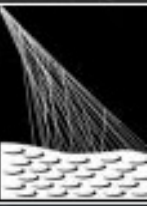


MAPSES Lecce 23-25 Novembre

Pierre Auger Observatory
studying the universe's highest energy particles



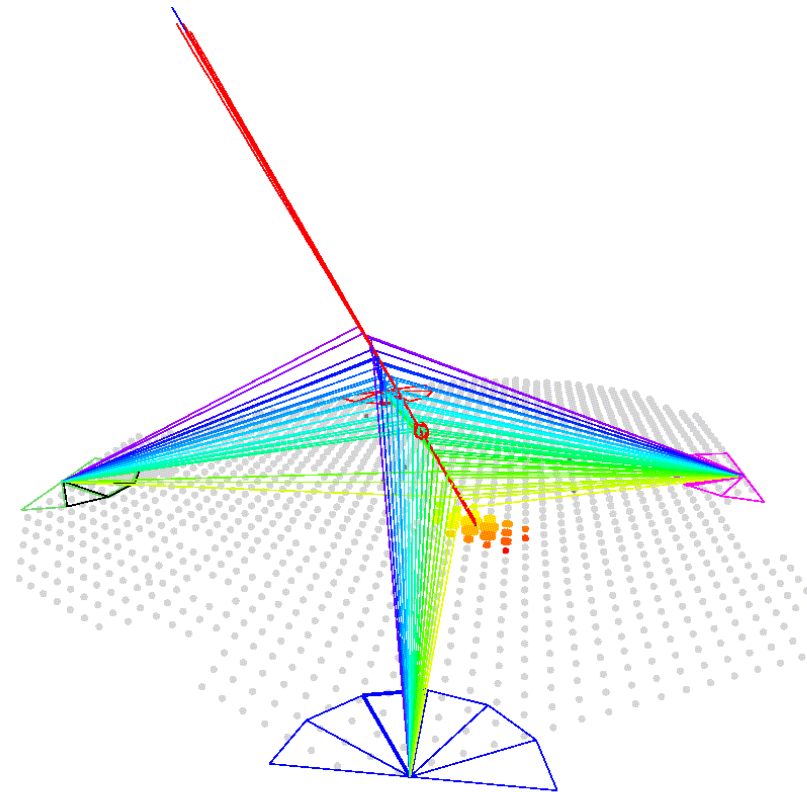
Tecniche di misura con l'Osservatorio Pierre Auger

Lorenzo Perrone

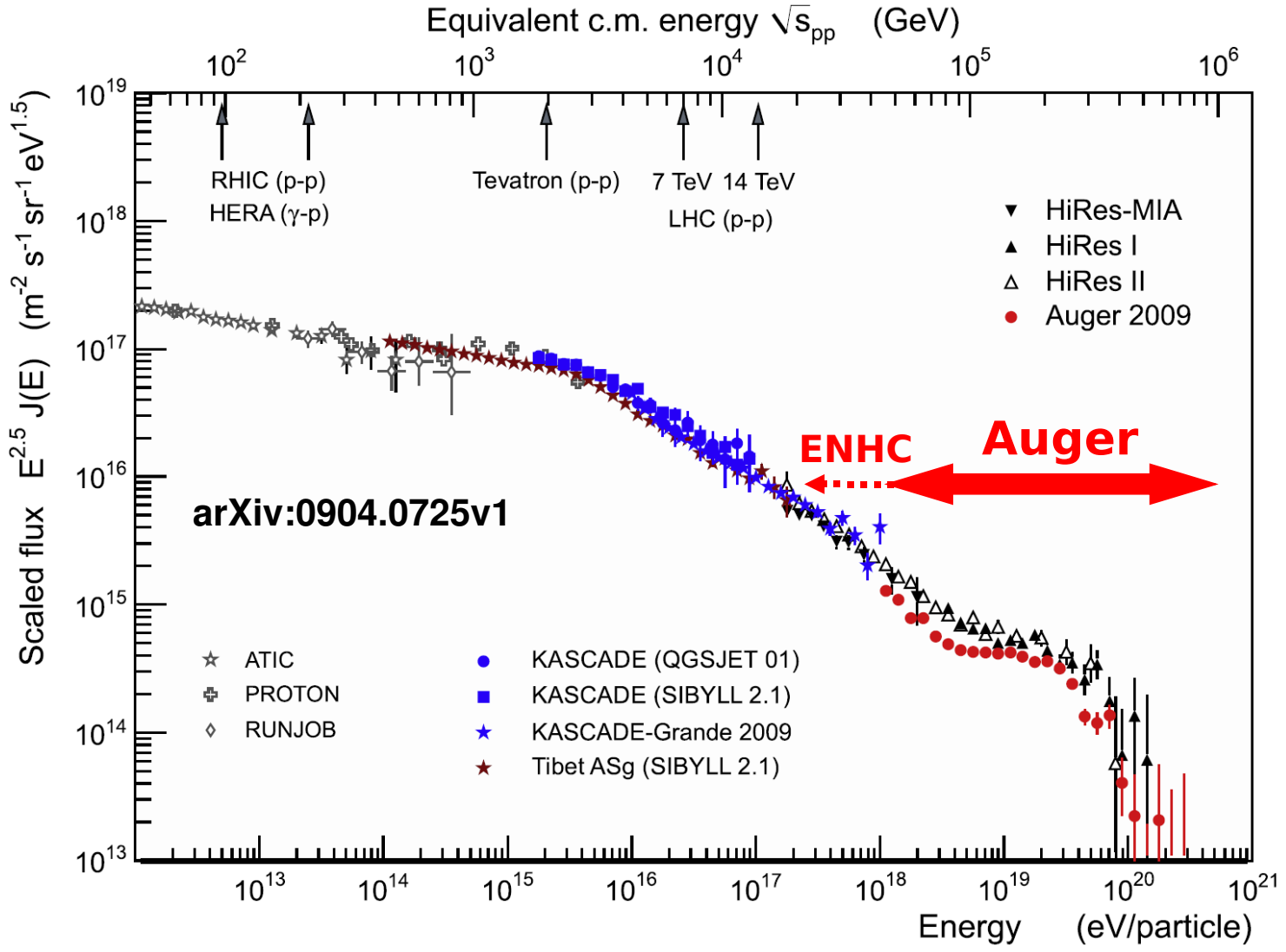
Università del Salento e INFN Lecce (Italy)

Outline

- Physics goals and operation range
- Detector description
- Performance and observables
- Results
- Enhancements



The Pierre Auger Observatory: range of operation



ENHC: Auger low energy extensions

Study of the transition between galactic and extra-galactic cosmic rays

- Ankle region

- 2nd Knee region (with lower energies extensions)

End of the spectrum (GZK region)

Energy spectrum

Arrival directions

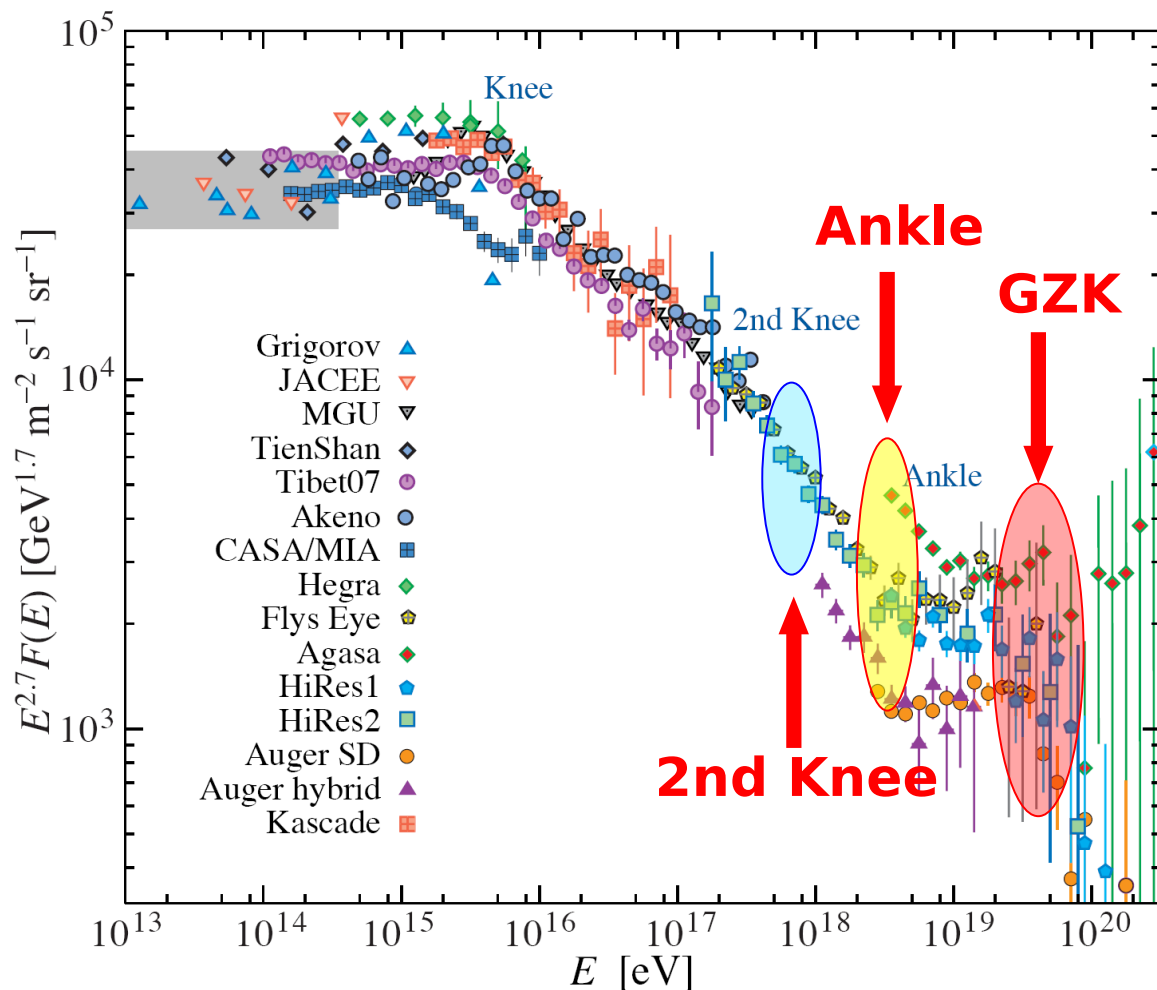
Composition

Search for photon and neutrinos as primary cosmic rays

Hadronic physics



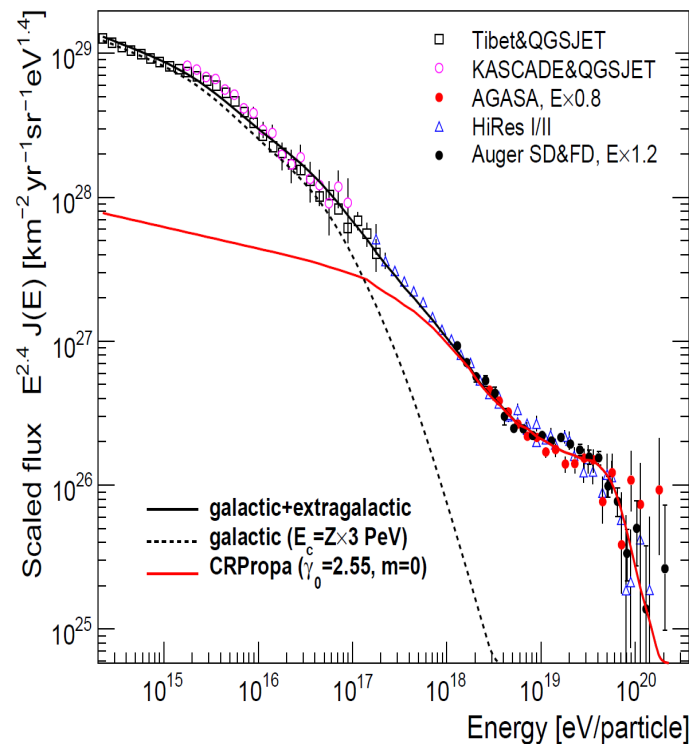
The physics case



Particle Data Group

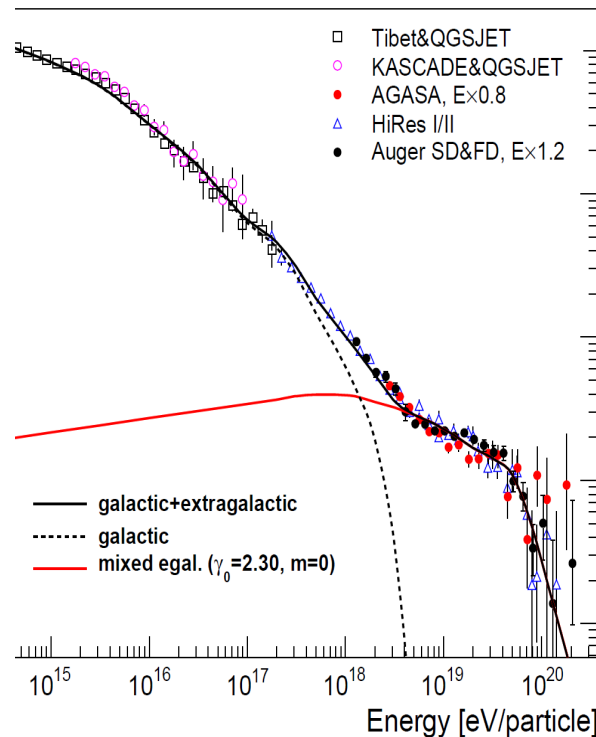
“the ankle”: models and hypotheses

M.Unger, arXiv:0812.2763 [astro-ph]



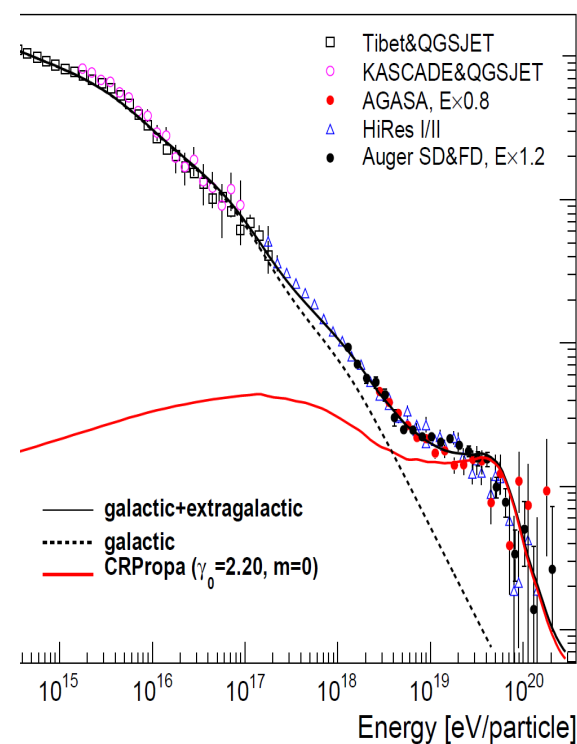
$$E_{\text{Gal-ExtraGal}} \sim 10^{17.5} \text{ eV}$$

Dip Model
Extragal. protons
(Berezinsky et al.)



$$E_{\text{Gal-ExtraGal}} \sim 3 \cdot 10^{18} \text{ eV}$$

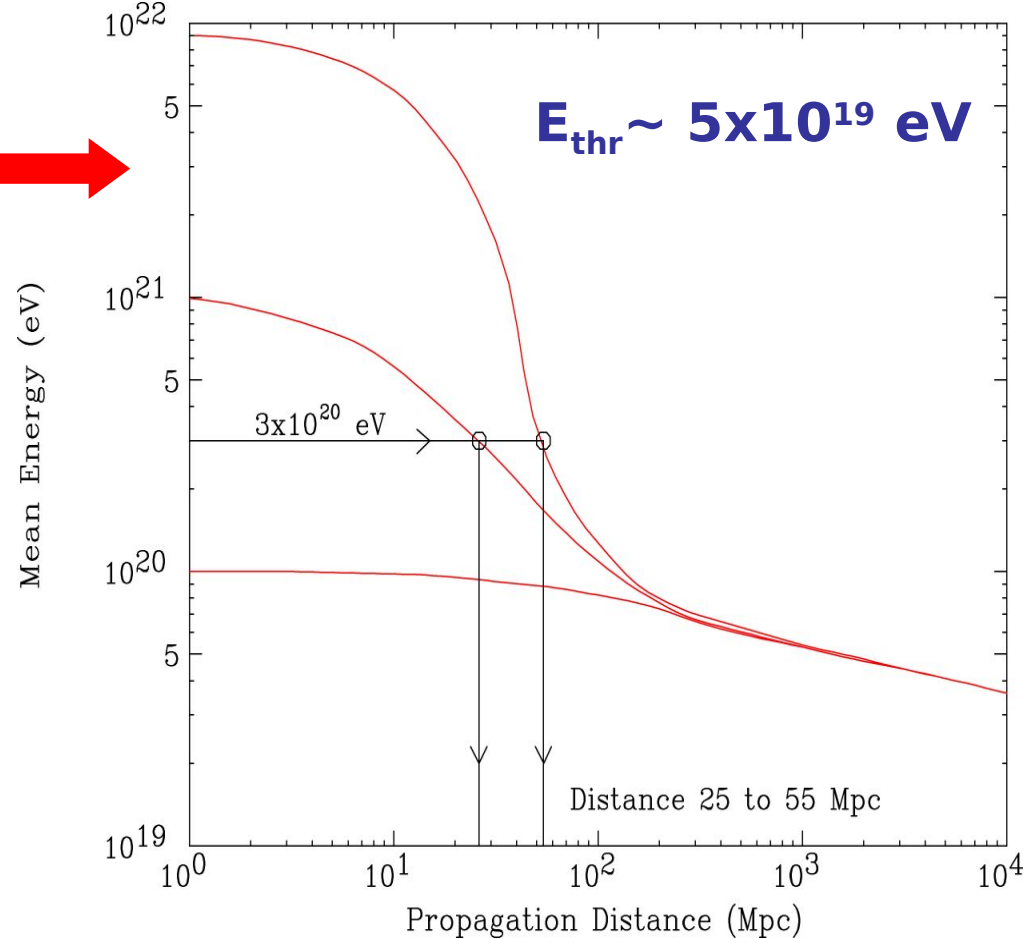
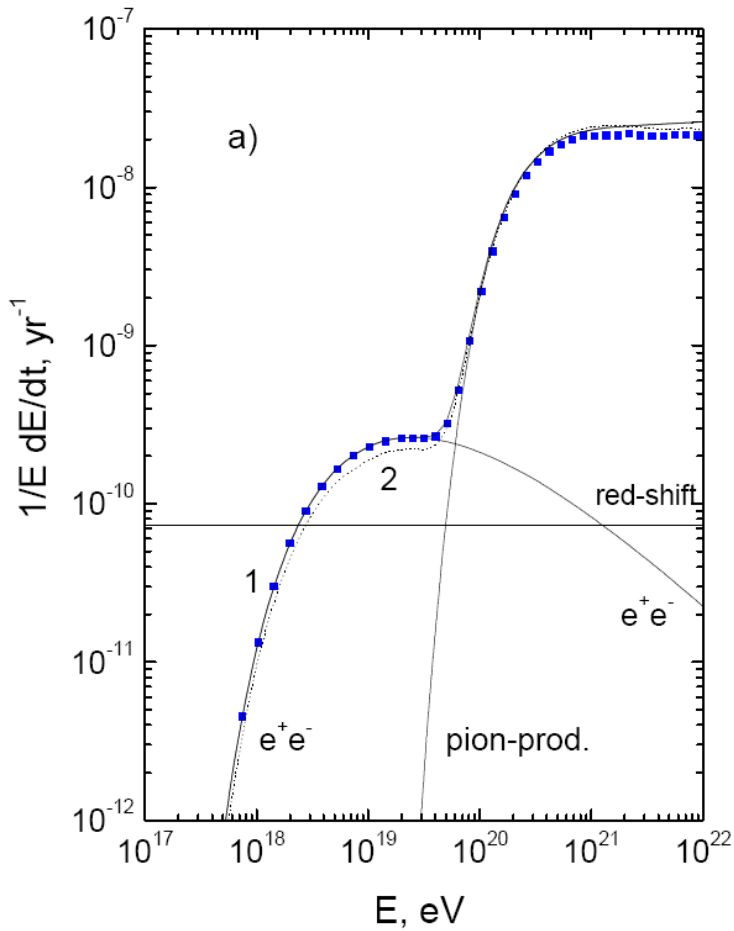
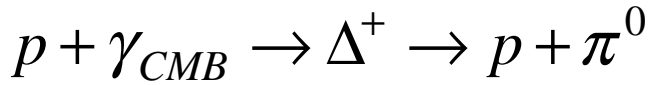
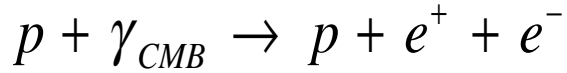
Mixed comp. of
extragal. component
(Allard et al.)



$$E_{\text{Gal-ExtraGal}} \sim 10^{19} \text{ eV}$$

Extragal. protons
(ankle model)

Propagation of CR: implications



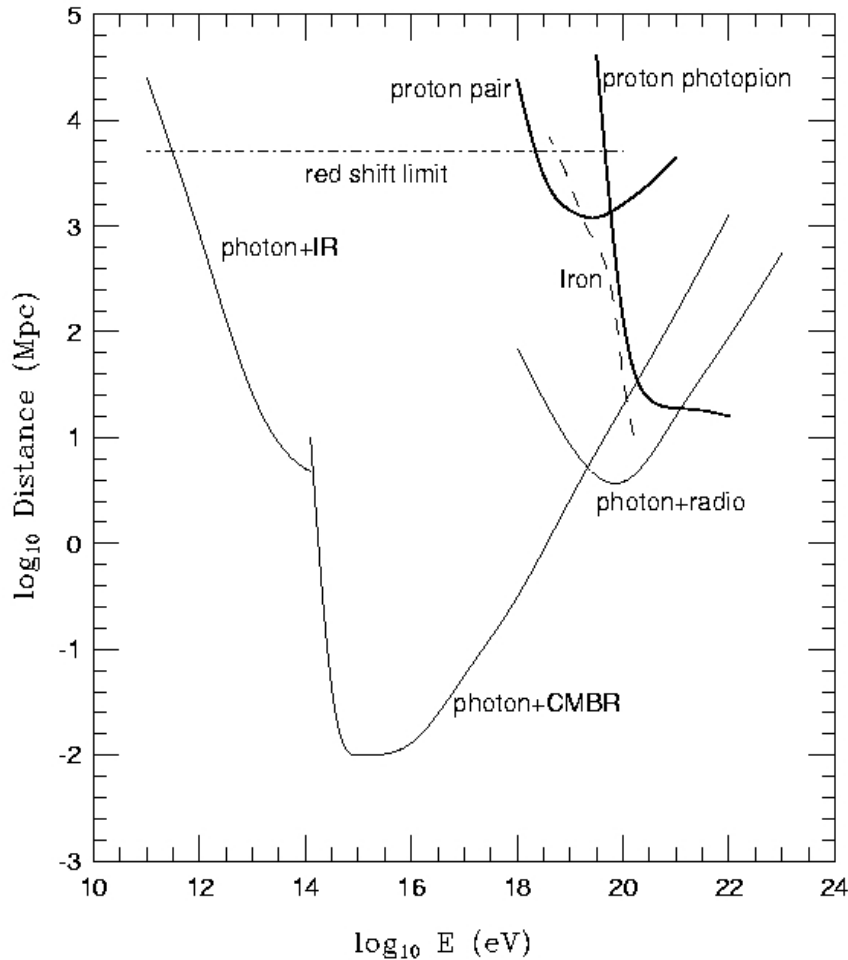
Flux Suppression (GZK cut-off)

Protons at $E > 10^{20}$ eV within 100 Mpc

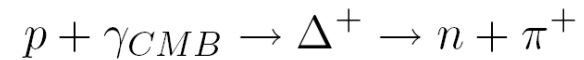
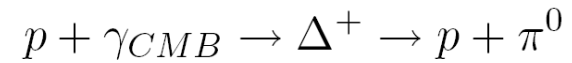
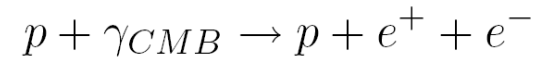
End to the cosmic ray spectrum?

Greisen Zatsepin Kuz'min effect (1966):

Interaction with the cosmic microwave background (CMB)



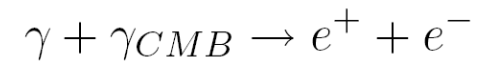
protons:



nuclei: photo-disintegration and pair production on CMB (RB IR)

“horizon” (p and nuclei) ~ 100 Mpc ($\sim 10^{20}$ eV)

photons:



$$E_{thr}(eV) \sim \frac{3 \cdot 10^{14}}{\epsilon_{\gamma}(eV)}$$

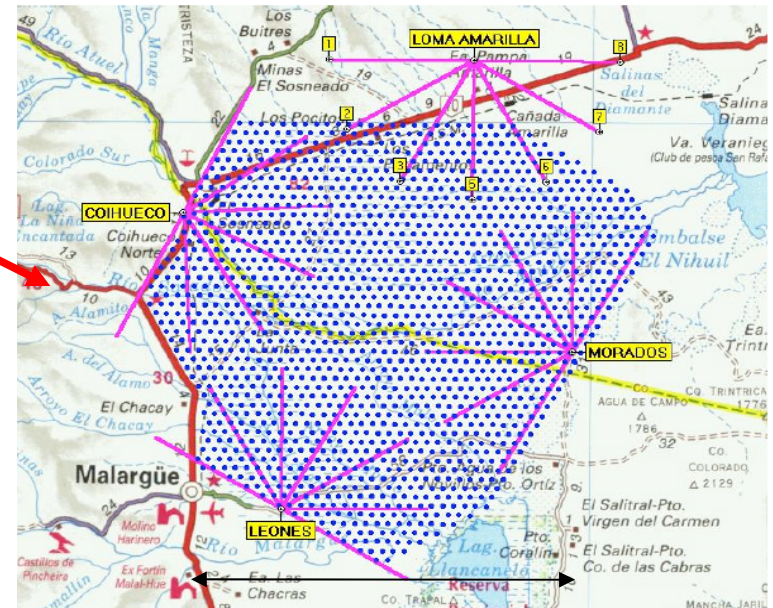
The Pierre Auger Observatory

17 Countries, 63 Institutions ~ 350 members



Southern hemisphere (3000 km²)
Malargüe (Mendoza) Argentina

- *large and flat region*
- *low density of population (low background due to artificial light)*
- *clean and dry atmospheric conditions (small cloud coverage)*



~ 50 km

The Pierre Auger Observatory

- *Surface detector*

an array of 1600 Cherenkov stations on a 1.5 km hexagonal grid ($\sim 3000 \text{ km}^2$)

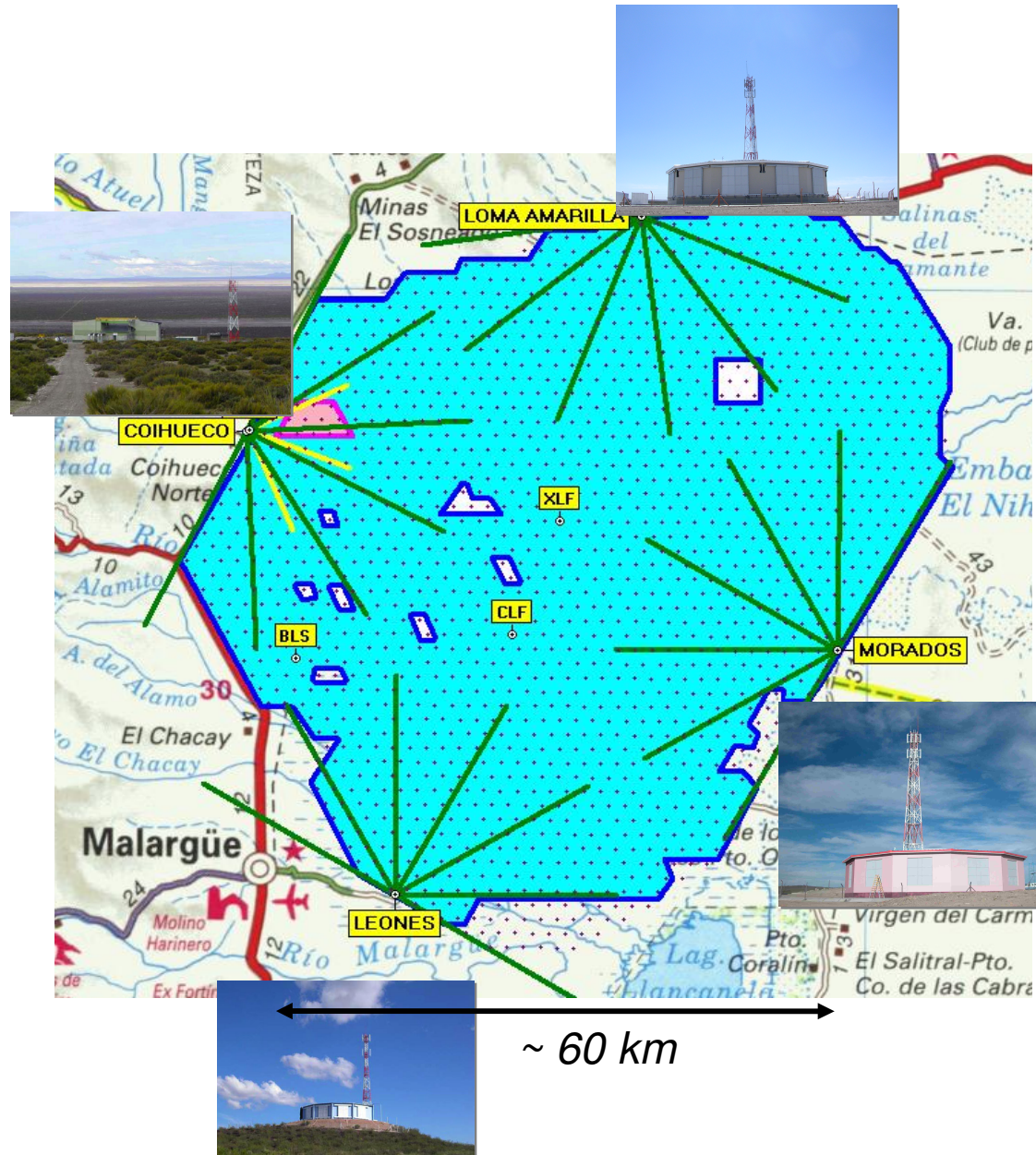
- *Fluorescence detector*

4 buildings overlooking the array

Low energy extensions

AMIGA: dense array plus muon detectors

HEAT: three further high elevation FD telescopes



The Hybrid Concept

Surface Detector Array

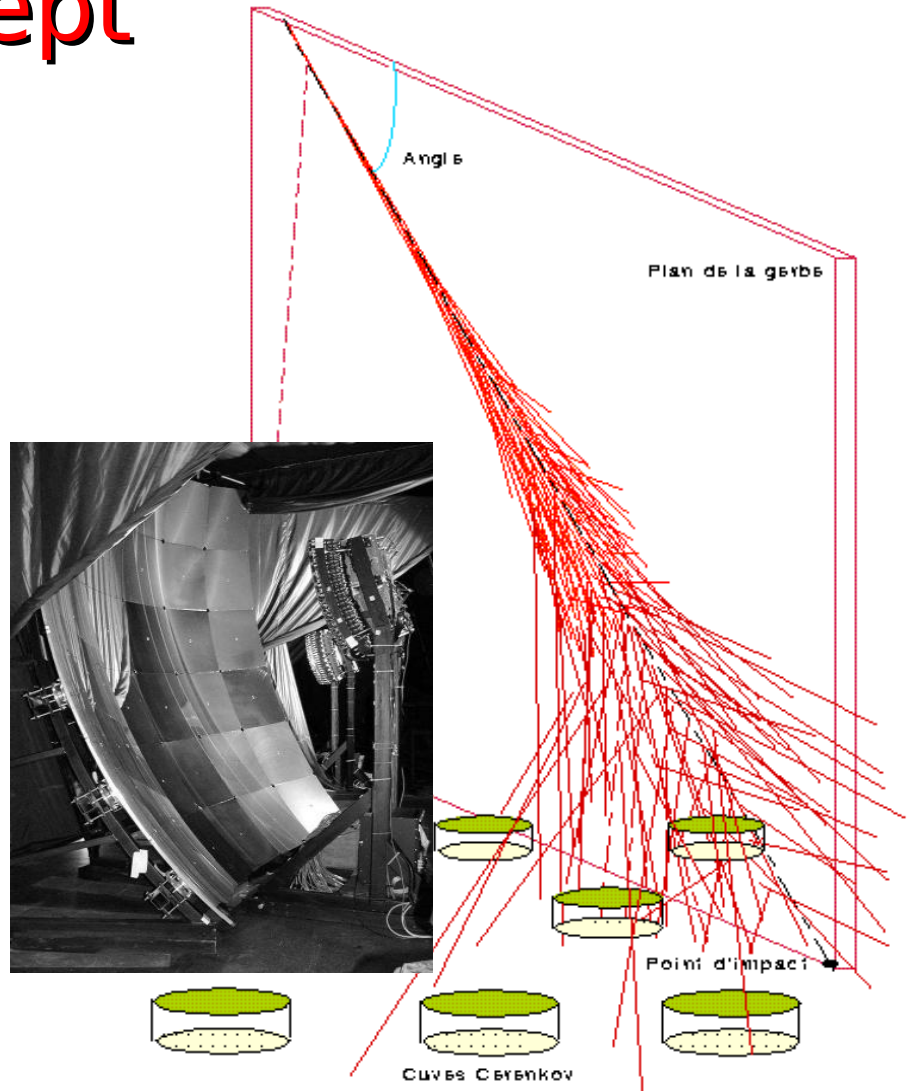
lateral distribution, 100% duty cycle

Air Fluorescence Detectors

Longitudinal profile, calorimetric energy measurement, ~15% duty cycle

accurate energy and direction measurement

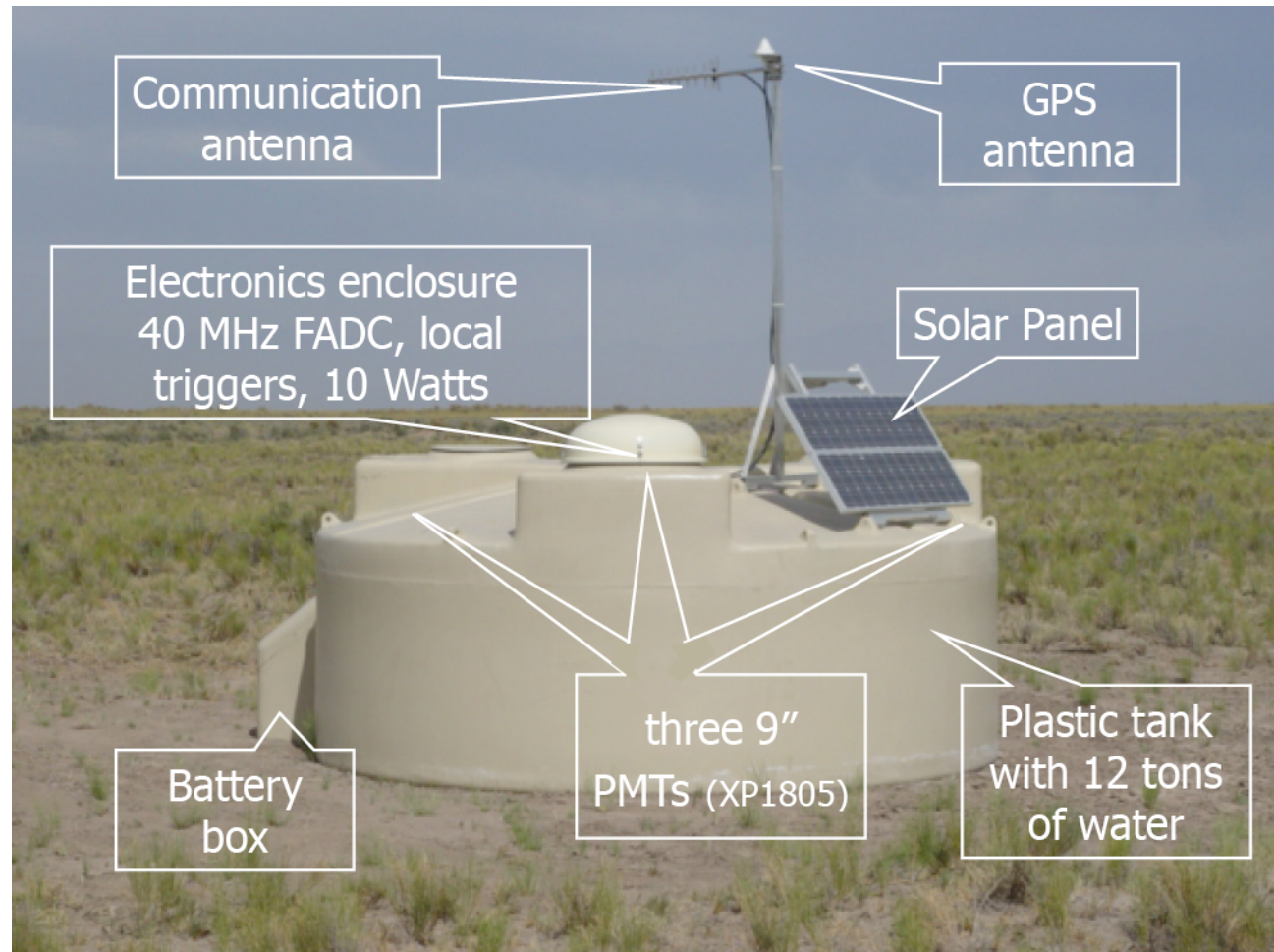
mass composition studies in a complementary way



“In order to make further progress, particularly in the field of cosmic rays, it will be necessary to apply all our resources and apparatus simultaneously and side-by-side.”

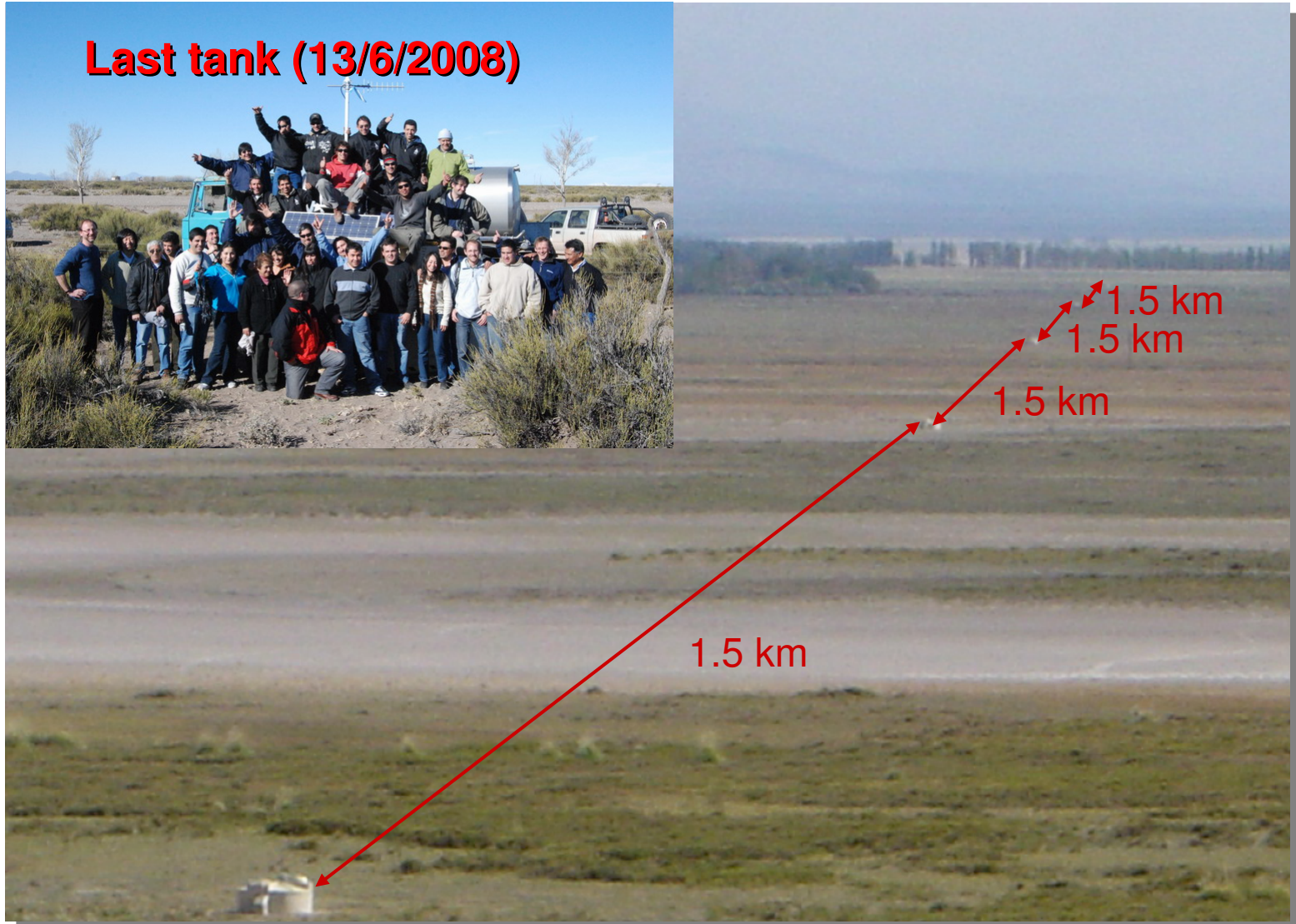
A station of the Surface Detector

- Plastic Tank
- Ultra-reflective tyvek liner
- 12 m³ purified water
- 3 PMTs (9 inches)
- Independent power supply (solar panels)
- GPS antenna
- Communication antenna



DAQ : 40 MHz FADC sampling (10 bit resolution)

The surface detector (SD)



Not only muons hit the tank!!!!

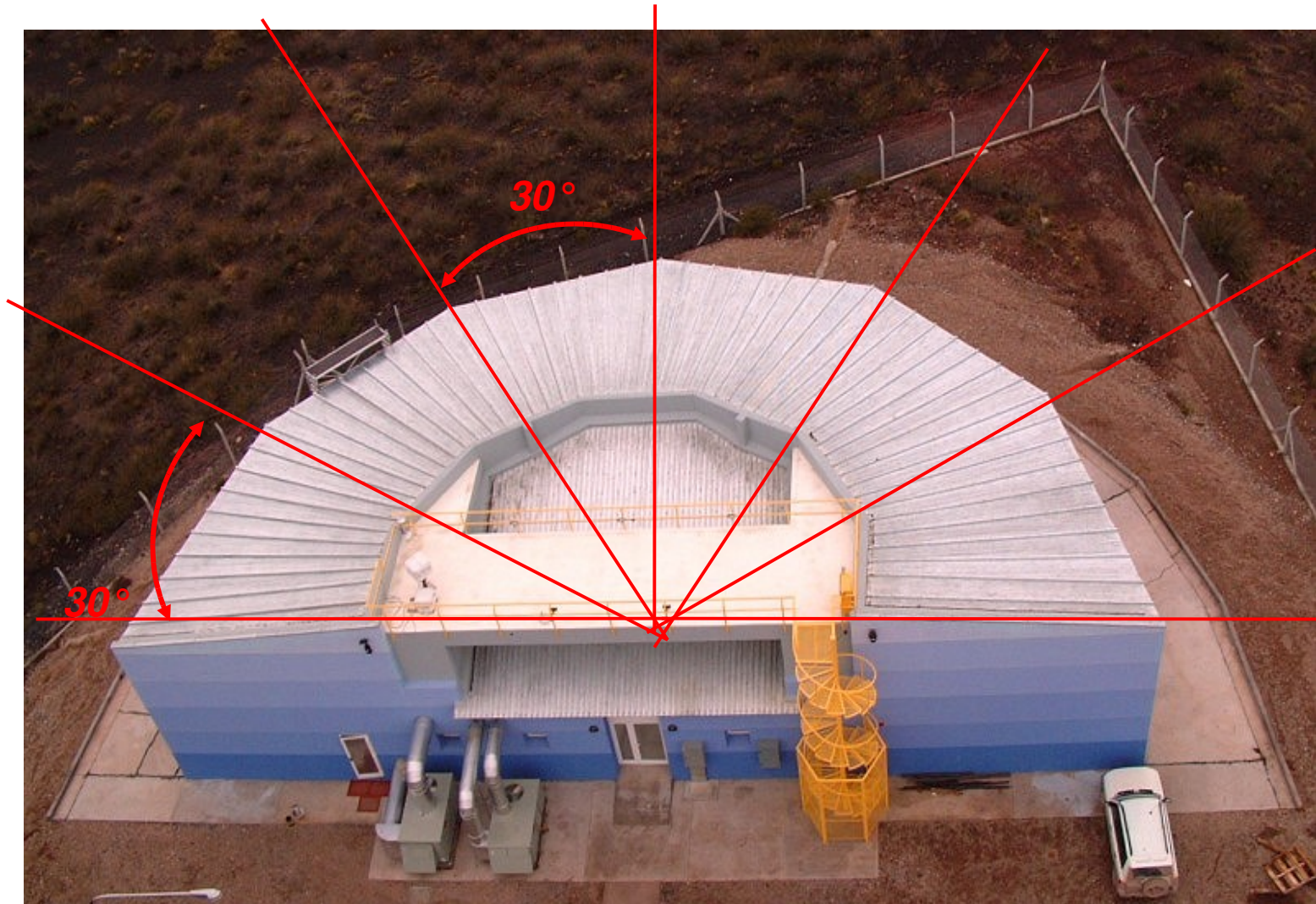


**Bird droppings
together with dry
weather degrade
solar panels.**



**Bird nests behind
solar panels
sometimes catch
fire.**

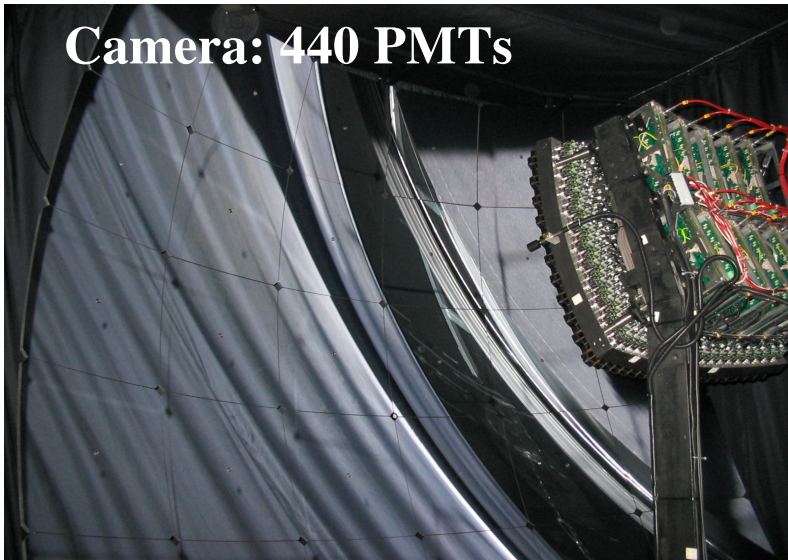
The fluorescence detector (FD)



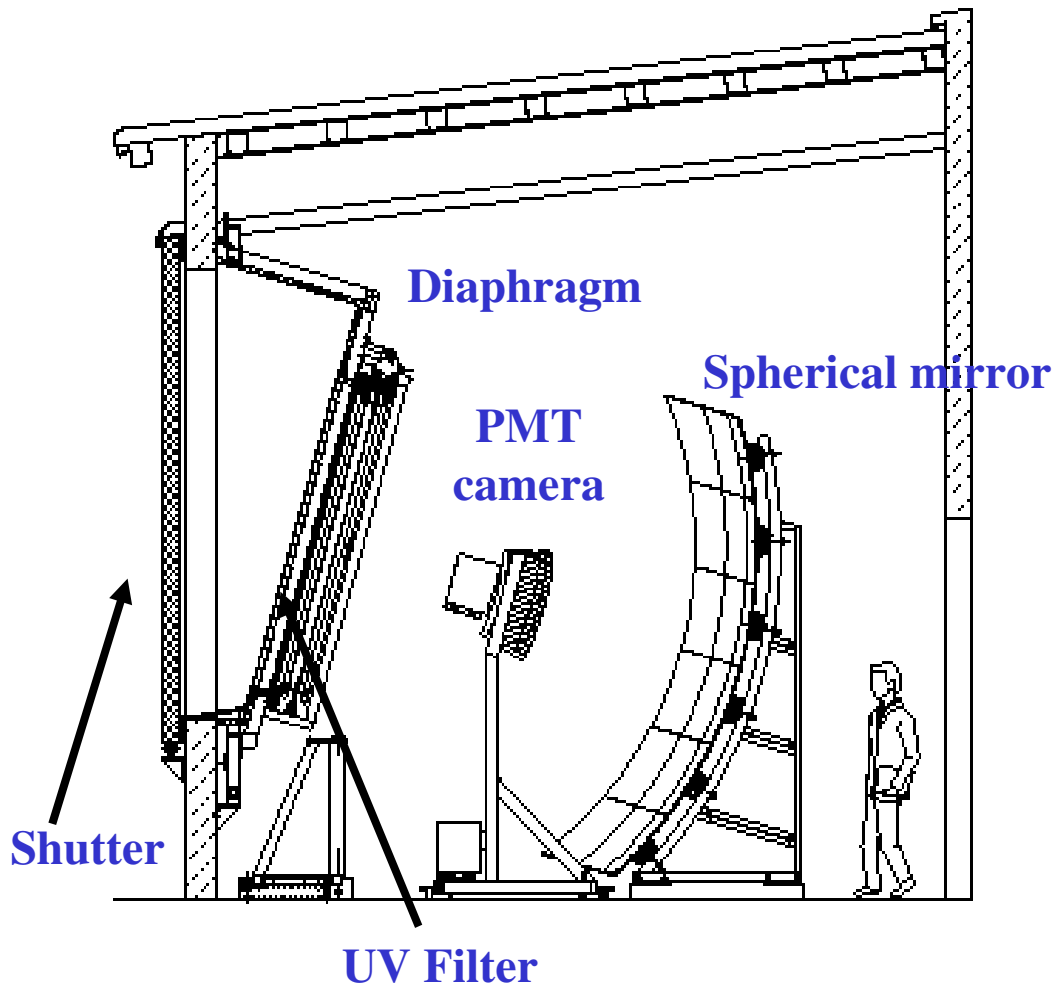
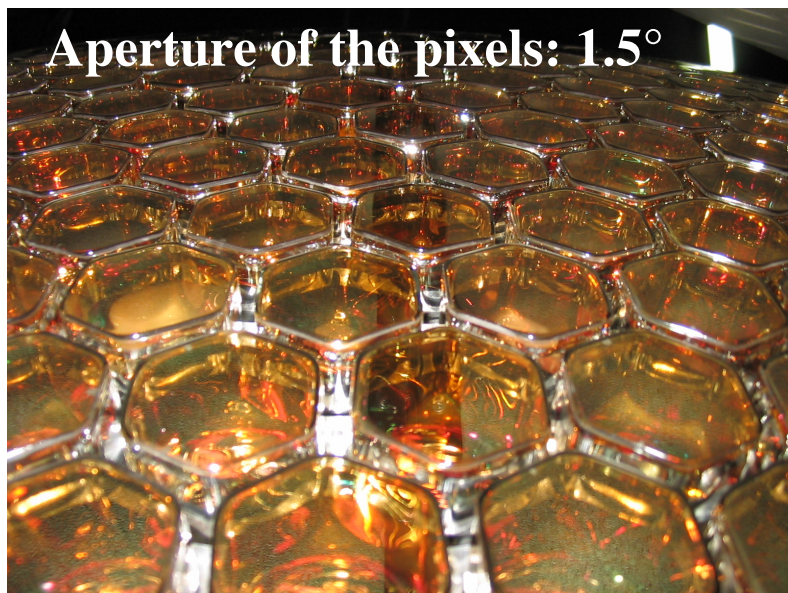
6 telescopes, each with 30° x 30° FOV

The fluorescence detector (FD)

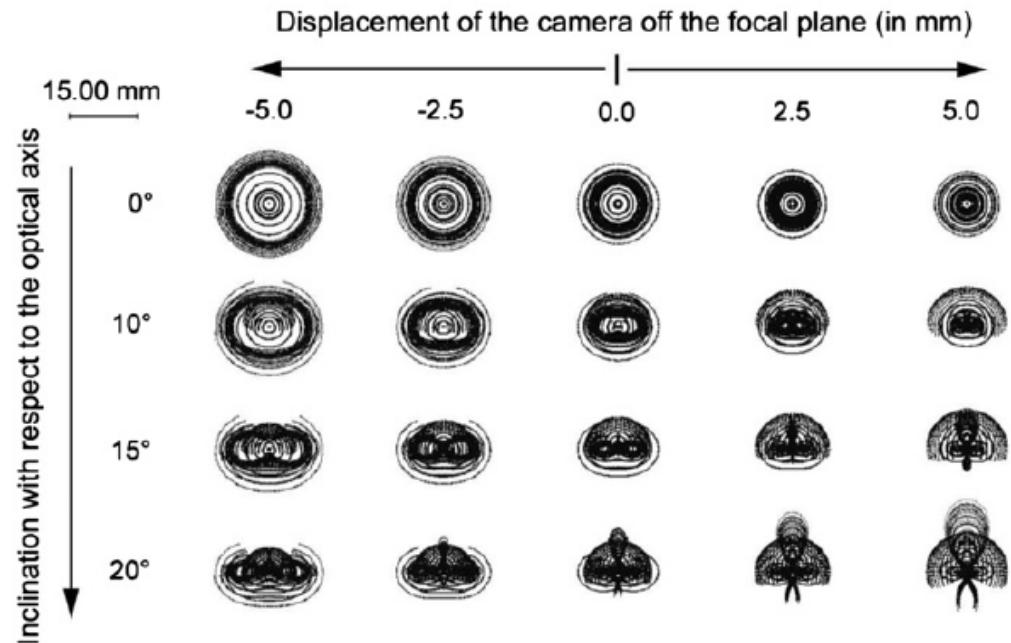
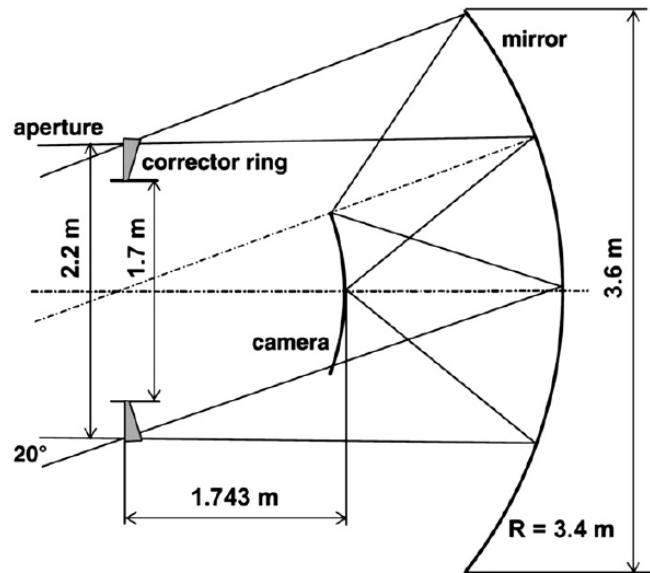
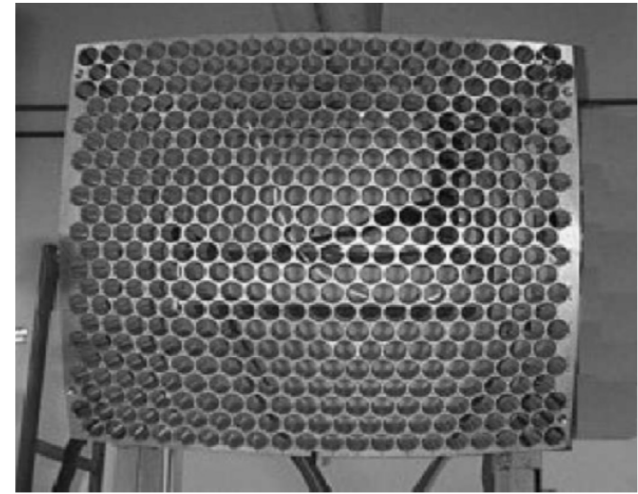
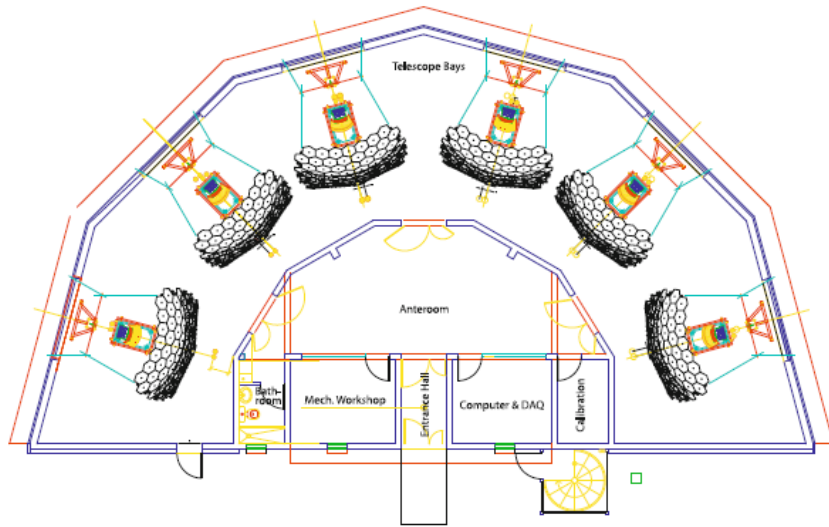
Camera: 440 PMTs



Aperture of the pixels: 1.5°

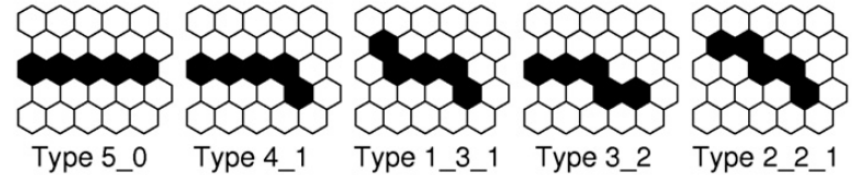


The fluorescence detector (FD)

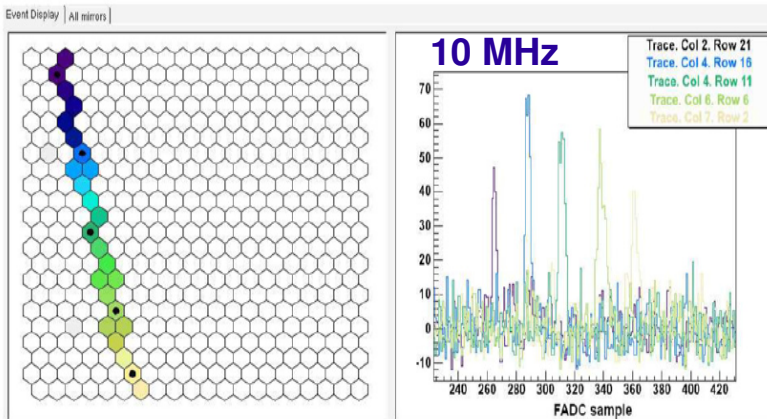


Trigger strategy for FD

- T1** individual pixel above threshold - 100 Hz/pixel
- T2** on specific patterns (~40000) - 0.1 Hz/telescope
- T3** software trigger (event builder) 0.02 Hz/FD-site

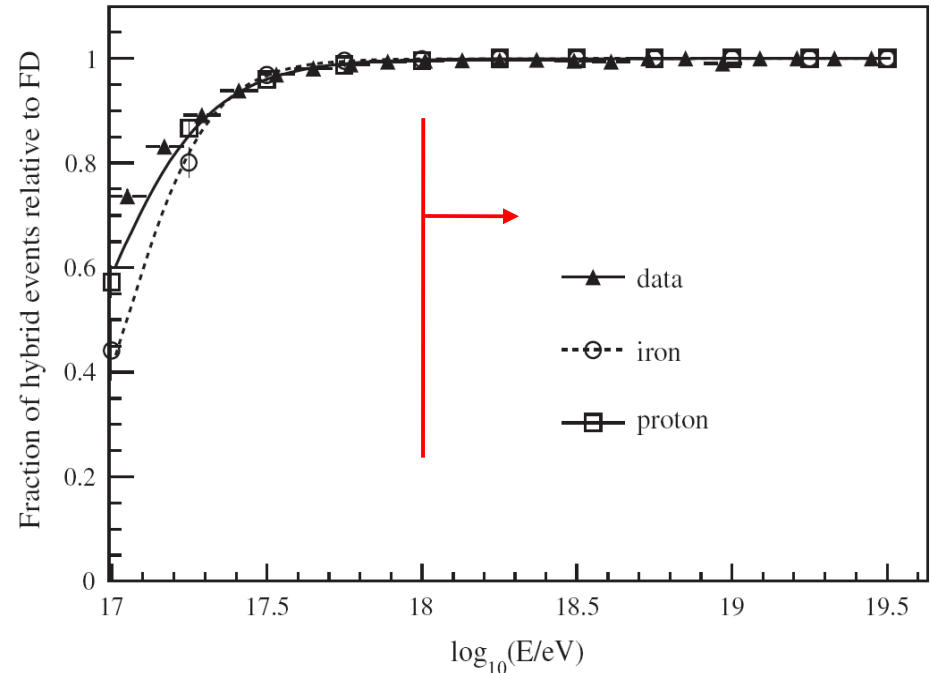


Event Display

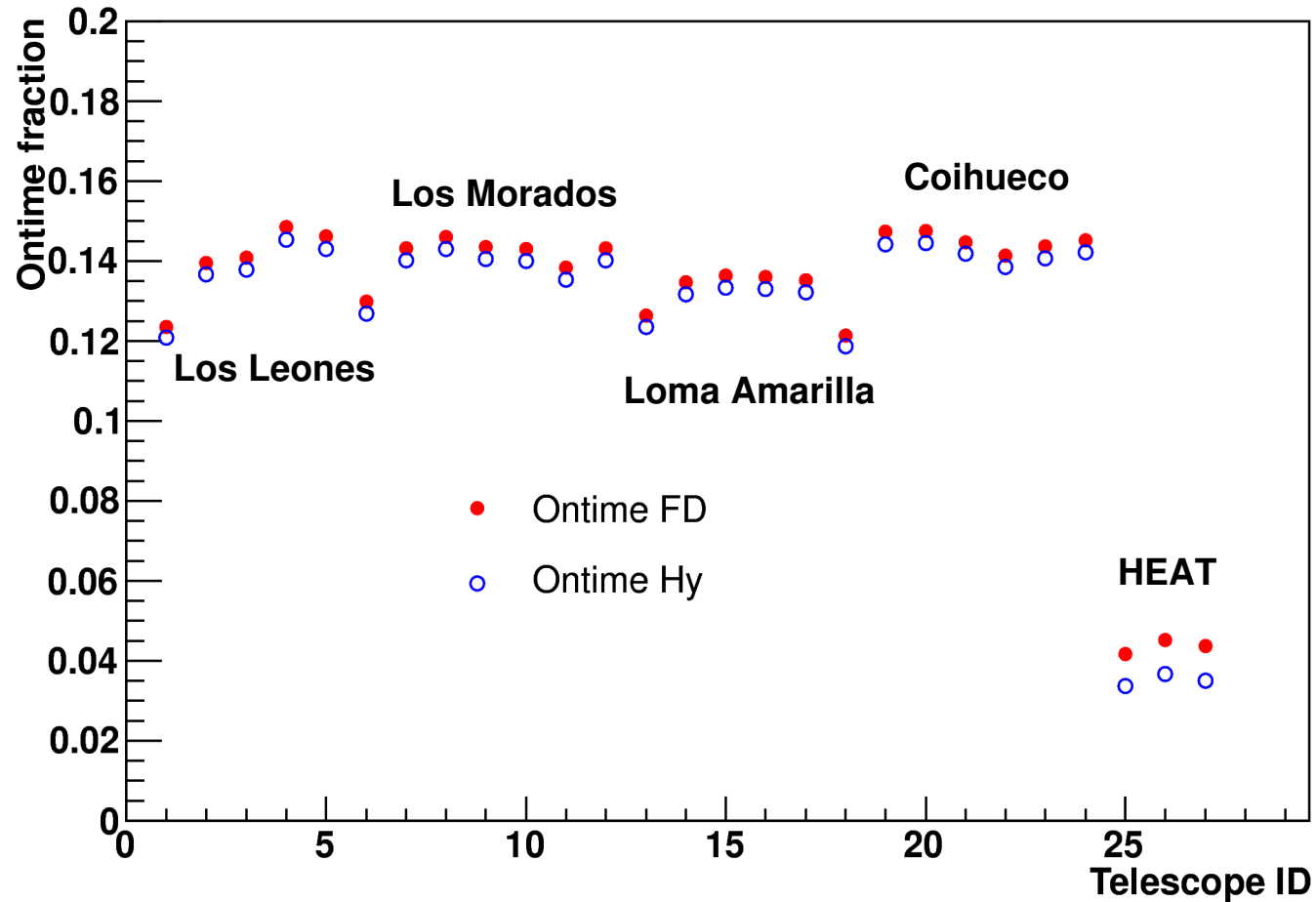


At energy above 10^{18} eV each FD event has at least one station, regardless of its primary mass if hadron

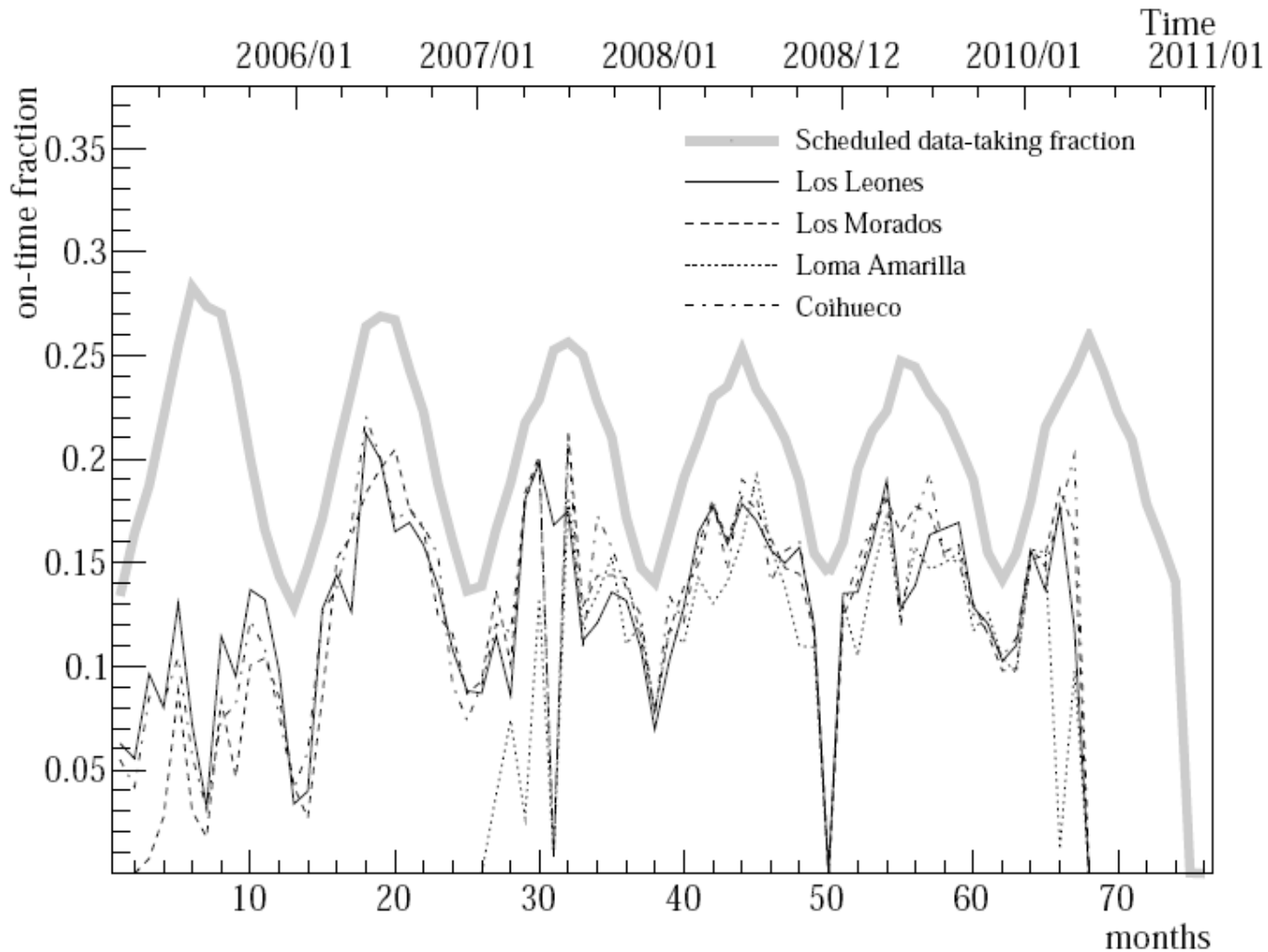
Time and geometrical info of each T3 sent to SD -> **Hybrid trigger!**



FD On-time fraction



FD On-time fraction

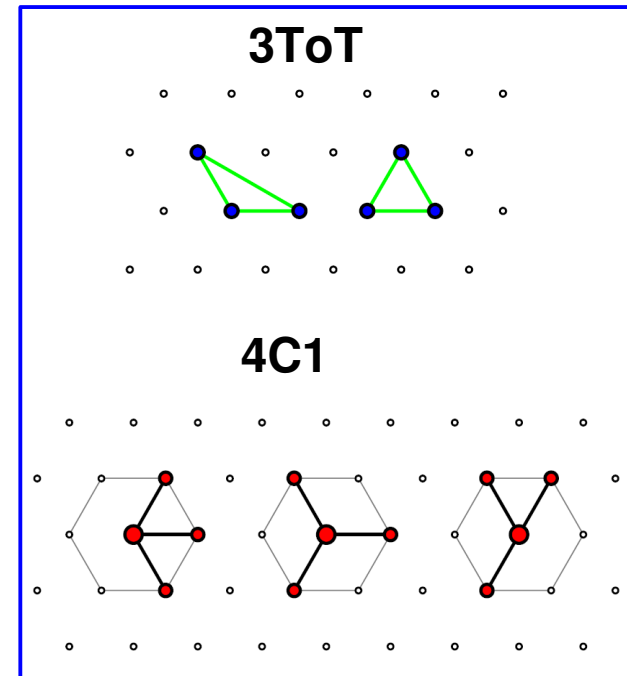


Trigger strategy for SD

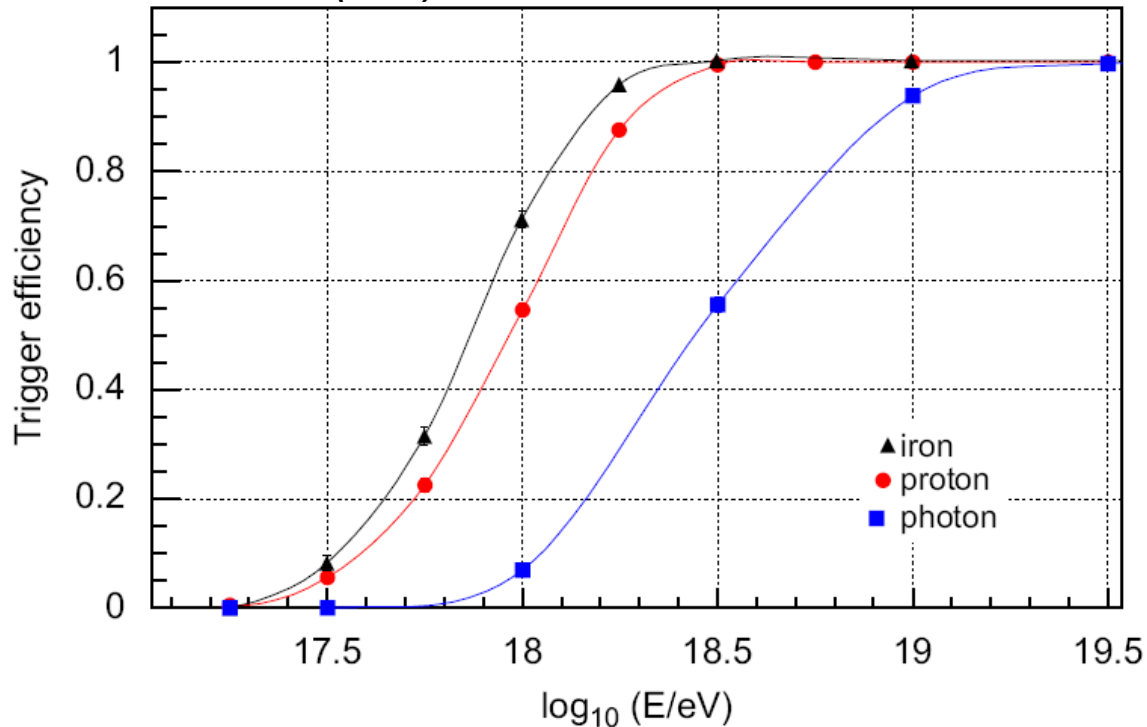
Station trigger

- T1** 3 PMTs above threshold 1.75 VEM – 100 Hz
- ToT** 13 time bins above a threshold of 0.2 VEM in 2 PMTs – 20 Hz
- T2** ToT || threshold above 3.2 VEM in 3 PMTs

Event



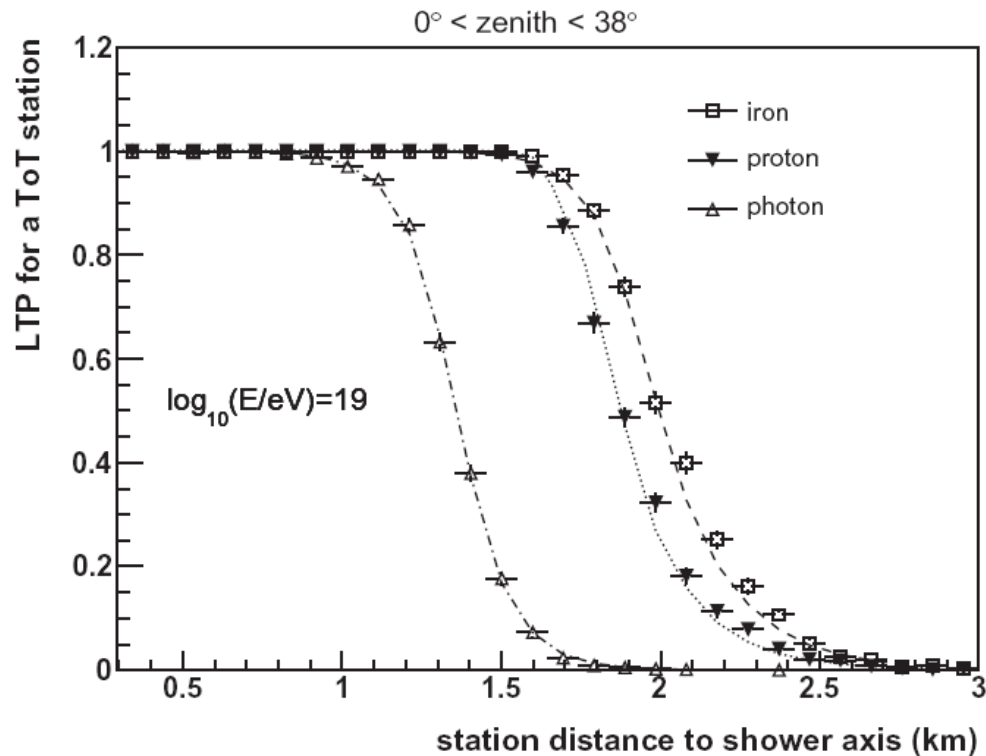
NIM A 613 (2010) 29–39



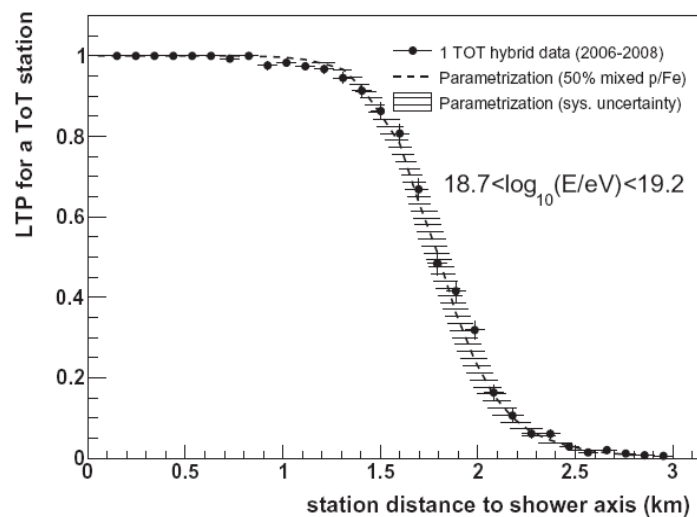
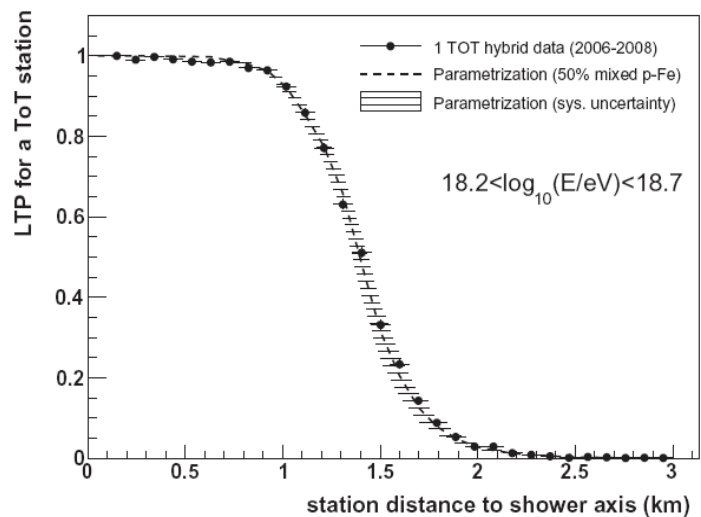
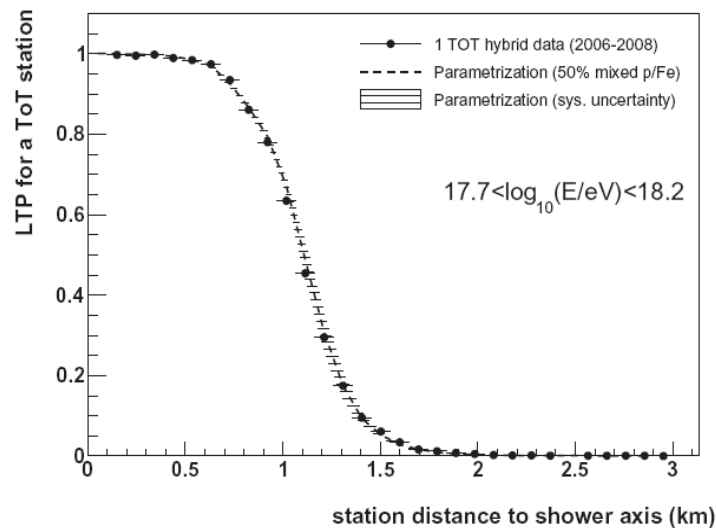
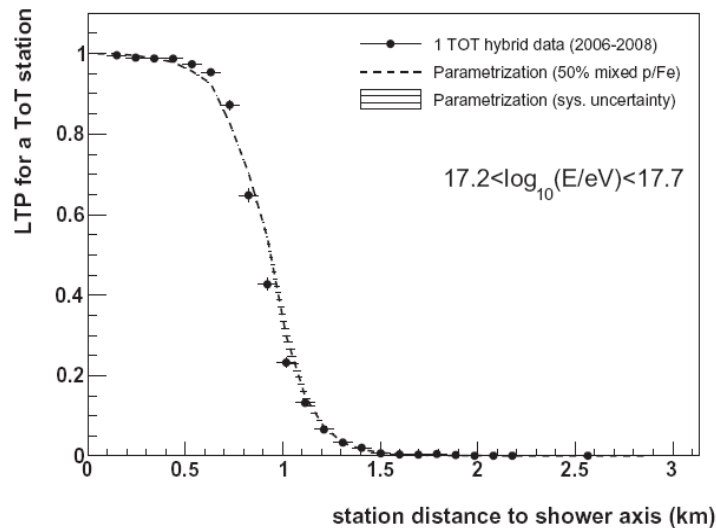
Full efficiency at energy above $10^{18.5}$ eV, regardless of its primary mass if hadron

Lateral Trigger Probability Function

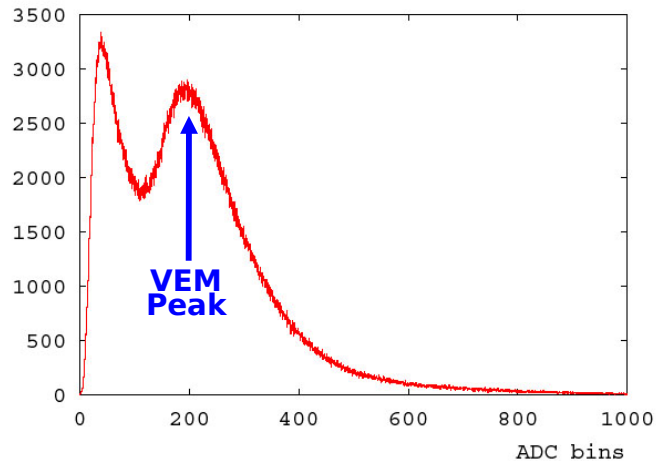
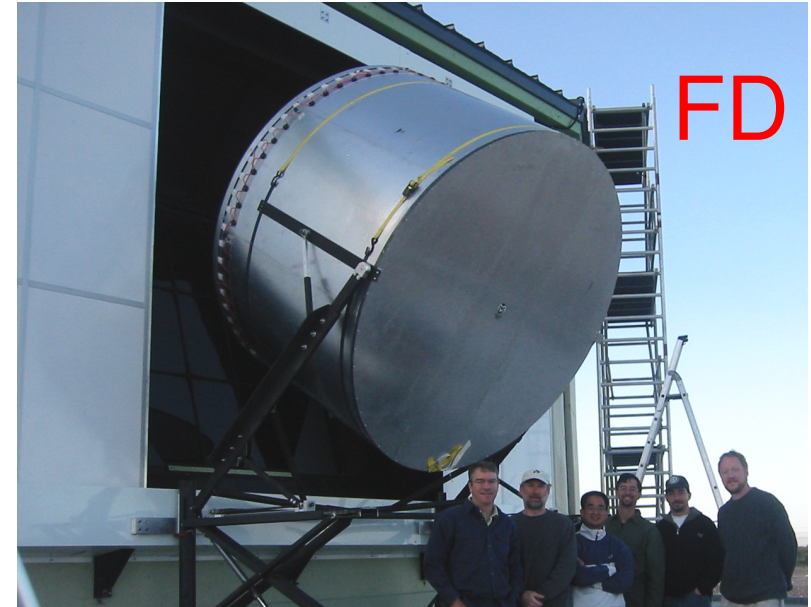
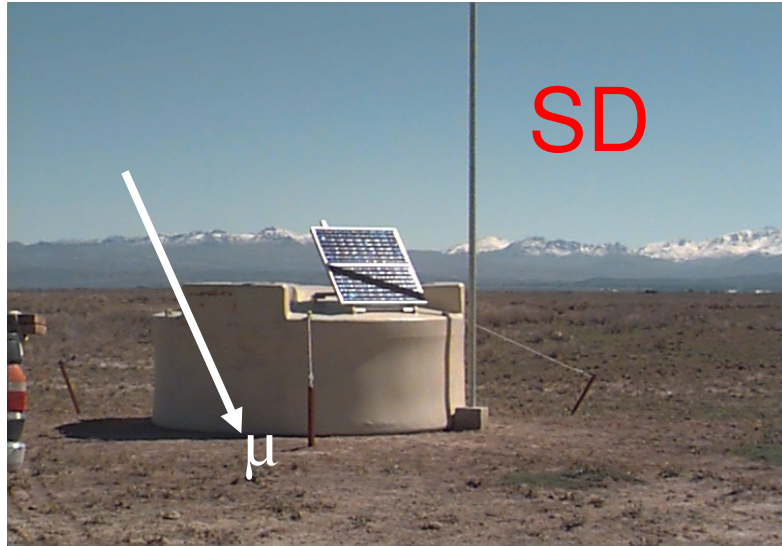
The probability for an Extensive Air Shower to trigger an individual detector of a ground based array as a function of distance to the shower axis, taking into account energy, mass and direction of the primary cosmic ray



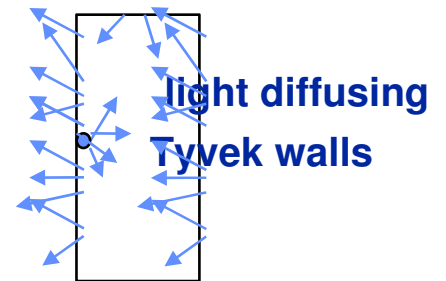
Lateral Trigger Probability Function



SD e FD Calibration



light flux measured
by absolutely
calibrated PMT



Drum: uniform camera illumination

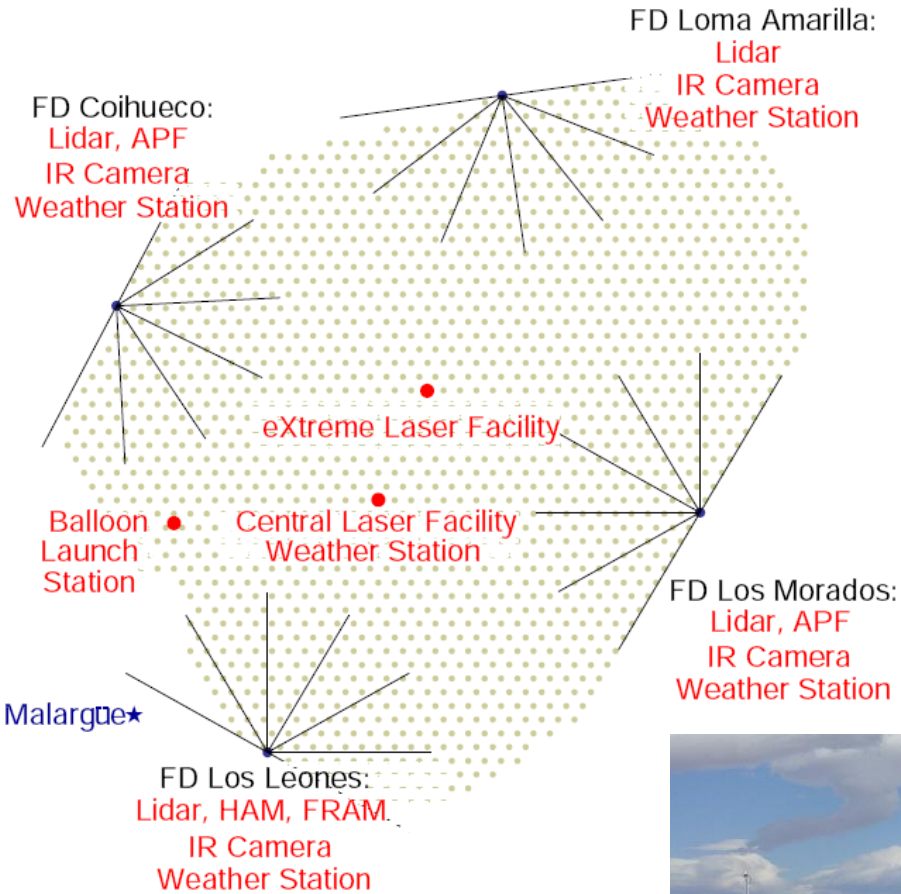
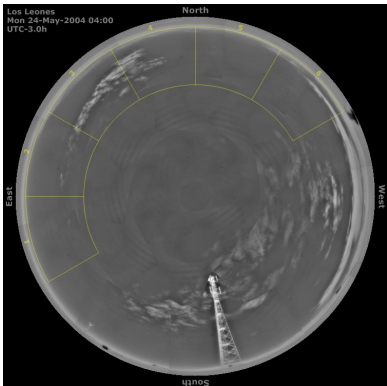
Through-going cosmic muons

Atmospheric monitoring

balloons



IR cloud camera



backscatter Lidar



Central Laser Facility



K. Louedec @ ICRC 2011

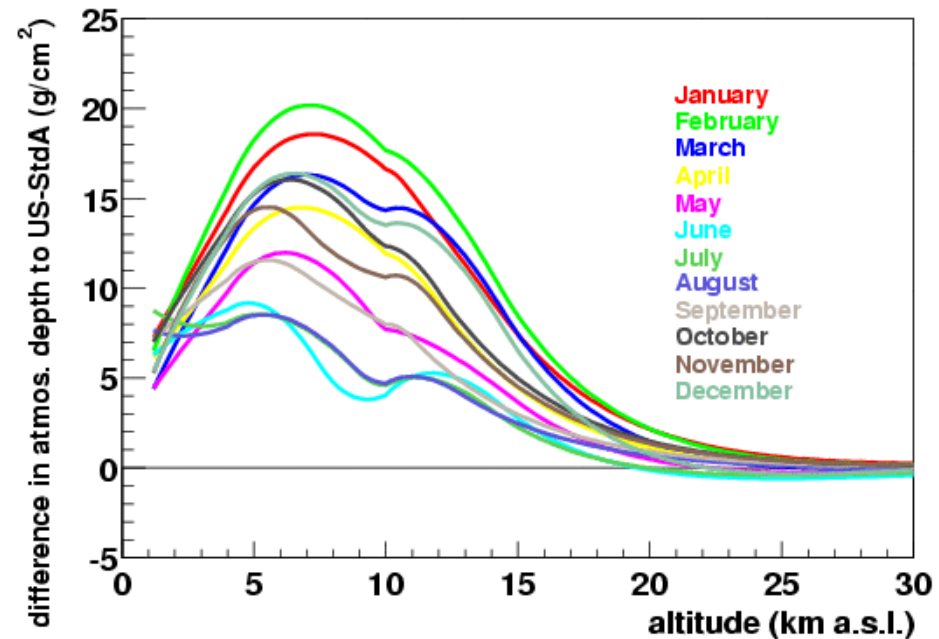
Atmospheric profiles

Local measurements with:

- radio sondes
- ground based weather stations

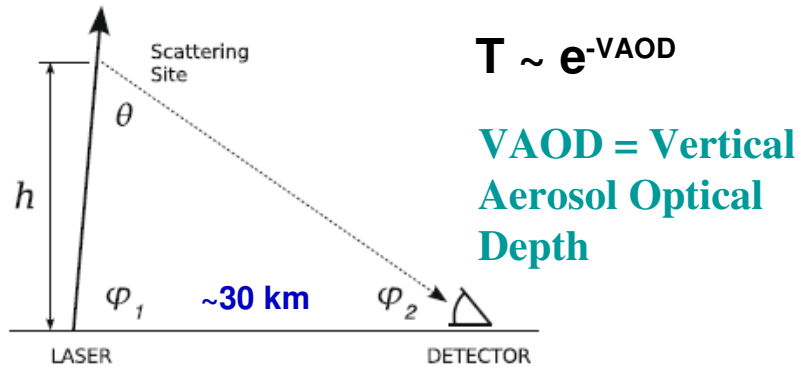


Malargue monthly models

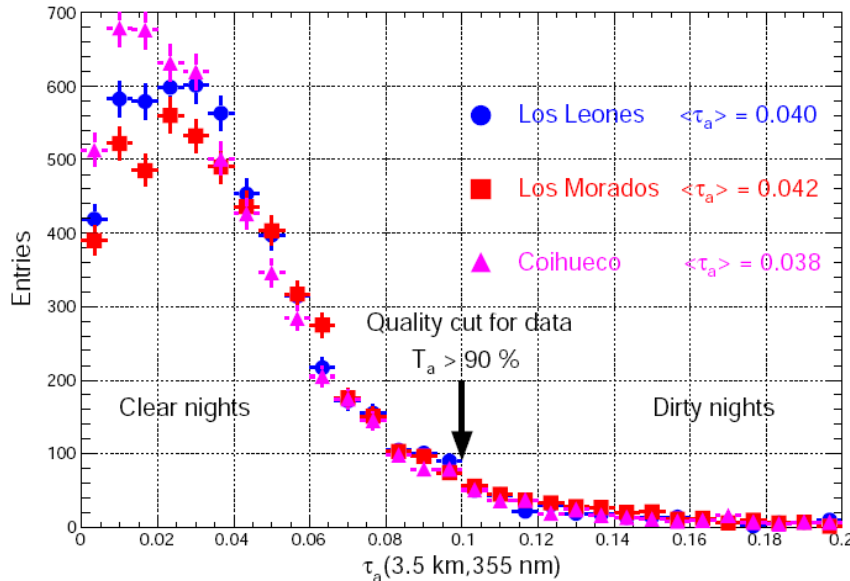


Global Data Assimilation System (GDAS) developed
by the National Oceanic and Atmospheric Administration

Central Laser Facility



Aerosol optical depth @ 3.5 km



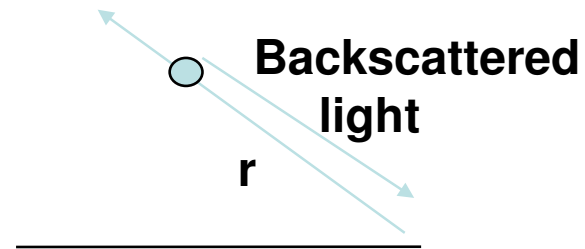
Vertical aerosol optical depth at 3.5 km above the fluorescence Telescopes measured between January 2004 and December 2010. The transmission coefficient is defined as $T = \exp(-\tau_a)$.

Aerosol monitoring

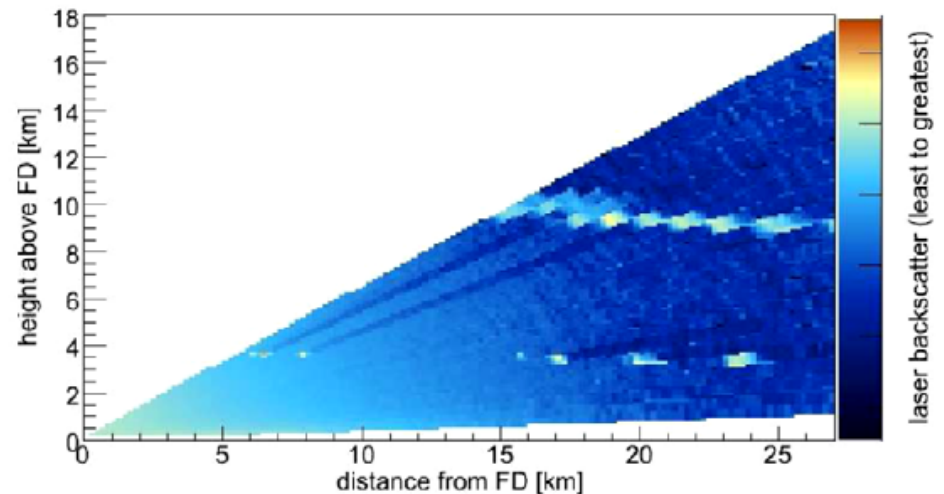
- Aerosols: clouds, dust, smoke and other pollutants

Backscatter Lidars

- 1 steerable laser per eye
- hourly scan of aerosols and “shoot the shower”

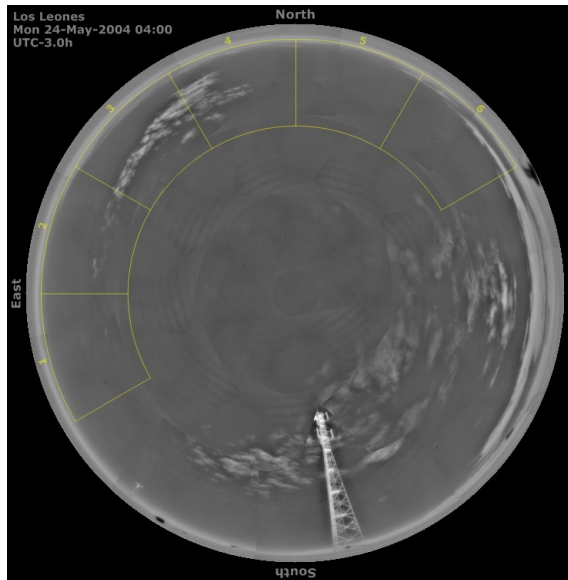


Cloud image

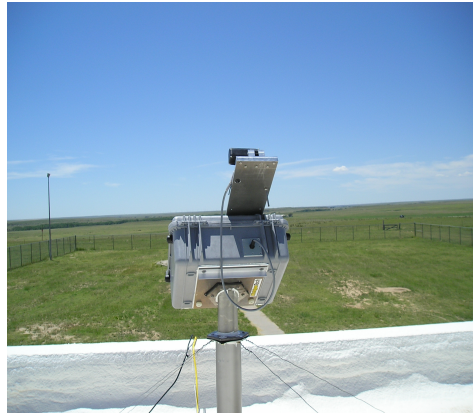
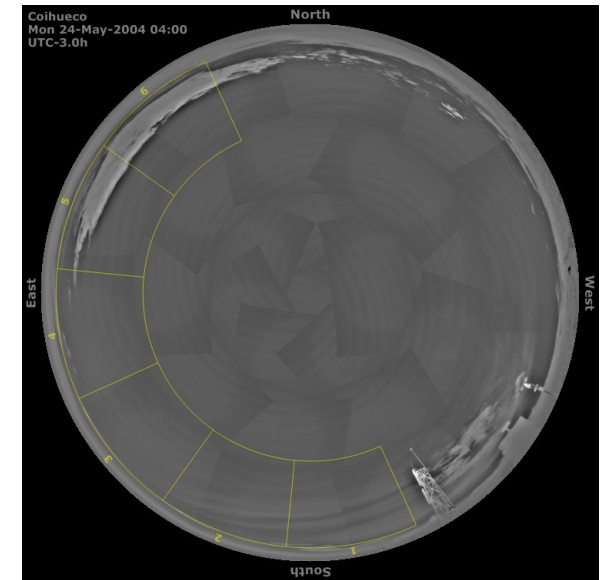


Infrared cloud monitoring

Los Leones

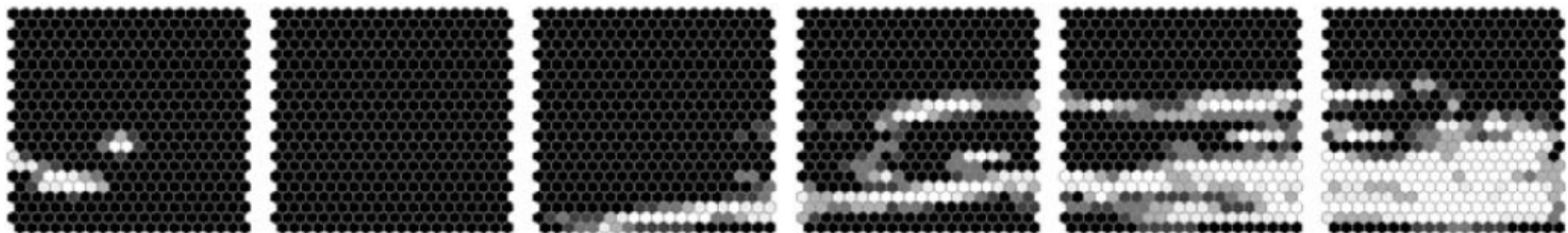


Coihueco



Finely pixelated infrared
Raytheon 2000B camera

Full sky cloud scan

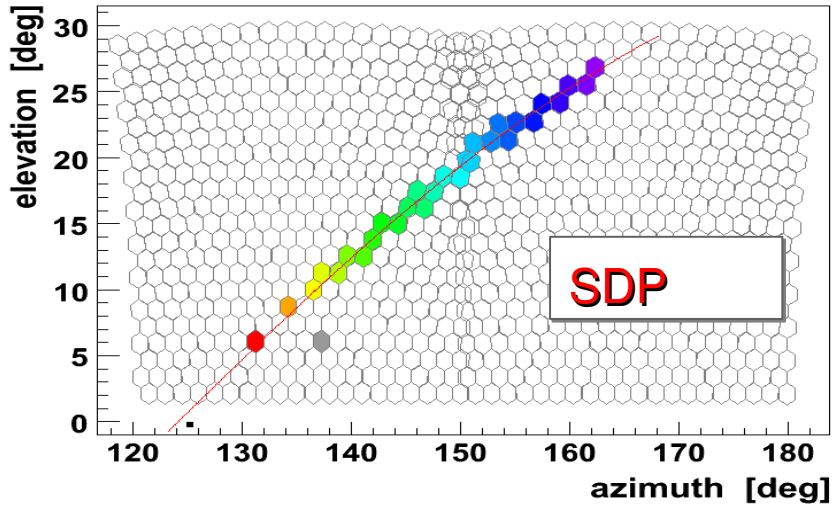


Pixel-wise mask for shower reconstruction

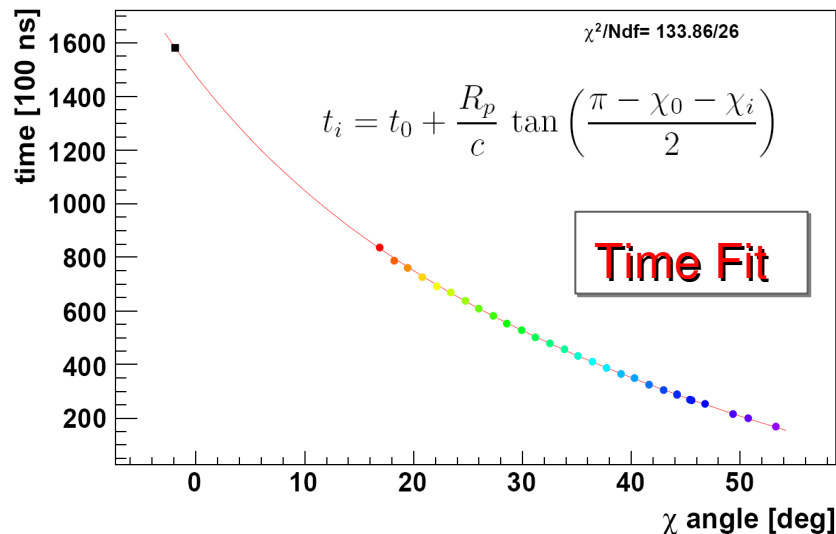
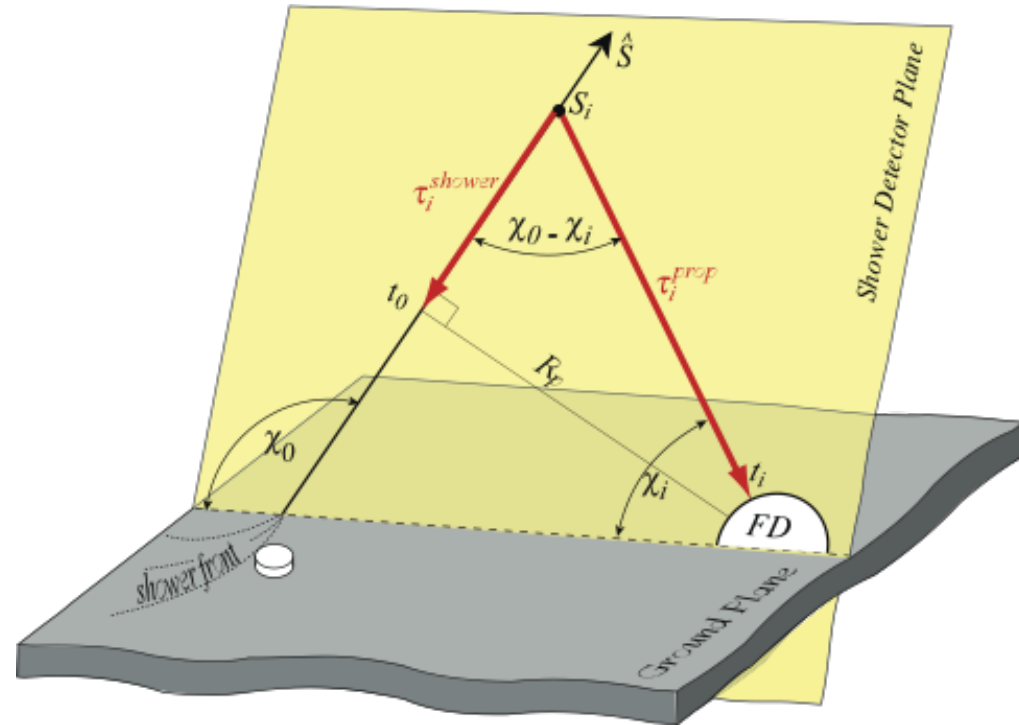
Observables and Detector Performance

- Reconstruction of arrival directions with FD/SD/Hybrid
- Reconstruction of longitudinal profile
- Energy determination

FD-Hybrid geometry reconstruction

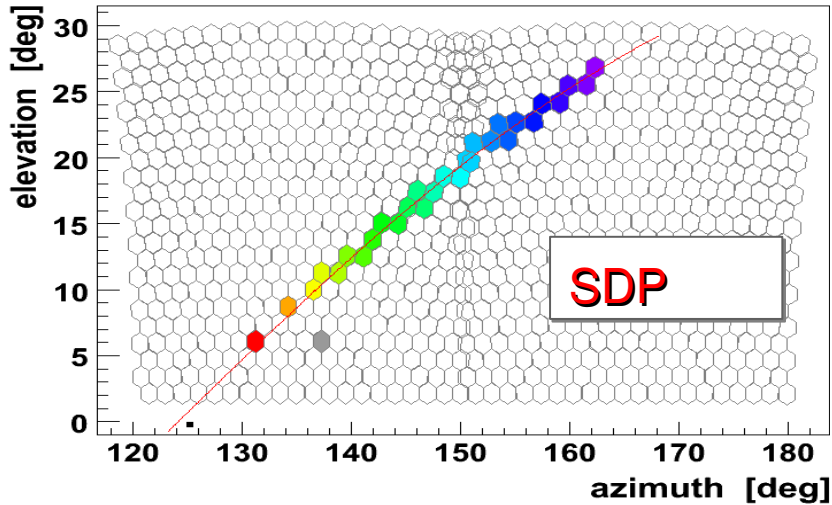


Shower-Detector Plane (SDP) using the directions of the triggered pixels

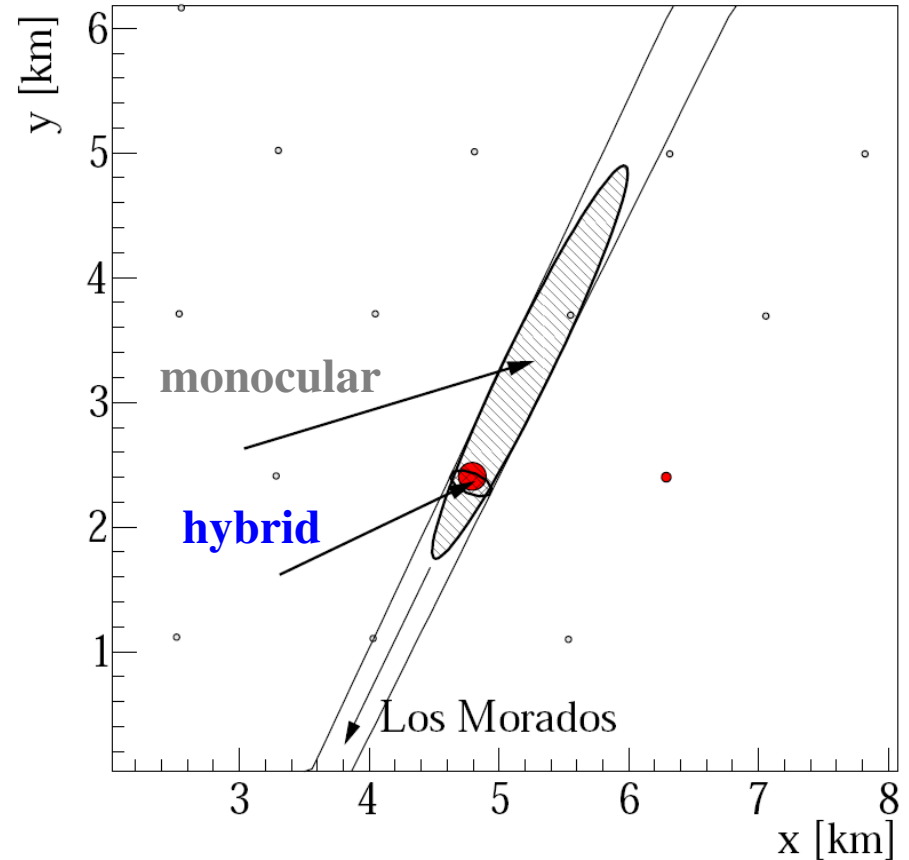


- Shower axis from the time-sequence of triggered FD pixels plus the information from the “hottest” SD station

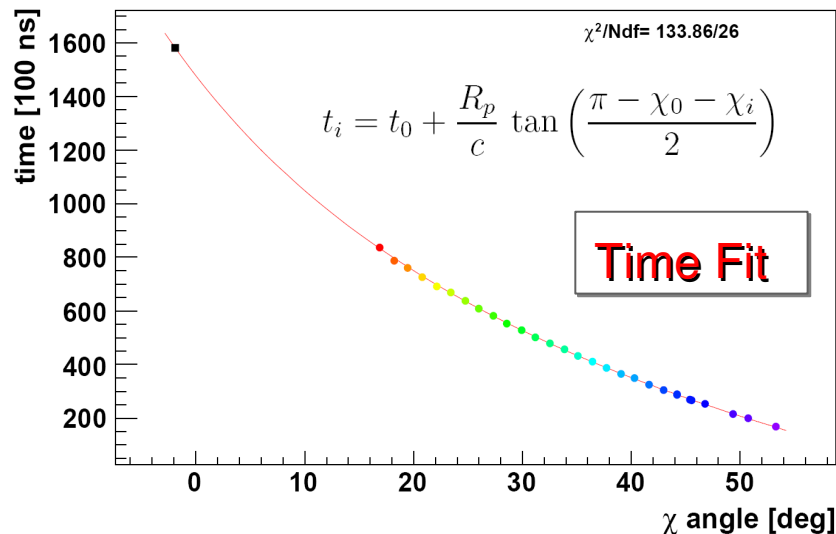
FD-Hybrid geometry reconstruction



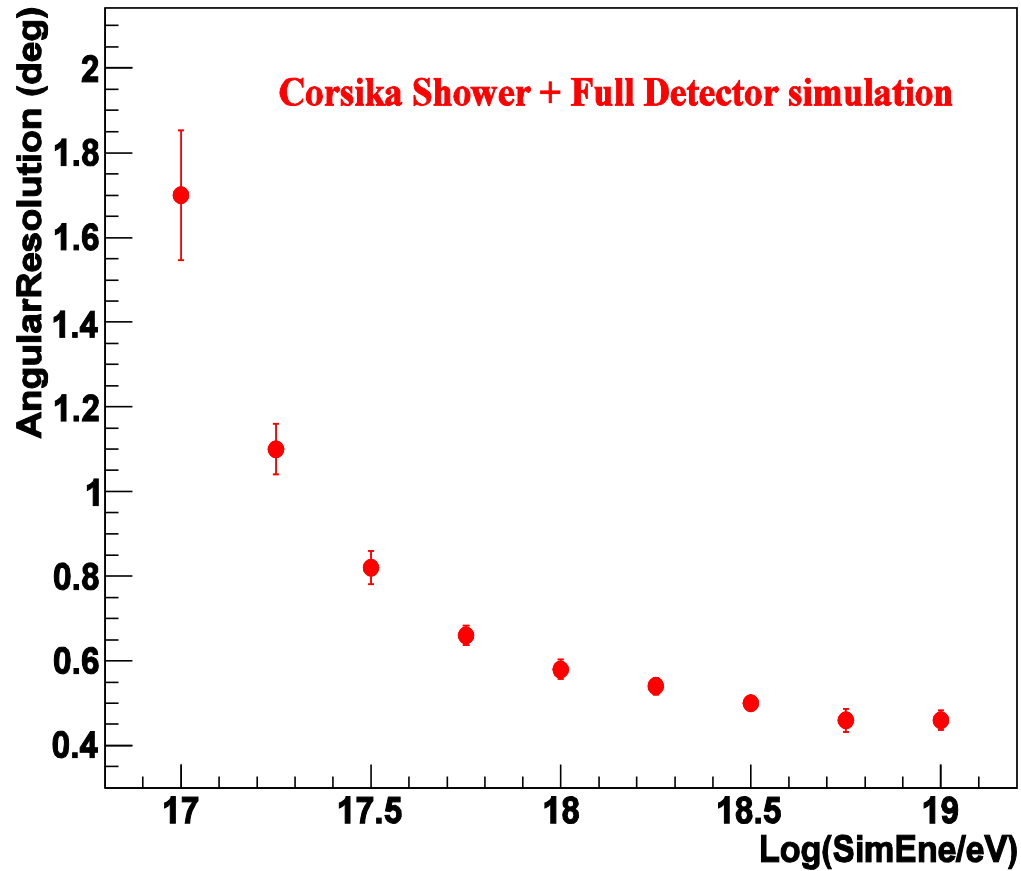
Shower-Detector Plane (SDP) using the directions of the triggered pixels



Hybrid angular resolution $\sim 0.6^\circ$
Core resolution about 50 meters



Hybrid Angular resolution



Angular Resolution:

the angular radius that contains 68% of the showers coming from a given point source

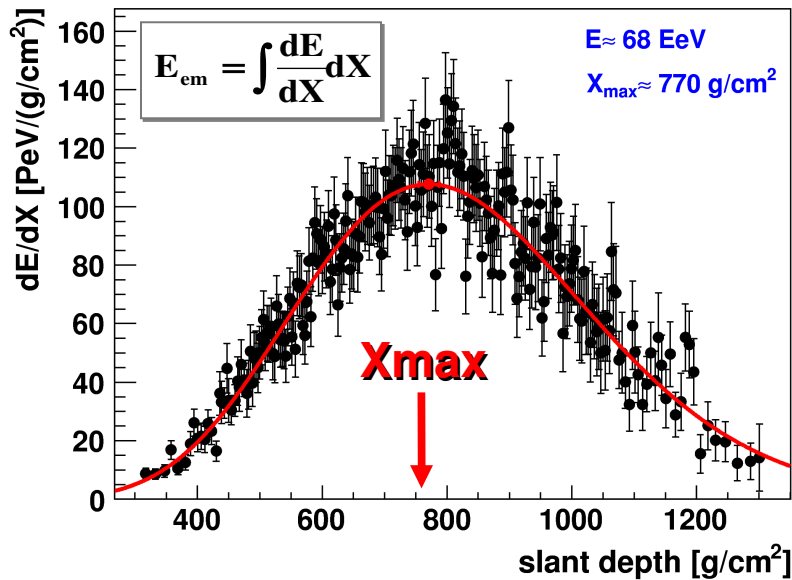
Hybrid angular resolution from simulation

$E \sim 10^{18}$ eV AR $\sim 0.8^\circ$ ($\theta < 60^\circ$)

$E > 10^{19}$ eV AR $\sim 0.5^\circ$ ($\theta < 60^\circ$)

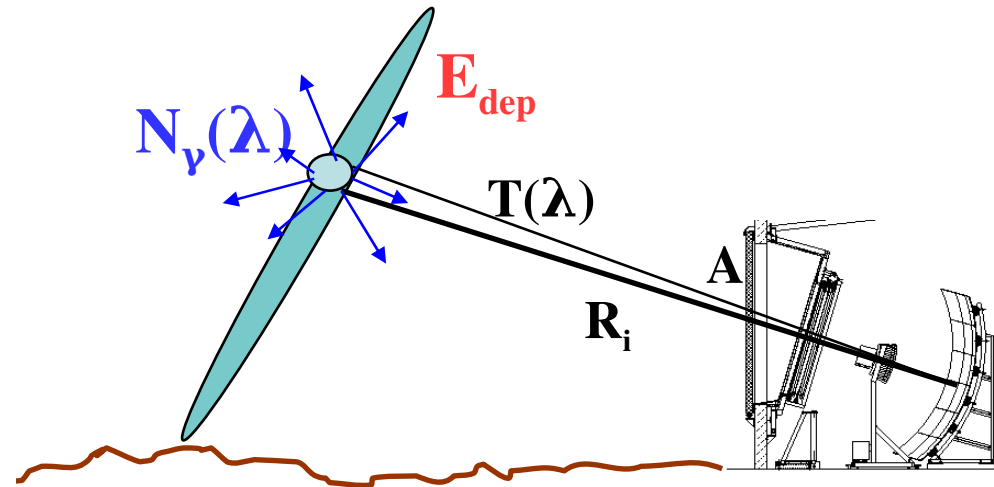
FD: energy determination

Longitudinal Profile



Energy “Calorimetric measurement”

Almost model independent



Fluorescence yield
 (from laboratory
 measurements)

Geometry

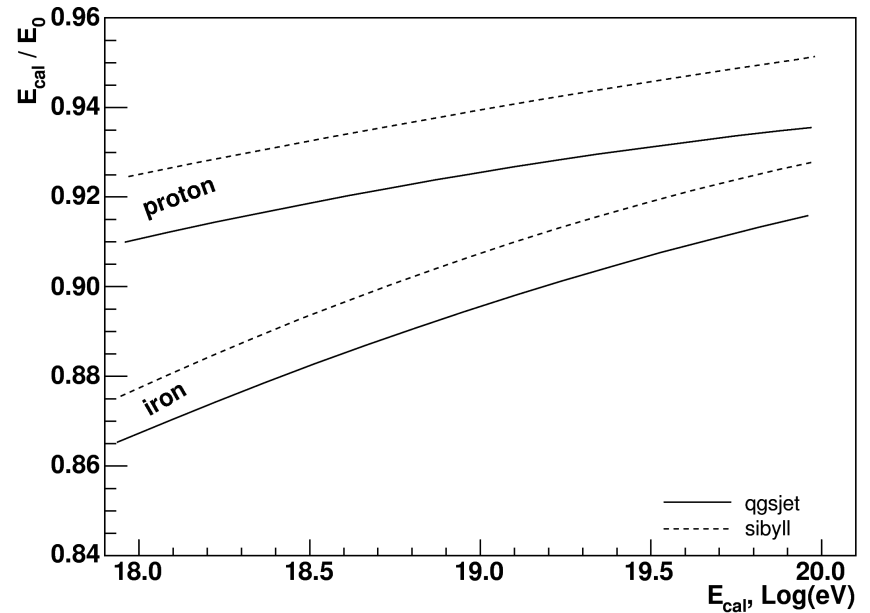
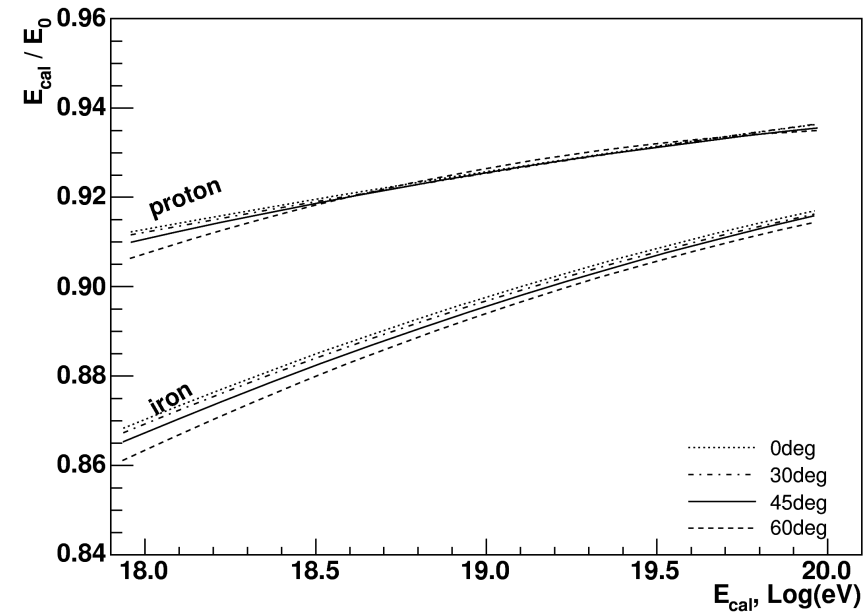
$$\frac{A}{R_i^2}$$

Atmosphere

$$T(\lambda)$$

Detector
 calibration

FD: the invisible energy



The “invisible” energy carried away mainly by muons and neutrinos has to be taken into account to reconstruct the primary energy

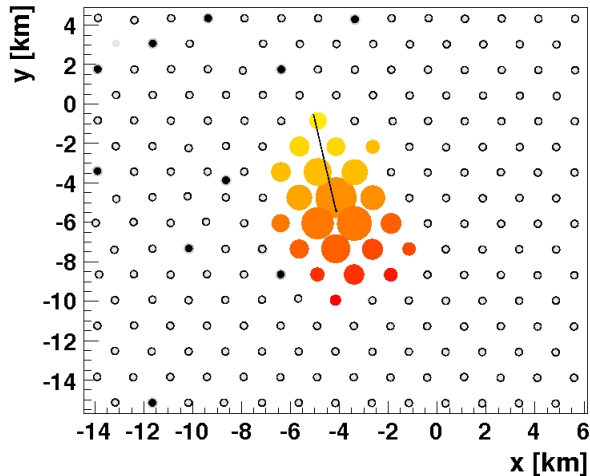
$$E_{FD} = (1 + f_{inv}) E_{cal}$$

This correction is mass and model dependent

SD reconstruction

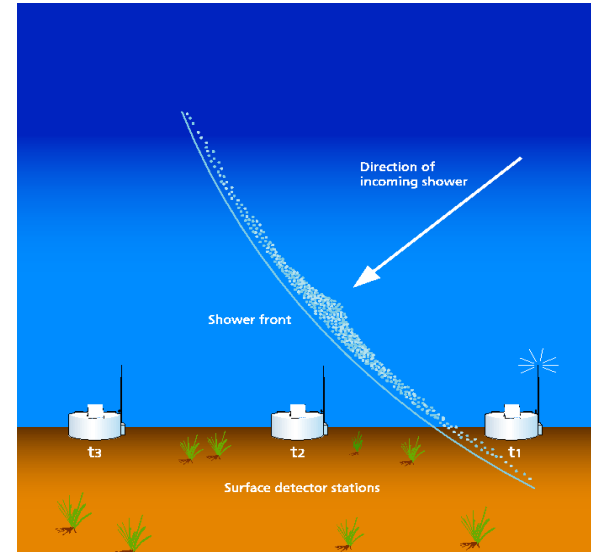
Direction:

fit to arrival times sequence of particles in shower front



Angular resolution

$E > 10^{18}$ eV, ~ 3 stations, $< 2^\circ$
 $E > 10^{19}$ eV, ~ 6 stations, $< 1^\circ$



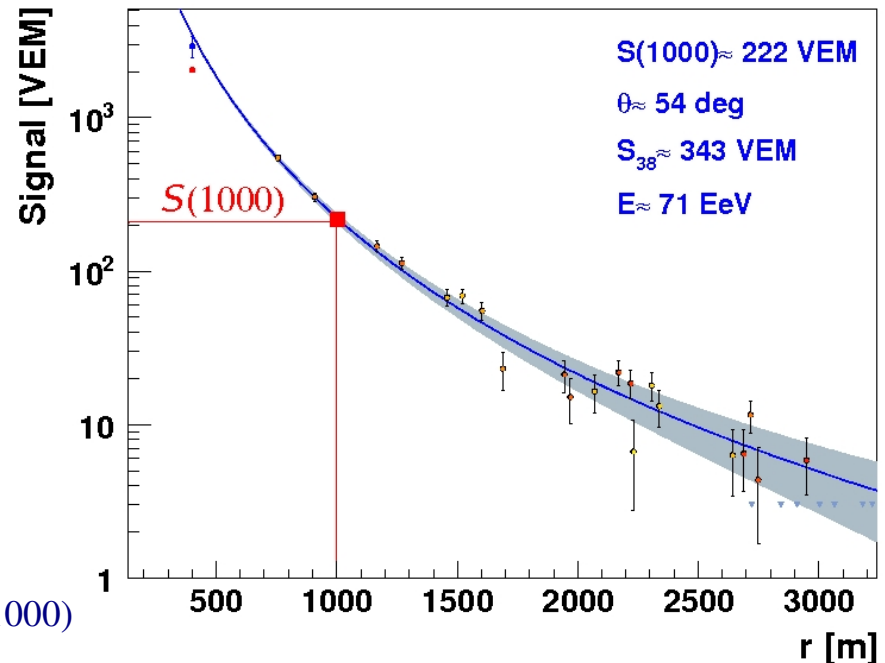
Determination of the arrival direction with χ^2 -method

Determination of the lateral particle density function and LDF with a Likelihood method to fit a NKG-type function

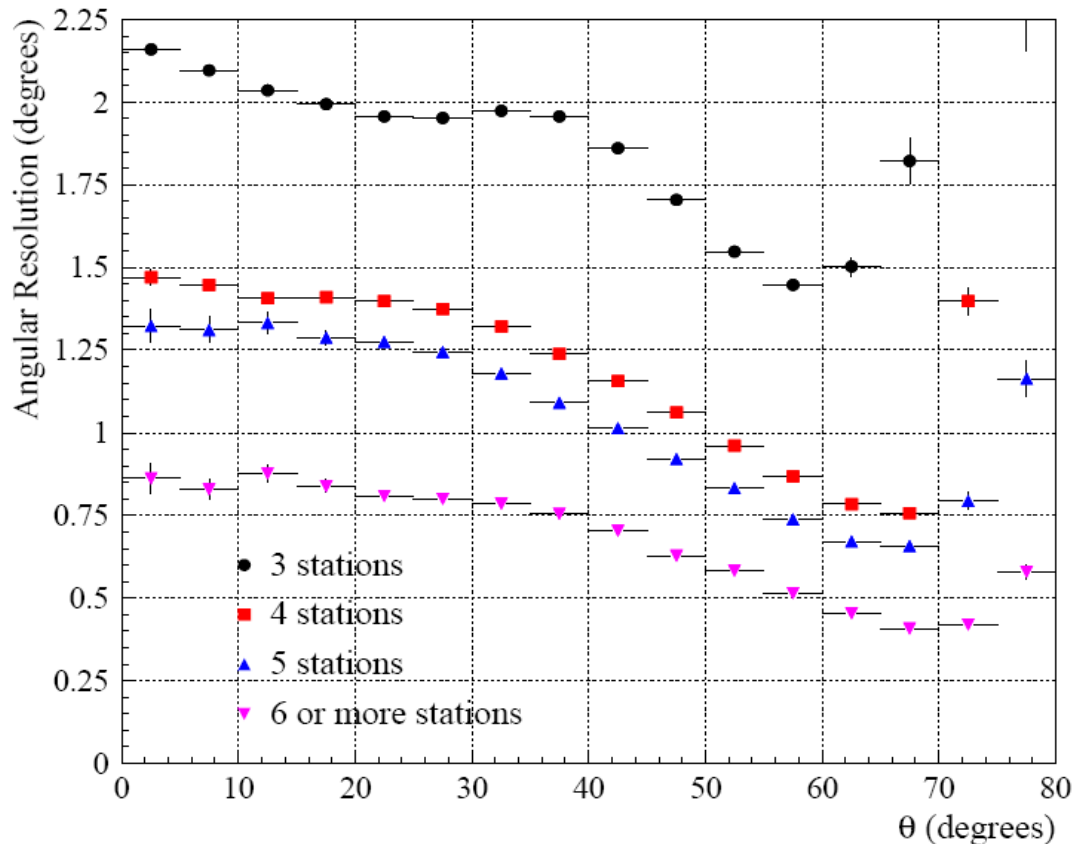
$$S(r) = S(1000) \left(\frac{r}{1000}\right)^{-\beta} \left(\frac{r+700}{1700}\right)^{-\beta}$$

Free parameters: core position and signal at 1000 m, $S(1000)$

β is parameterized as a function of shower zenith angle and $S(1000)$



Angular resolution with SD



Using the time variance model
 Astropart. Phys. 28 (2008) 523

$$F(\eta) = 1/2 (V[\theta] + \sin^2(\theta) V[\phi])$$

$V[\theta, \phi]$ = variances

η = space angle between true and reconstructed angle

$$AR = \sqrt{-2 \ln(0.32) F(\eta)}$$

SD angular resolution from data

3-fold $E < 4 \cdot 10^{18}$ eV $AR < 2.2^\circ$ ($\theta < 60^\circ$)

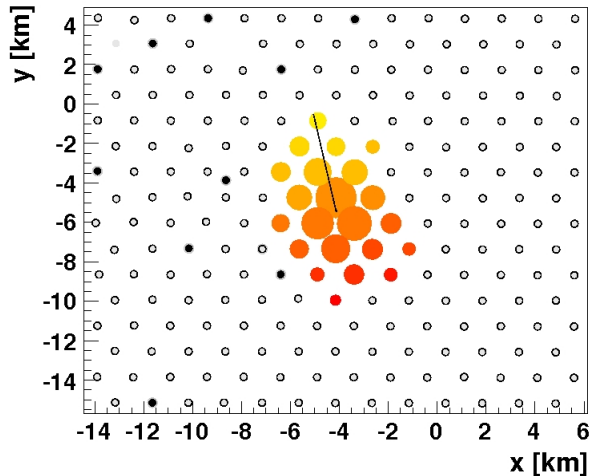
4/5-fold $3 \cdot 10^{18} < E < 10^{19}$ eV $AR < 1.5^\circ$ ($\theta < 60^\circ$)

More fold $E > 10^{19}$ eV $AR < 1^\circ$ ($\theta < 60^\circ$)

SD reconstruction

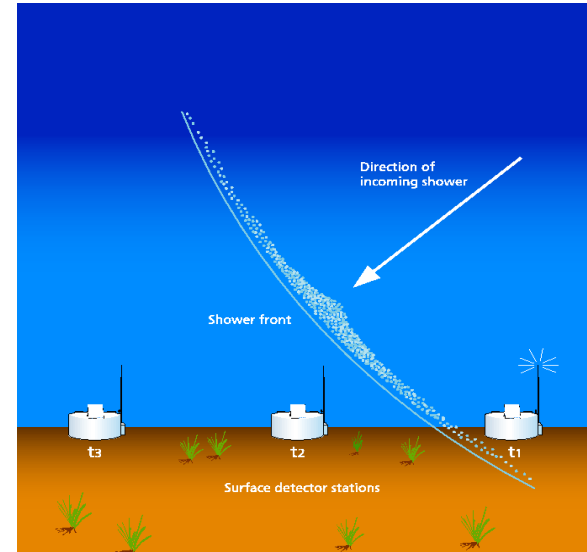
Direction:

fit to arrival times sequence of particles in shower front



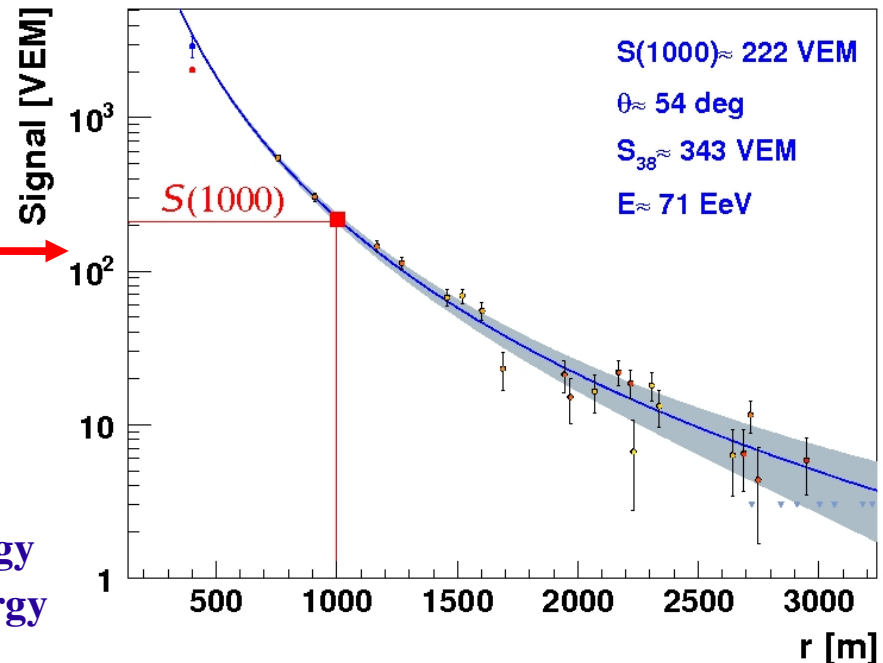
Angular resolution

$E > 10^{18}$ eV, ~ 3 stations, $< 2^\circ$
 $E > 10^{19}$ eV, ~ 6 stations, $< 1^\circ$



Energy estimator: S(1000)

particle density at 1000 m from shower axis

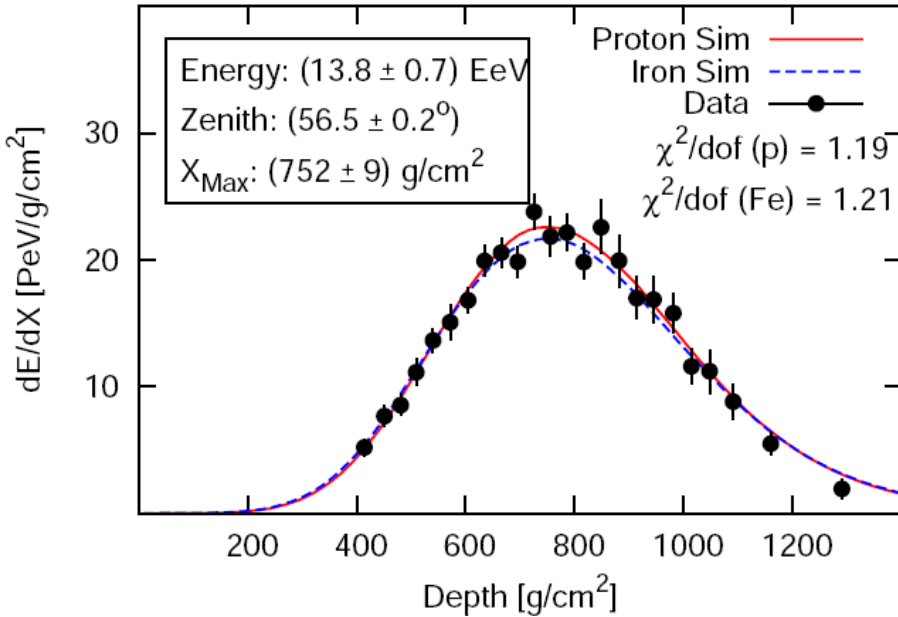


Systematic uncertainties on energy determination

- 30% from hadronic interaction models at high energy
- 10-20% from hadronic interaction model at low energy

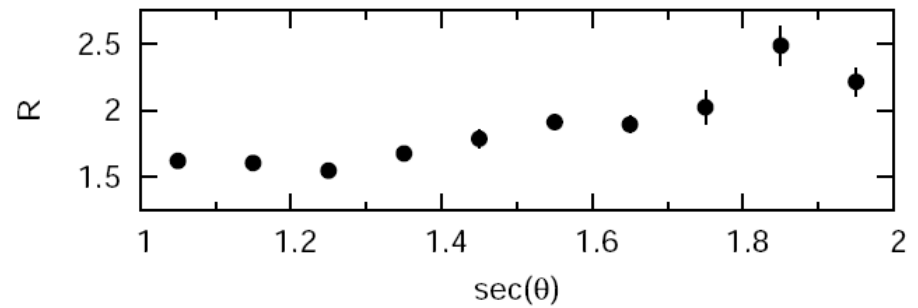
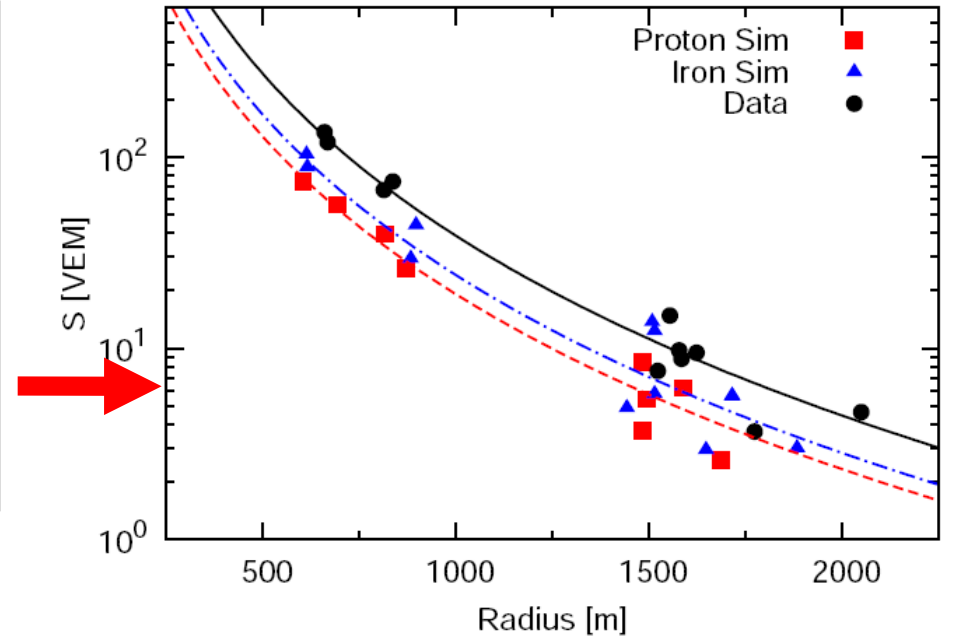
Muon puzzle....

J.Allen @ ICRC 2011

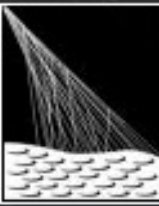


More muons in data than in simulation!

Not easy to reproduce with models these measurements



SD energy based on LDF systematically overestimated w.r.t. FD



Tecniche di misura con l'Osservatorio Pierre Auger

Lorenzo Perrone

Università del Salento e INFN Lecce (Italy)

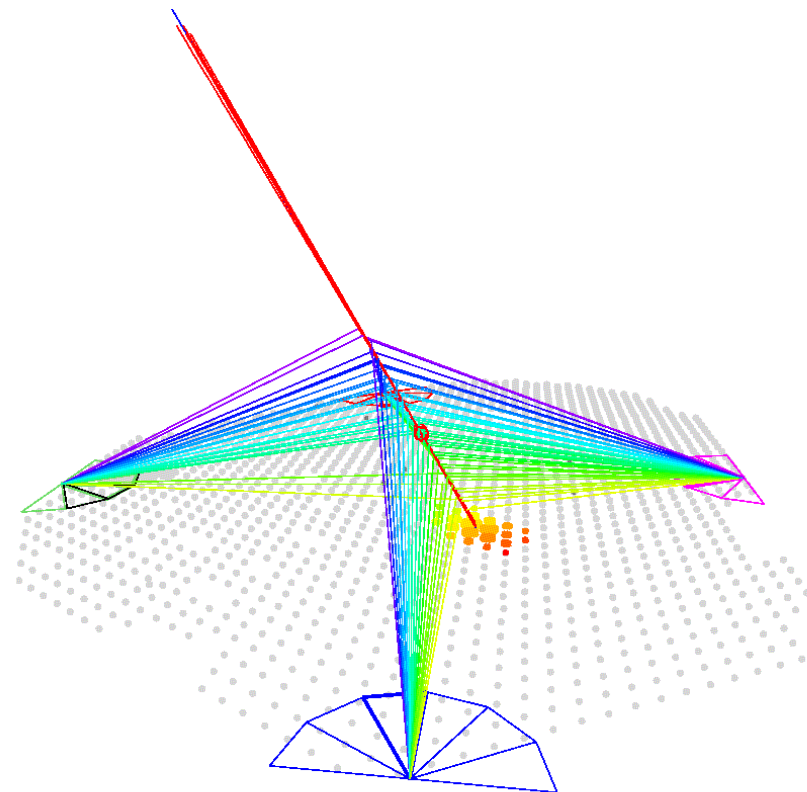
Outline

Physics goals and operation range

Detector description

Performance and observables

- Results
- Enhancements



Study of the transition between galactic and extra-galactic cosmic rays

- Ankle region

- 2nd Knee region (with lower energies extensions)

End of the spectrum (GZK region)

Energy spectrum

Arrival directions

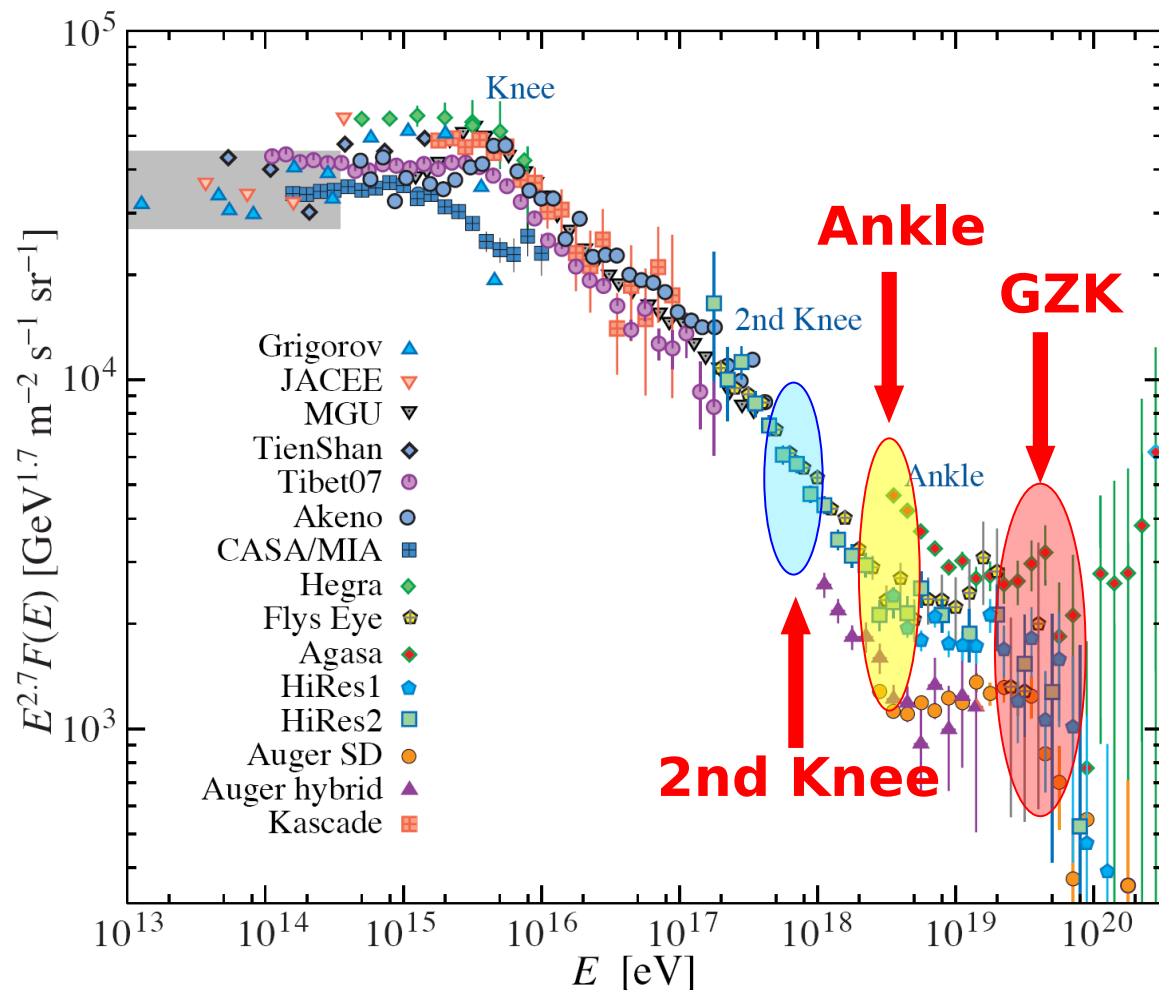
Composition

Search for photon and neutrinos as primary cosmic rays

Hadronic physics



The physics case



Particle Data Group

The Pierre Auger Observatory

- *Surface detector*

an array of 1600 Cherenkov stations on a 1.5 km hexagonal grid ($\sim 3000 \text{ km}^2$)

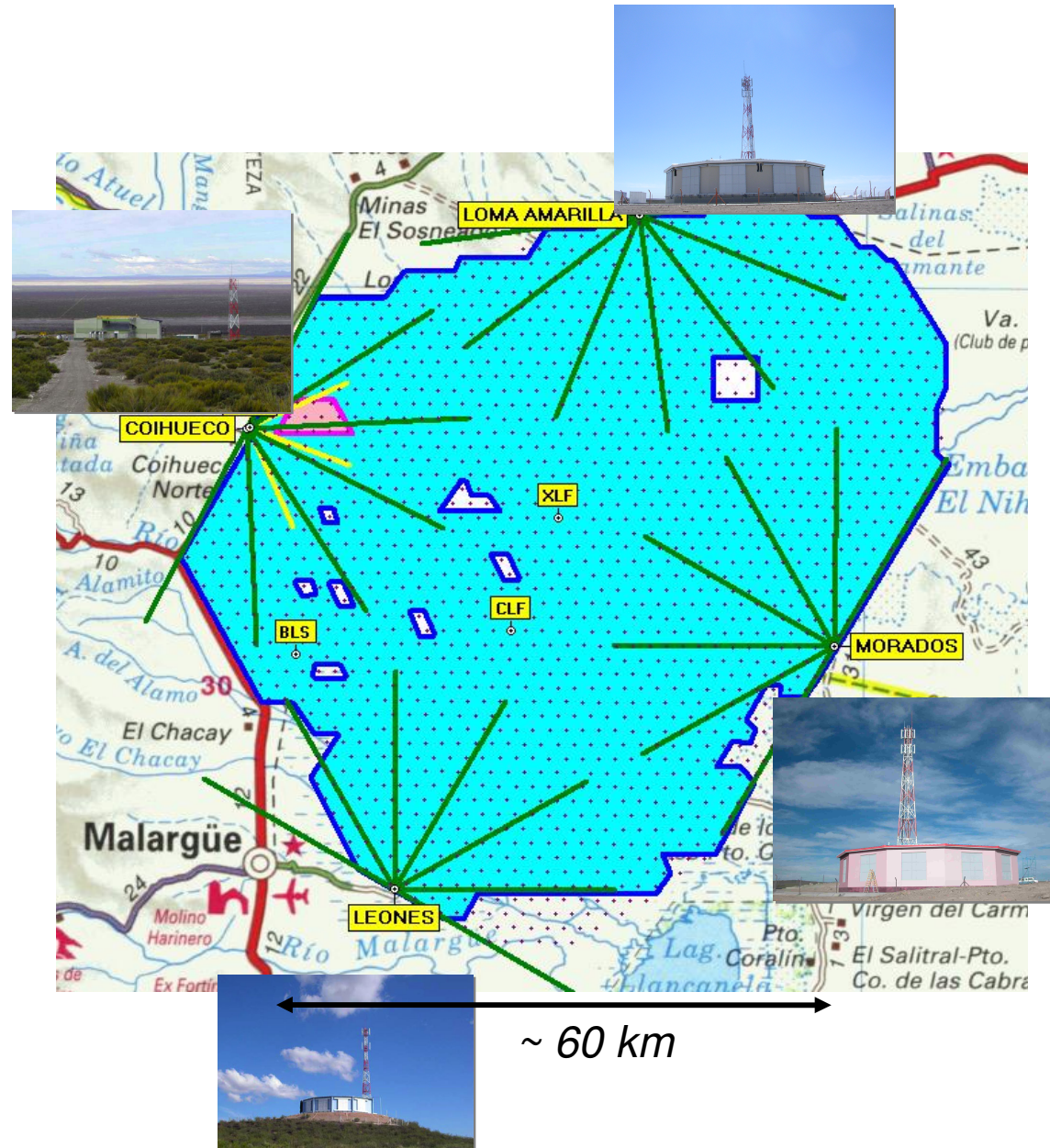
- *Fluorescence detector*

4 buildings overlooking the array

Low energy extensions

AMIGA: dense array plus muon detectors

HEAT: three further high elevation FD telescopes



The Hybrid Concept

Surface Detector Array

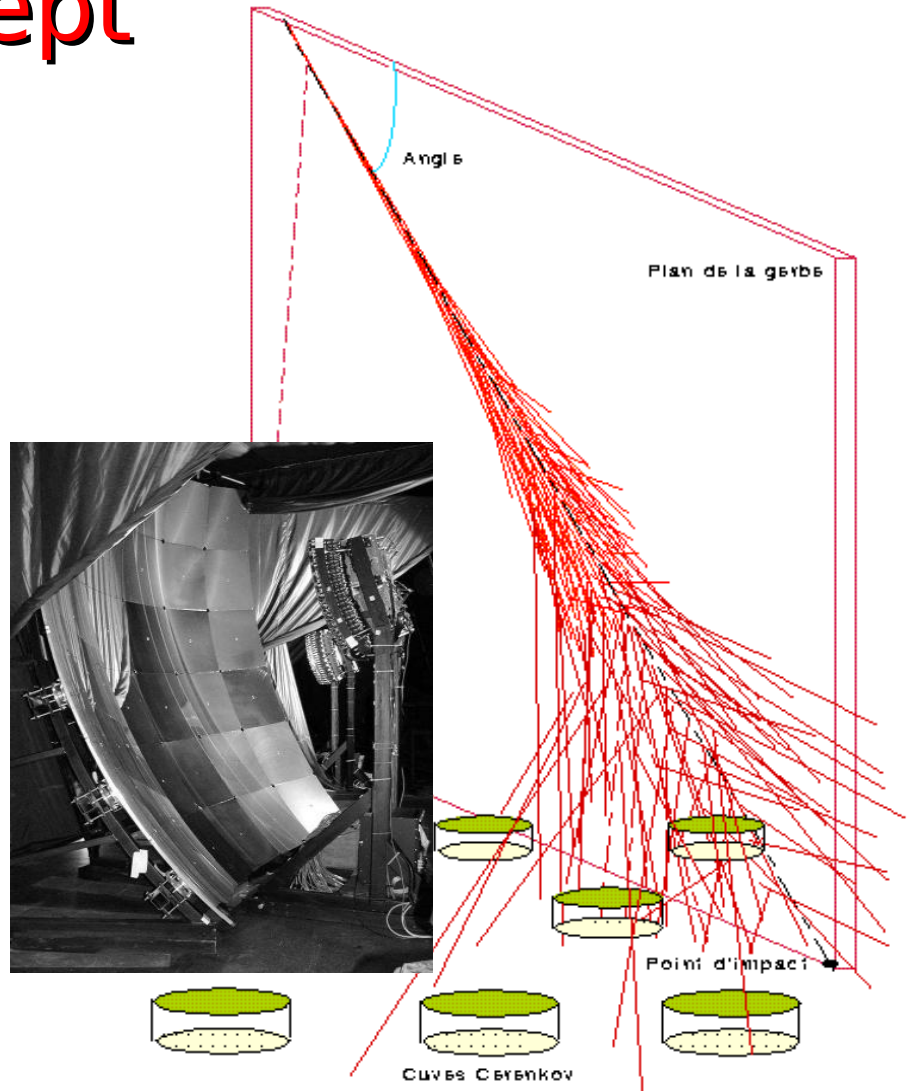
lateral distribution, 100% duty cycle

Air Fluorescence Detectors

Longitudinal profile, calorimetric energy measurement, ~15% duty cycle

accurate energy and direction measurement

mass composition studies in a complementary way



“In order to make further progress, particularly in the field of cosmic rays, it will be necessary to apply all our resources and apparatus simultaneously and side-by-side.”

V.H.Hess, Nobel Lecture, December 1936

FD-SD-Hybrid

	SD-only	FD-only	Hybrid
Duty-cycle	~100% (high stat)	~10-15%	~10-15%
Angular Res.	1-2 deg	~3 deg	~ 0.5 deg (>1 EeV)
Energy	relies on MC and composition	missing energy geometry bias	missing energy
Energy Range	~>10 ^{18.5} eV	~>10 ^{17,5} eV	~>10 ¹⁸ eV

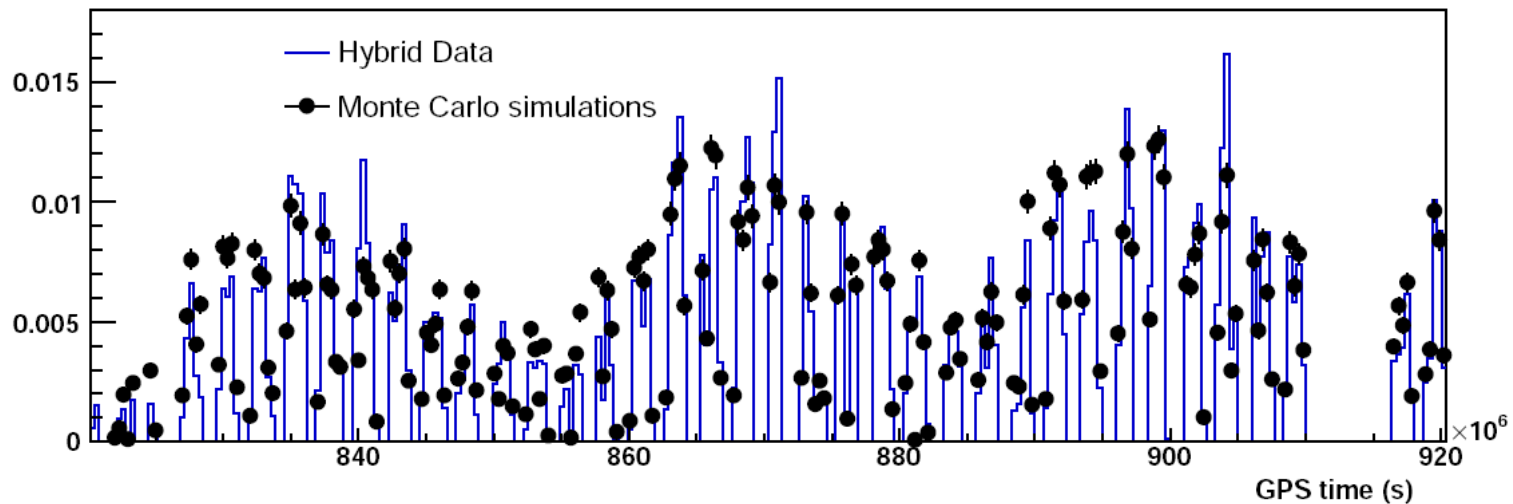
Results

- **Energy spectrum (Hybrid, SD, Combined)**
- Mass composition
- Hadronic interactions
- Search for photons and neutrinos
- Astrophysics

Hybrid Exposure

$$\mathcal{E}(E) = \int_T \int_{\Omega} \int_{A_{gen}} \varepsilon(E, t, \theta, \phi, x, y) \cos \theta \, dS \, d\Omega \, dt$$

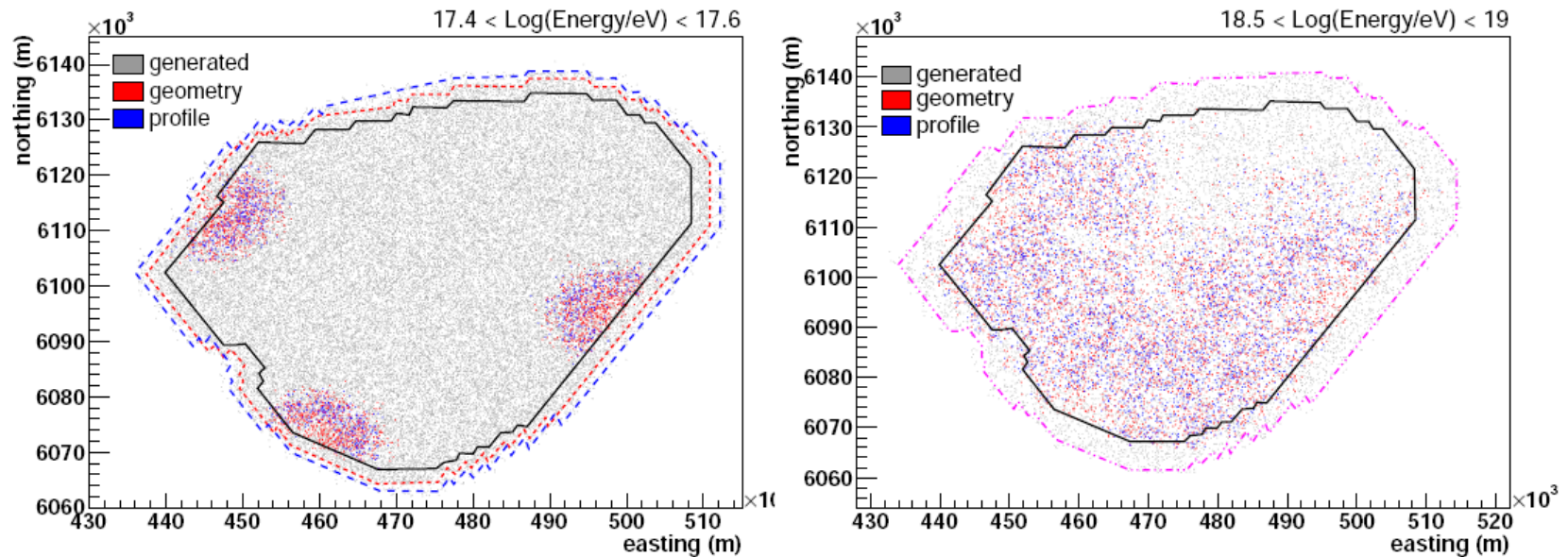
Time dependent simulations



FD on-time and SD stations status reproduced according to the actual data taking conditions along the considered time window

Efficiency

Simulations taking into account the FD and SD detector status plus the atmospheric conditions



Example: time period with only 3 FD sites, two different energy ranges

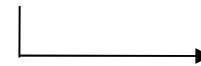
Hybrid Exposure

First Method : Conex profiles + LTPs (large statistics, no signal in the stations)

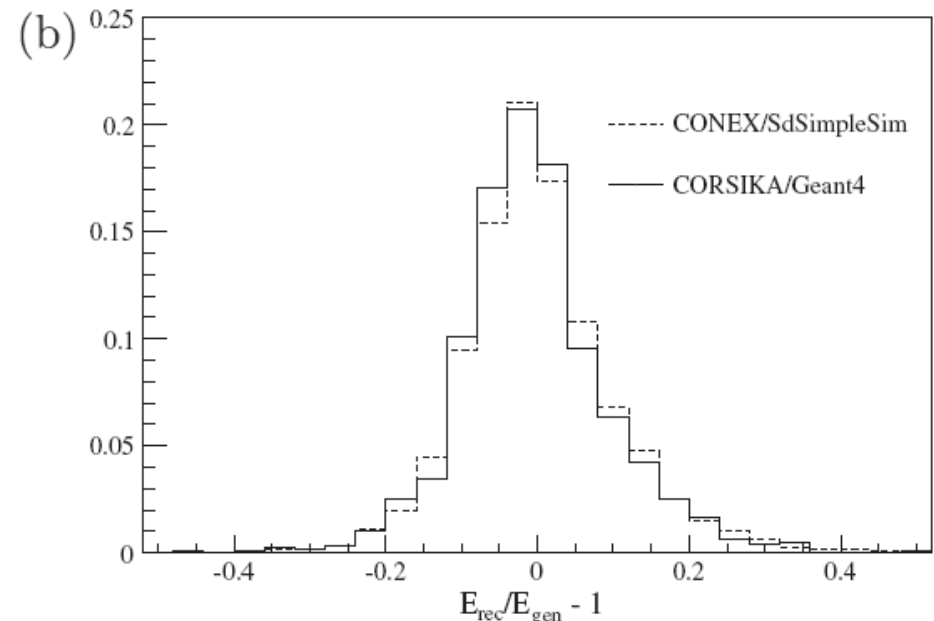
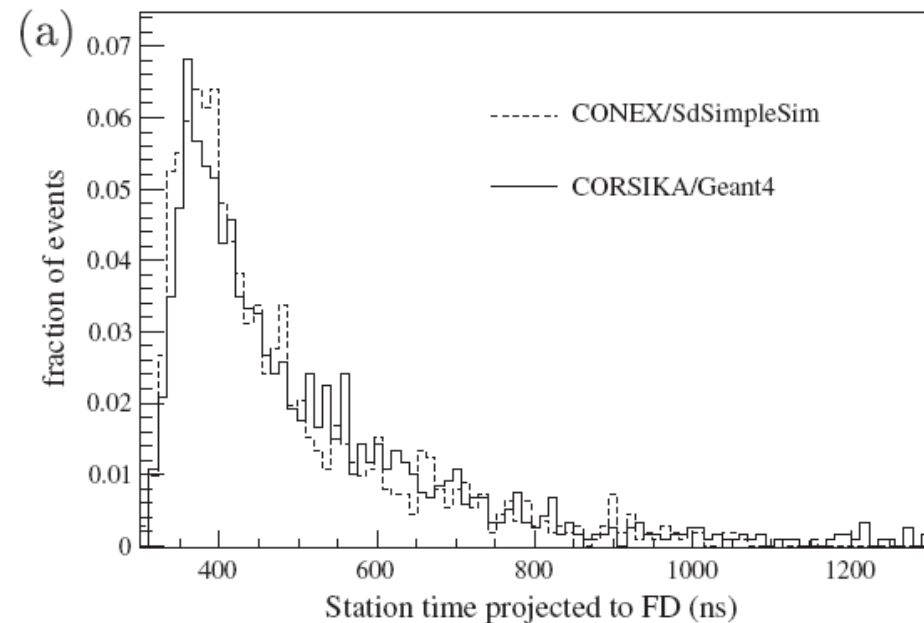
Longitudinal profile plus a parametrized station trigger response

Second Method : Corsika+Geant4 (less statistics, signal in the stations)

First method validated with the second

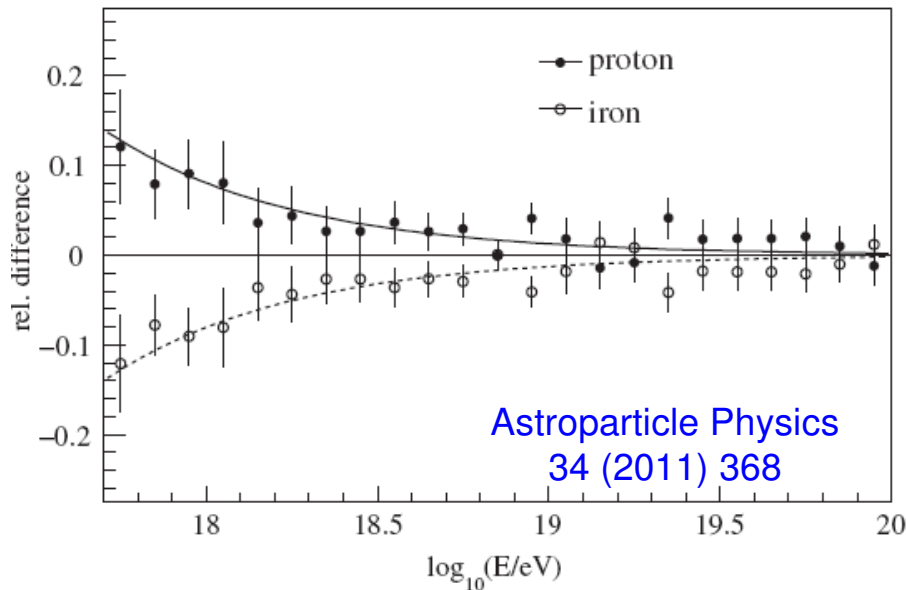


Astroparticle Physics
34 (2011) 368

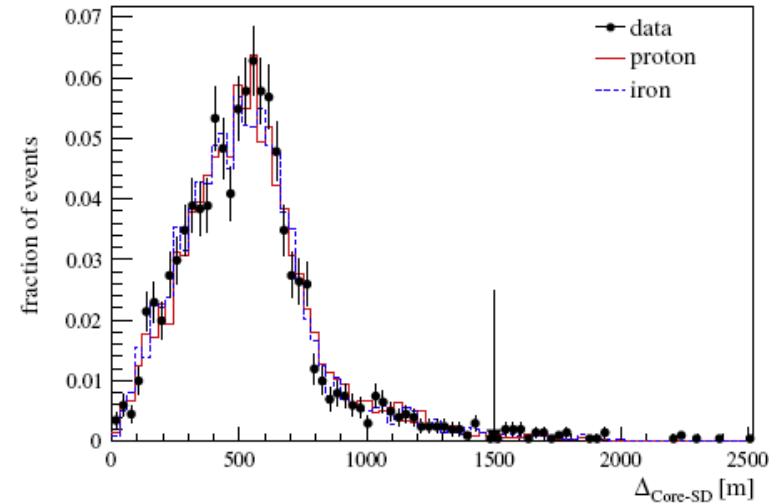


Hybrid Exposure

Weak dependence on primary mass above 1 EeV



Full agreement Data-MC

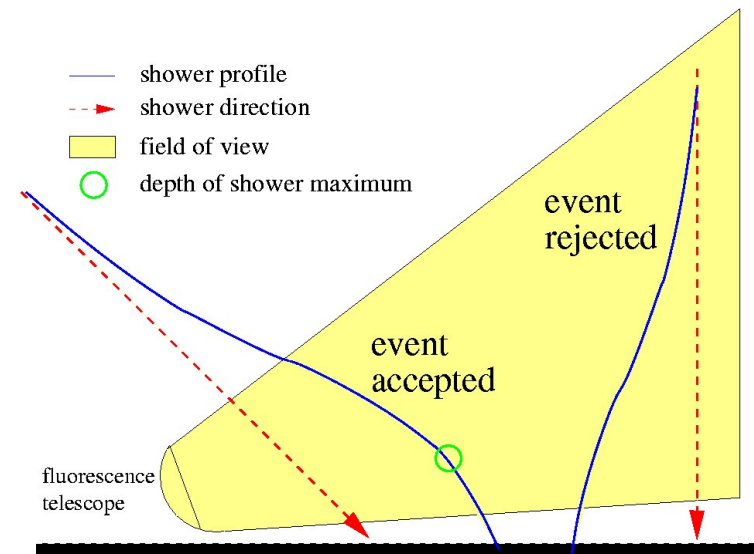


Quality cut

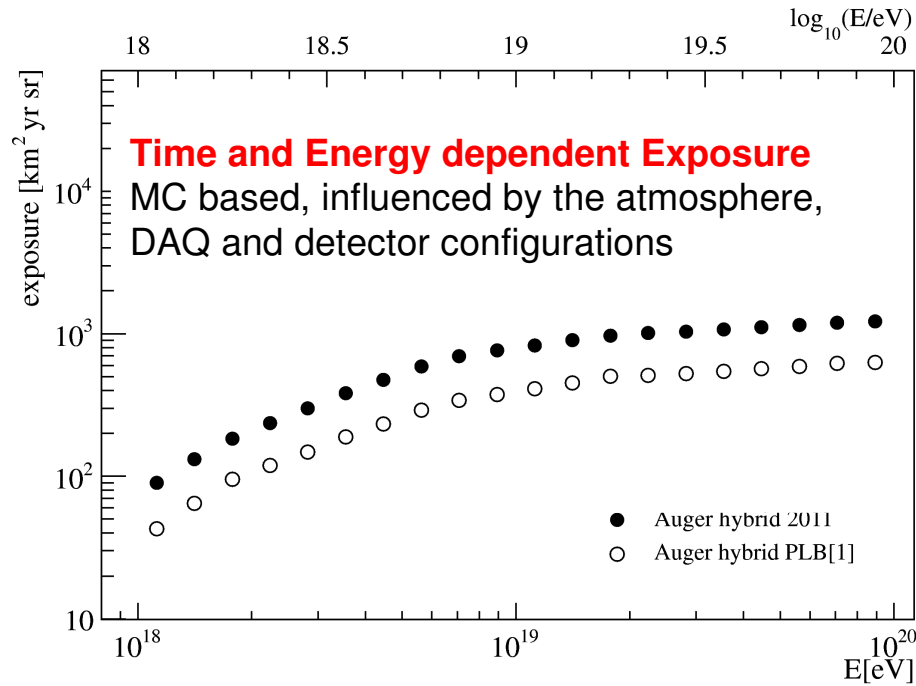
Fiducial cut

equal detection probability for all primaries

limited FD-site to shower axis distance to make the analysis robust against an energy shift within systematics



Hybrid Spectrum

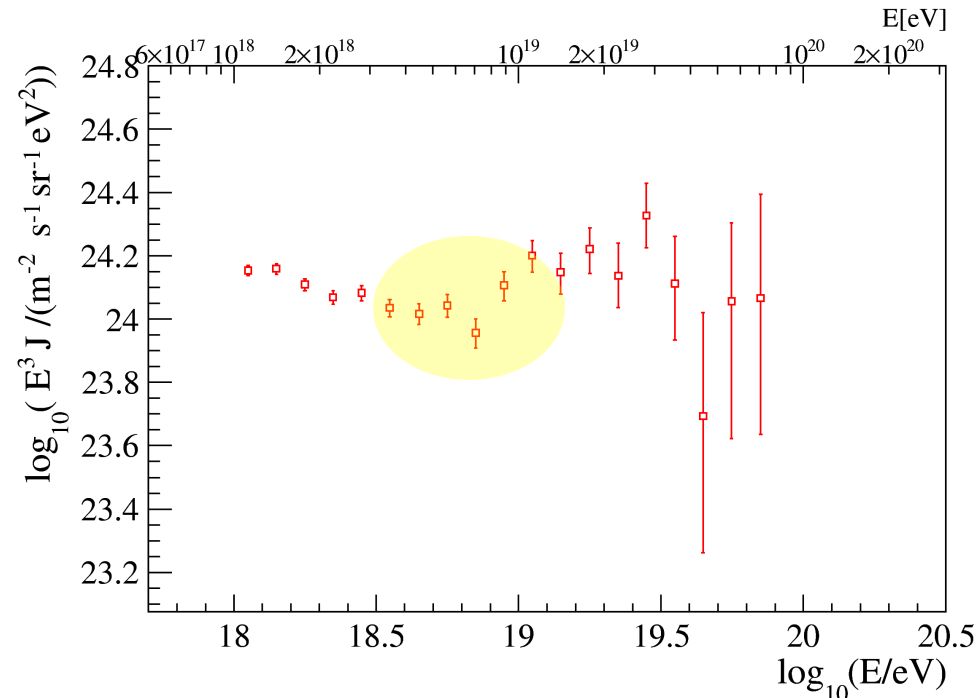


Data: Nov. 2005 – Sept. 2010

Systematic uncertainty on exposure
10% (6%) **E ~ 10¹⁸ eV** (>10¹⁹ eV)

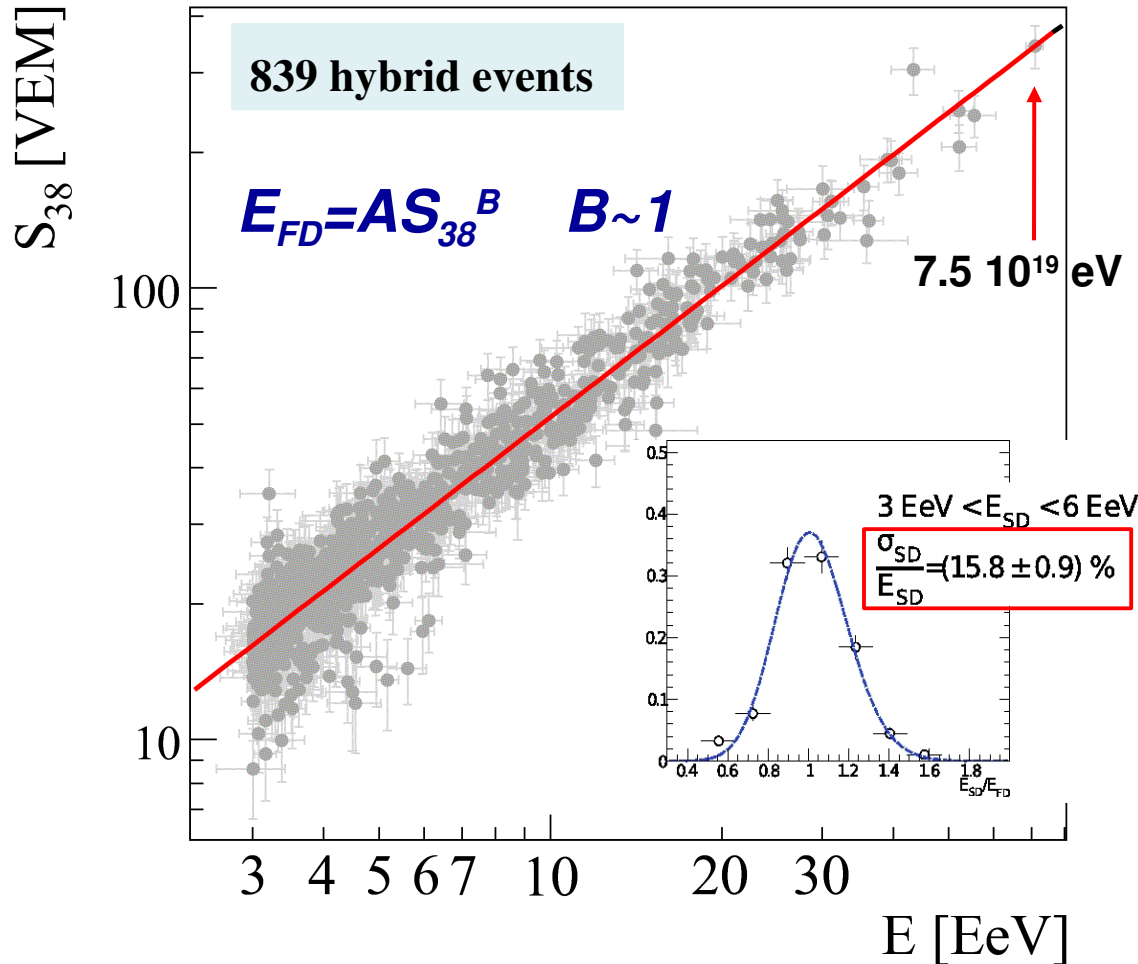
Clear indication of the *ankle*

- + Full efficiency at 10¹⁸ eV (ankle region)
- + Calorimetric measurement
- + Energy Resolution of 8%
- Limited duty cycle (~13%)



Energy calibration

R.Pesce @ ICRC 2011



Jan 2004 – Sept 2010
 $E > 3 \text{ EeV}$ - zenith $< 60^\circ$

Using hybrid events, the SD energy estimator is calibrated without relying on Monte Carlo

Method Systematic Uncertainties

7% a 10^{19} eV

15% a 10^{20} eV

FD Energy Systematics

- fluorescence yield 14%
- FD absolute calibration 9.5%
- invisible energy 4%
- reconstruction 10%
- atmospheric effects 8%

TOTAL: 22%

S_{38} -> S_{1000} that a shower would have produced had it arrived with a zenith angle of 38°

The attenuation curve

R.Pesce @ ICRC 2011

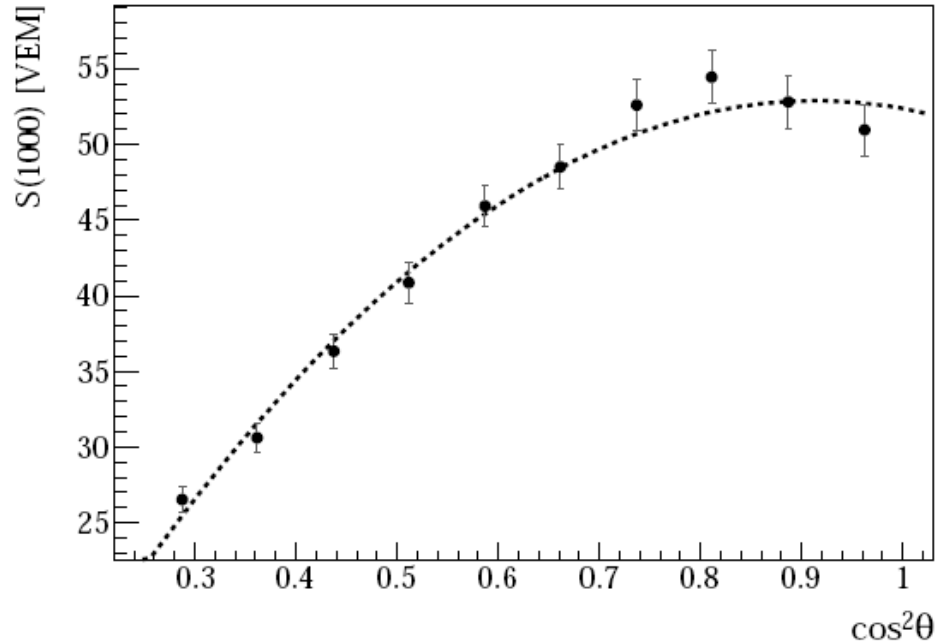
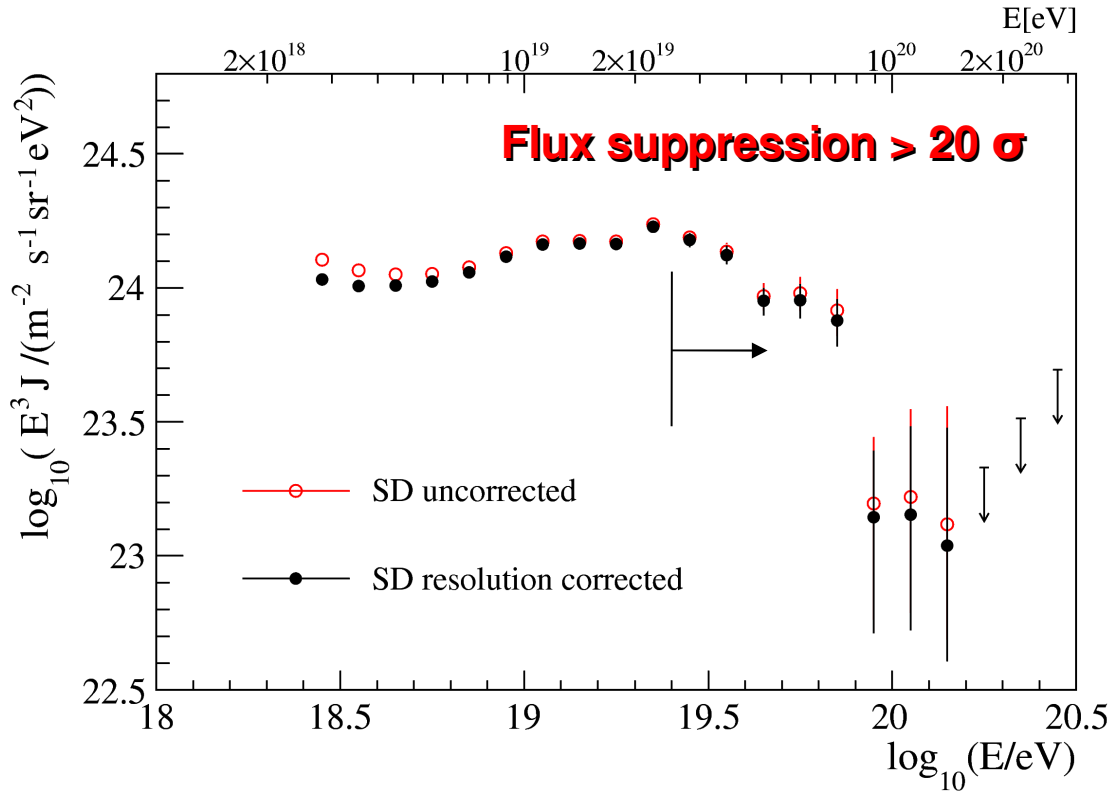


Figure 1: Attenuation curve, $CIC(\theta)$ fitted with a second degree polynomial in $x = \cos^2 \theta - \cos^2 \bar{\theta}$.

$$S_{38} \equiv S(1000)/CIC(\theta)$$

SD Energy spectrum



SD Exposure

$E > 3 \text{ EeV}$ and zenith $< 60^\circ$

- 20905 km² sr yr (Jan 04 - Dec 10)
- geometrical, counting active hexagons. Not relying on simulations, full efficiency
- independent of primary mass
- 3% systematic uncertainty

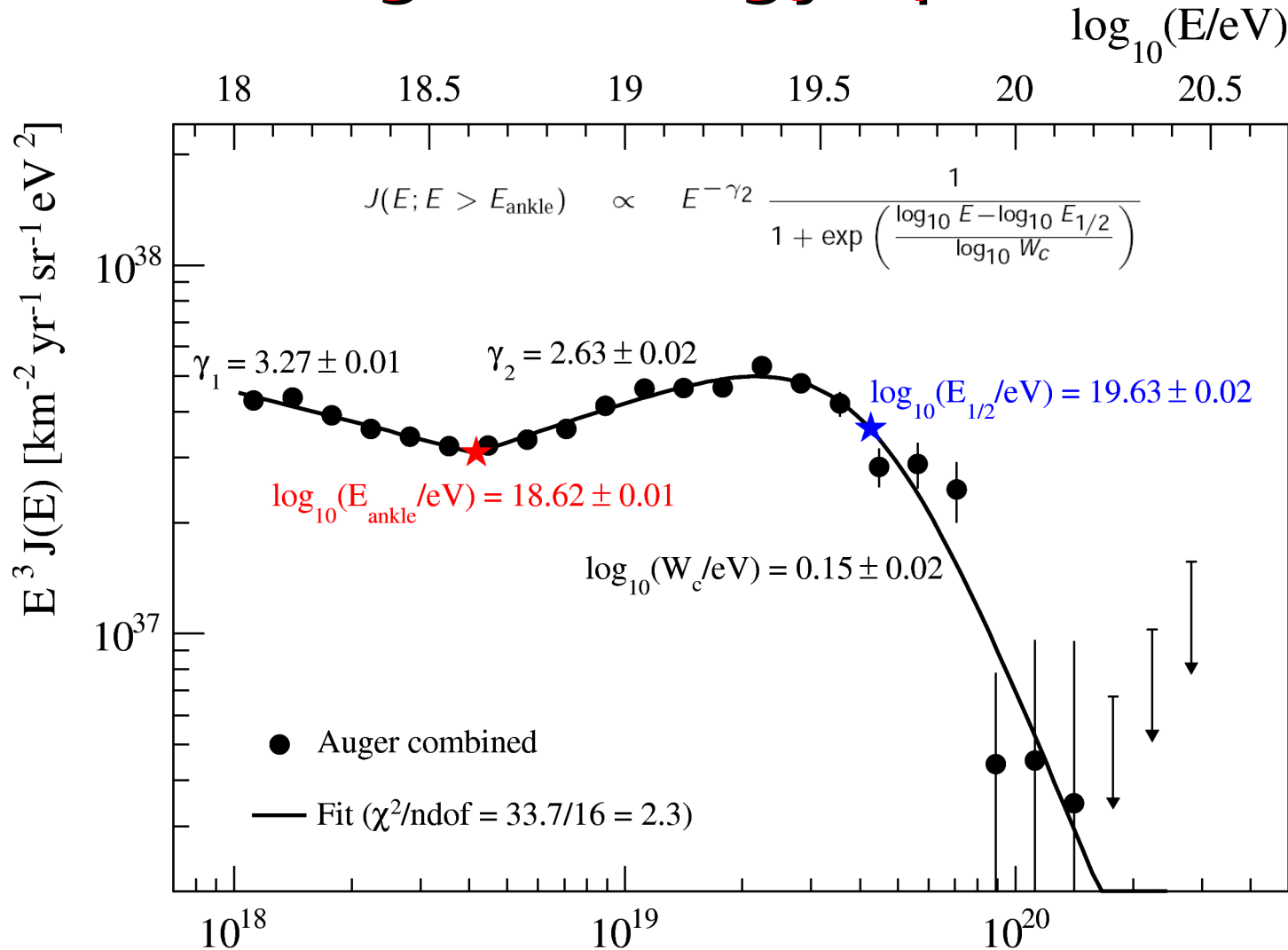
64000 (5000) events $E > 3 \cdot 10^{18} \text{ eV}$ ($> 10^{19} \text{ eV}$)

Energy scale from FD

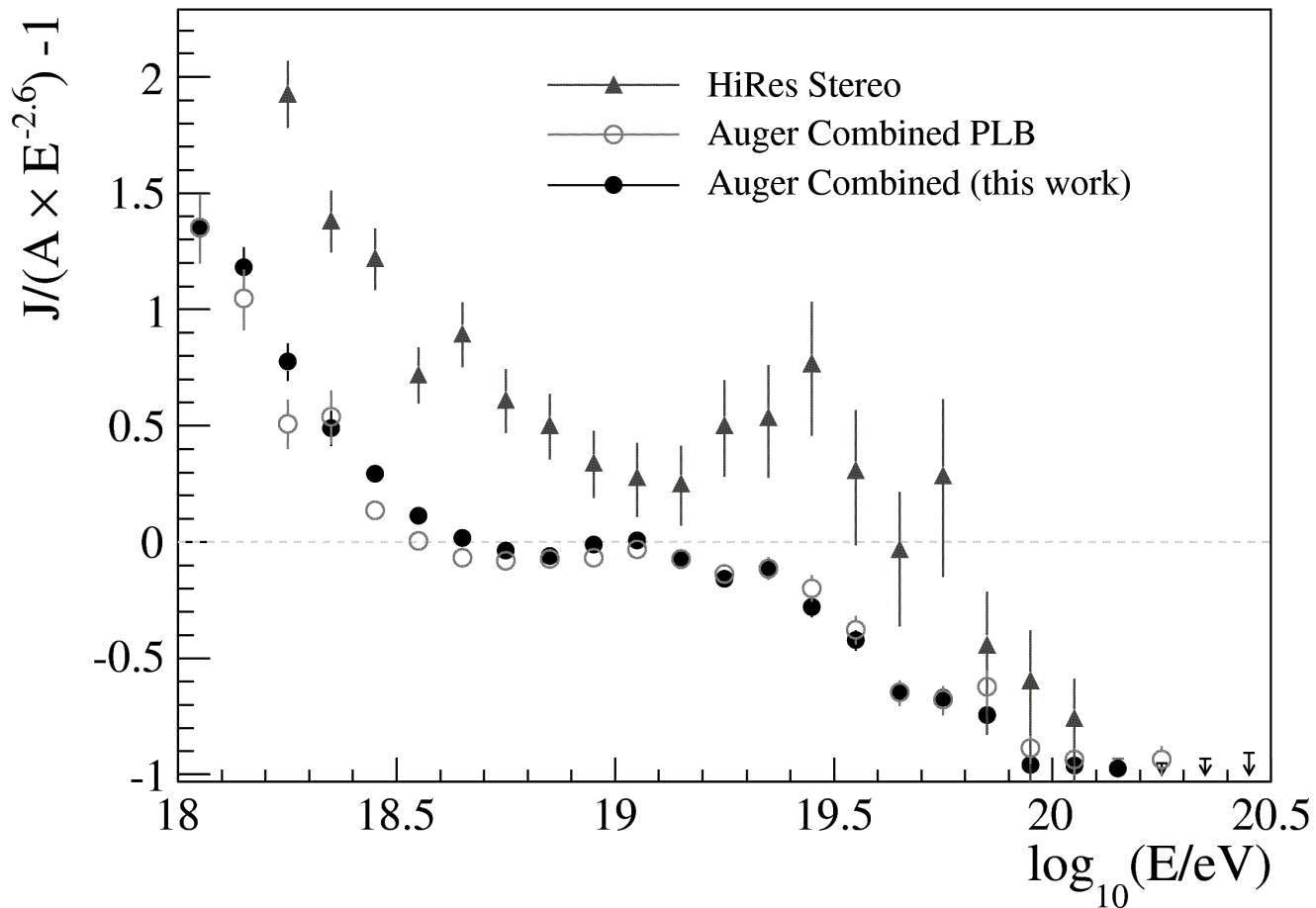
Energy resolution ~ 15%
forward folding method to correct
for the bin-to-bin migration

Total systematic uncertainty on flux ~ 6%
22% on the energy scale

The Auger Energy spectrum

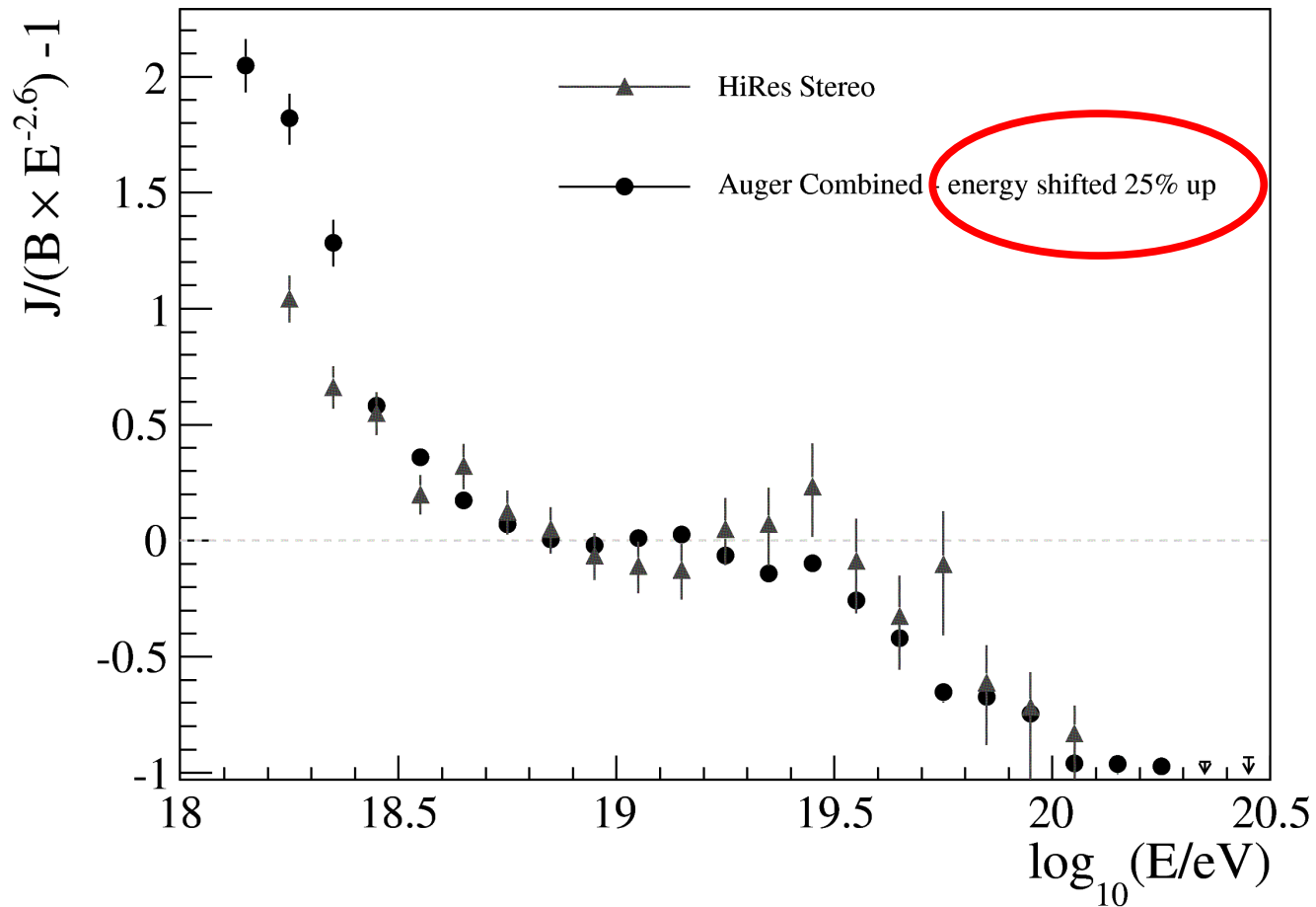


Energy spectrum: Auger vs HiRes



- Difference with respect to PLB 2010 due to changes of calibration curve
- Spectral features very well defined
- Compatible with HiRes within the energy scale systematic uncertainty

Energy spectrum: Auger vs HiRes



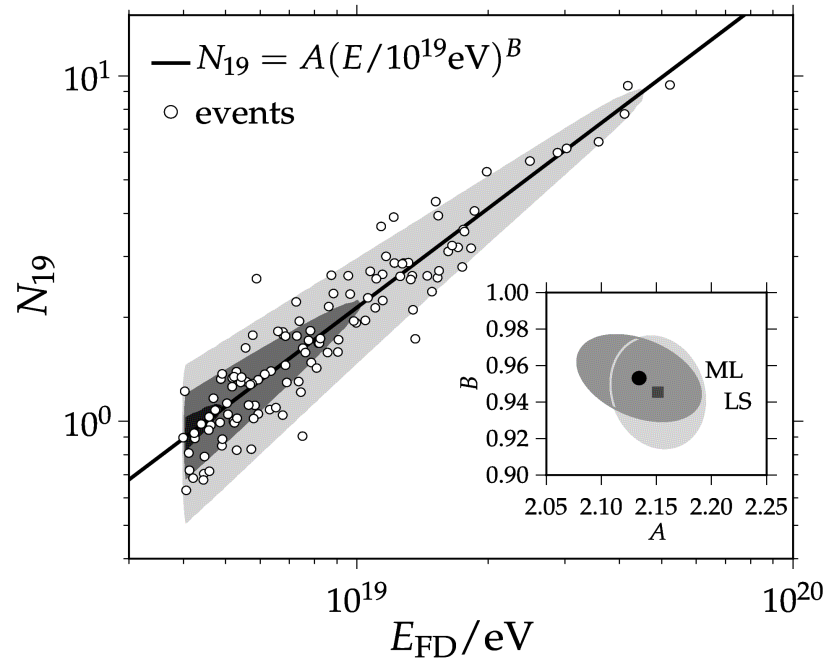
- Auger Energy Scale shifted of 25%
- Main spectrum features observed by both experiments

Spectrum with inclined events

Energy Calibration with FD energy

- Energy > $4 \cdot 10^{18}$ eV

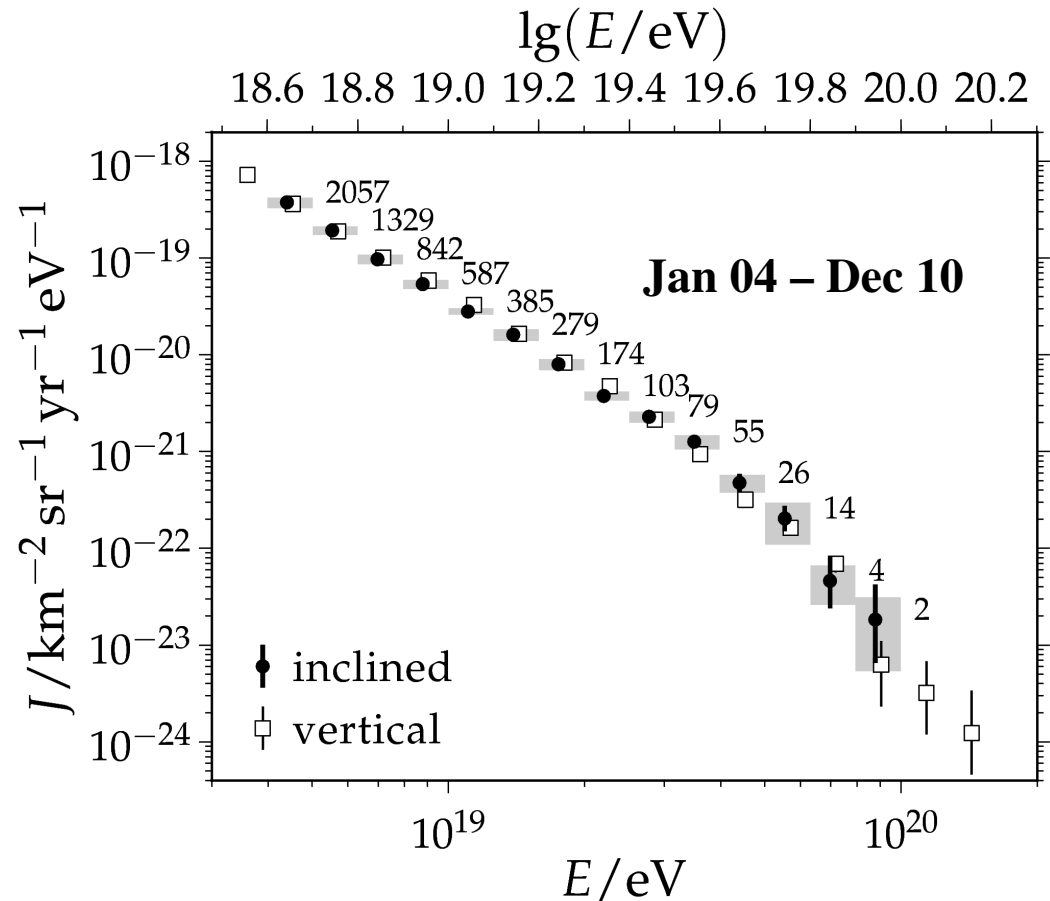
- $62^\circ < \text{Zenith} < 80^\circ$



Energy estimator:

N_{19} -> lateral muon density

**Full agreement with
flux from vertical showers**



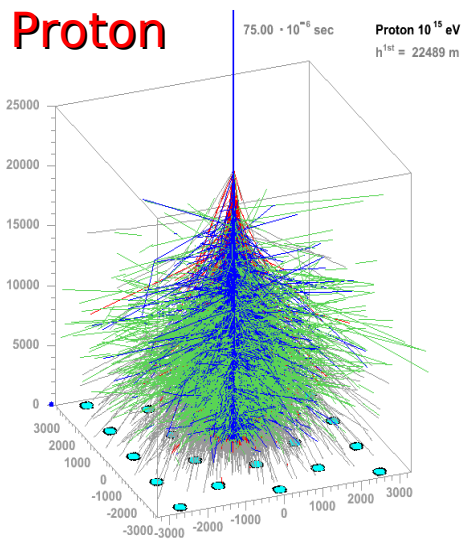
Results

- Energy spectrum
- **Mass composition**
- Hadronic interactions
- Search for photons and neutrinos
- Astrophysics

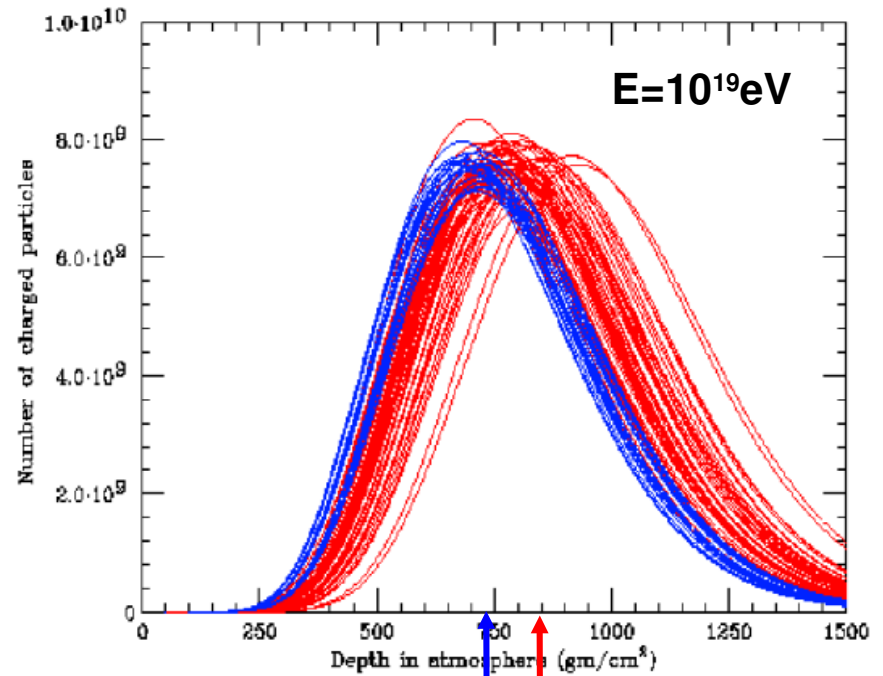
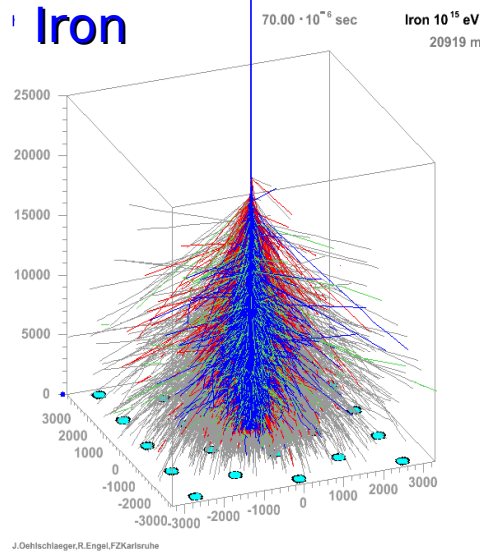
X_{\max} as indicator of mass composition

Atmospheric depth of shower maximum correlated with primary type
 (Example: proton showers develop deeper than iron, $X_{\max,pr} > X_{\max,Fe}$)

Proton



Iron



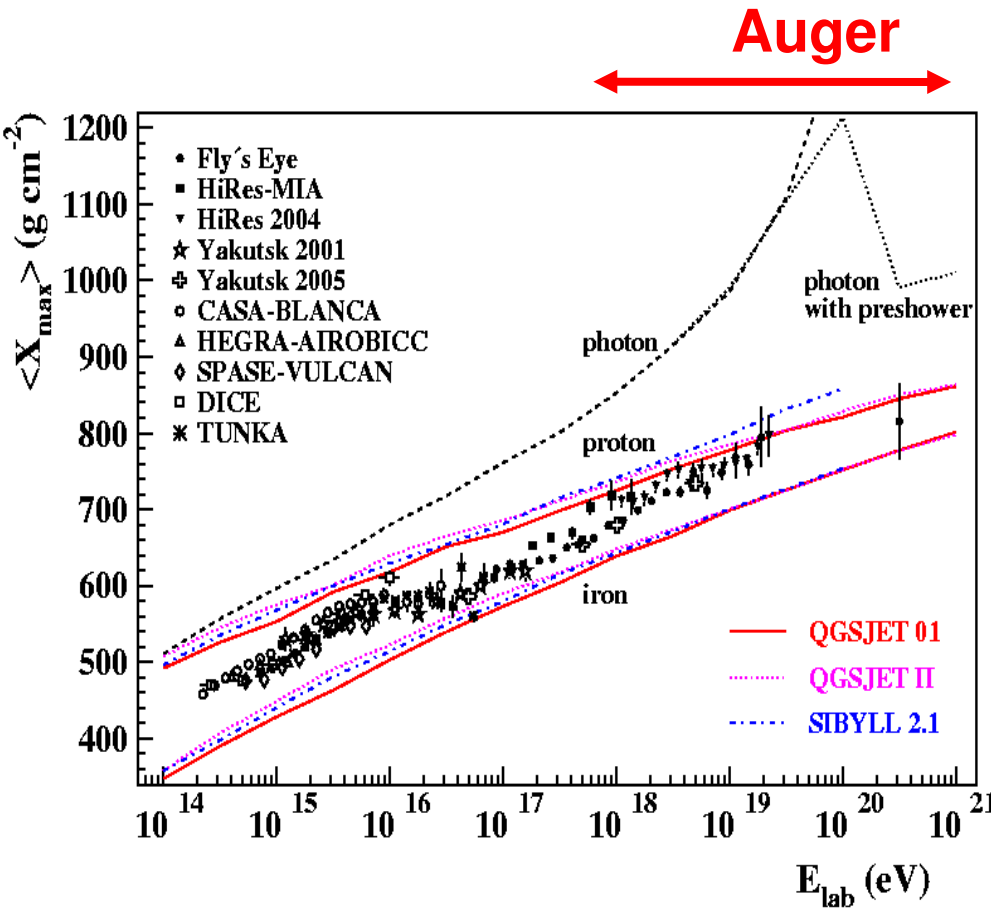
hadrons muons electrs neutrals

<http://www-ik.fzk.de/corsika>

$X_{\max,Fe} \sim 700 \text{ g/cm}^2$

$X_{\max,p} \sim 800 \text{ g/cm}^2$

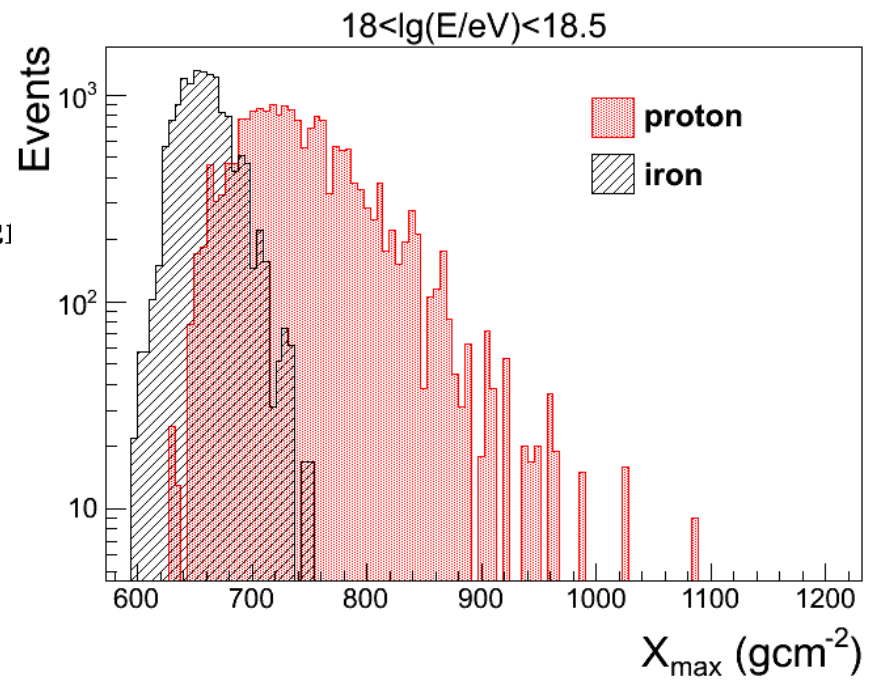
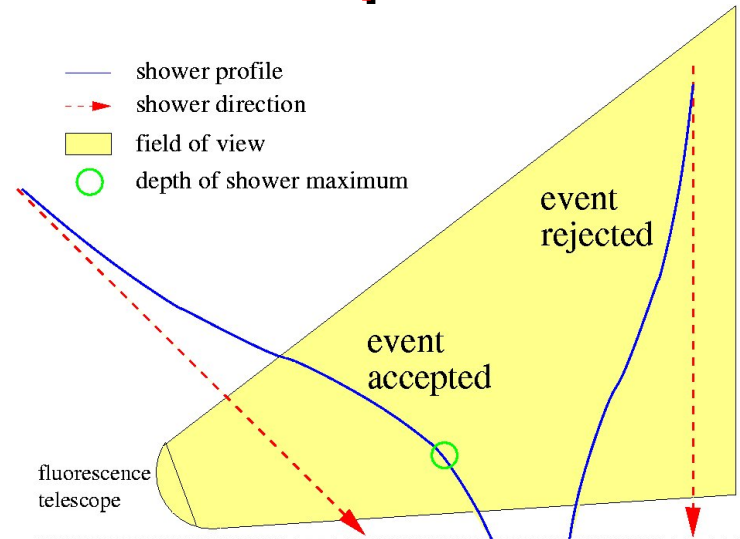
Observation of longitudinal profile



$$\langle X_{\max} \rangle = \alpha(\ln E - \langle \ln A \rangle) + \beta$$

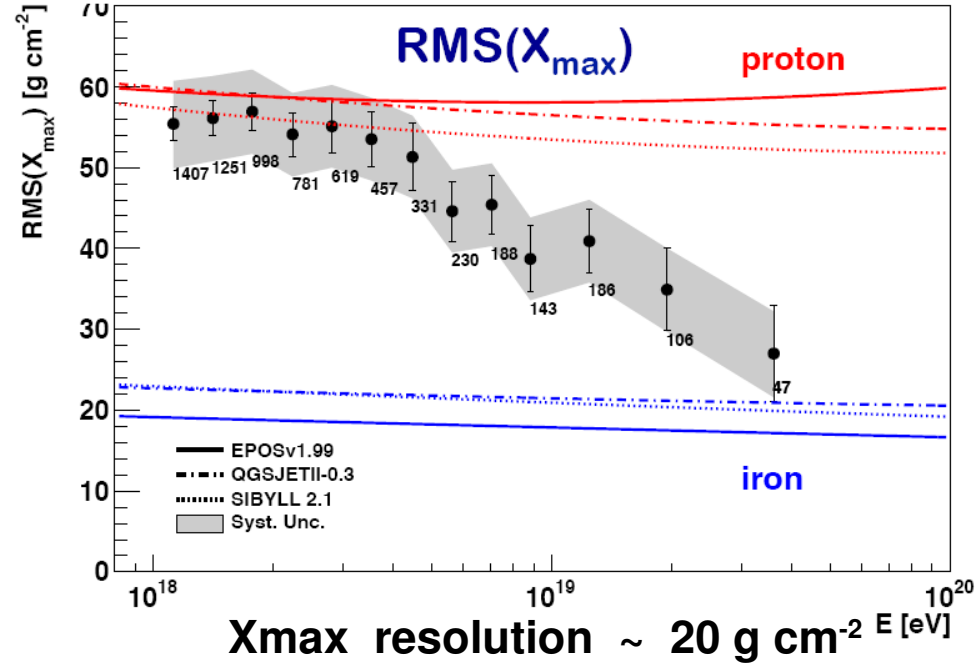
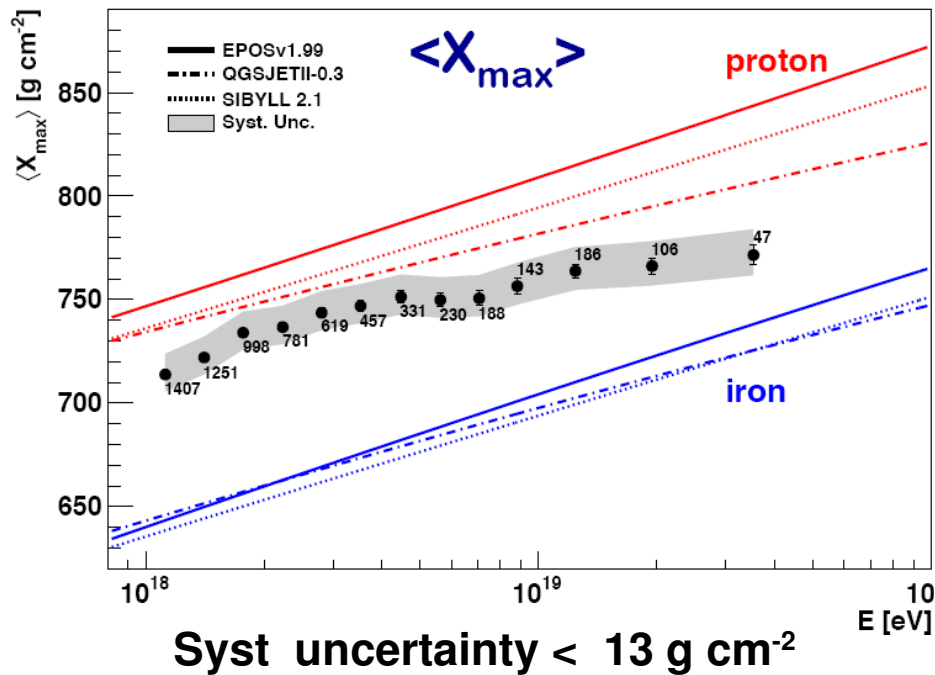
$\langle X_{\max} \rangle$ and its RMS

- sensitive to mass composition
- key observables for composition studies



Mass Composition: mean X_{\max} and its RMS

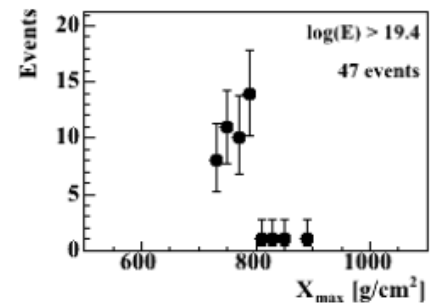
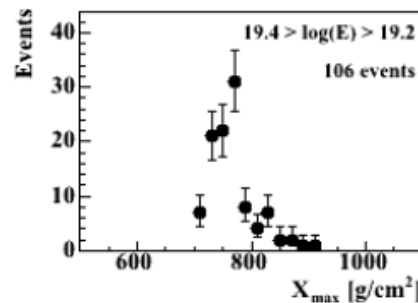
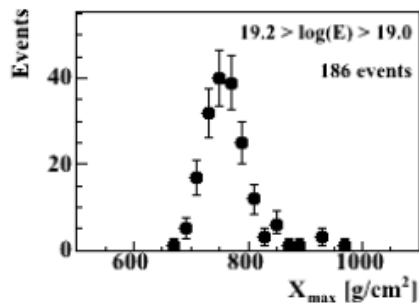
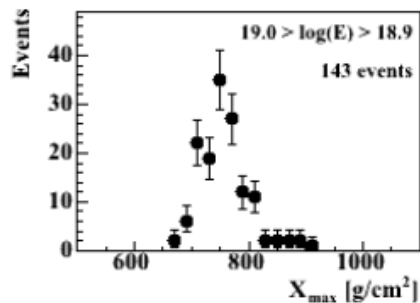
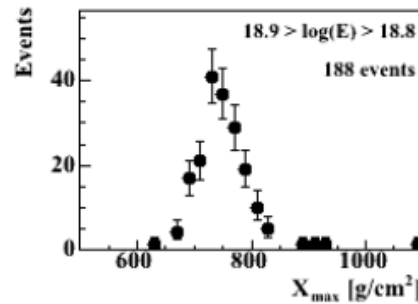
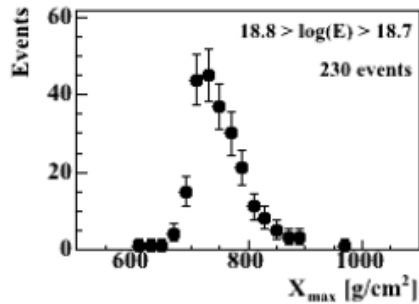
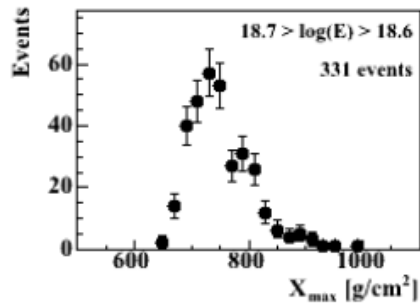
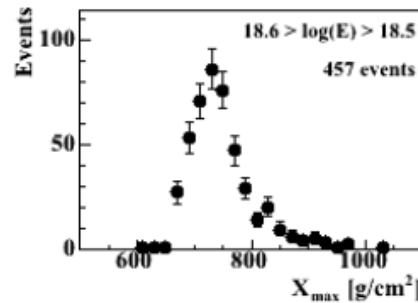
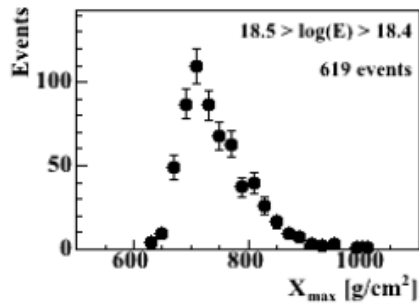
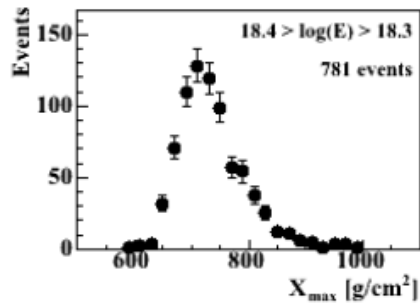
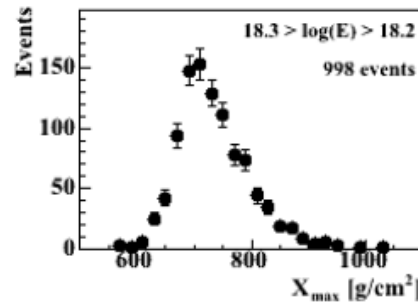
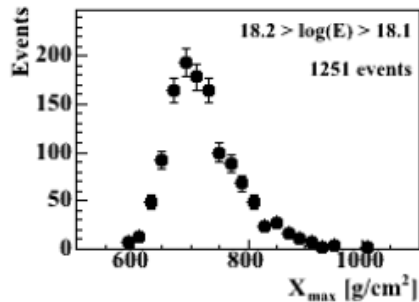
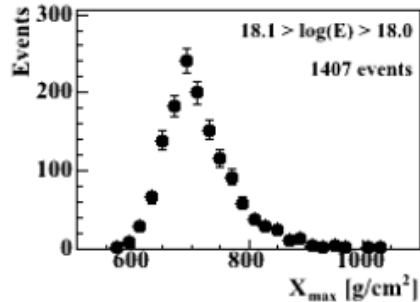
G. Pinto, P.Facal @ ICRC 2011



6744 hybrid events (Dec 2004 – Sept 2010) $E > 10^{18}$ eV

- interpretation depends on hadronic interaction models
- increase of the mean mass with the energy
- **Open issue: HiRes (and first results of TA) suggest a lighter composition**

X_{\max} distributions



As the energy increases:

- distributions become narrower, and

- deep X_{\max} tail becomes less evident

Interpretation, especially at high energy, is difficult since we have to rely on the extrapolation provided by the different models

Distributions – Shape

Subtract $\langle X_{\max} \rangle$ to each of the distributions and compare only the shapes

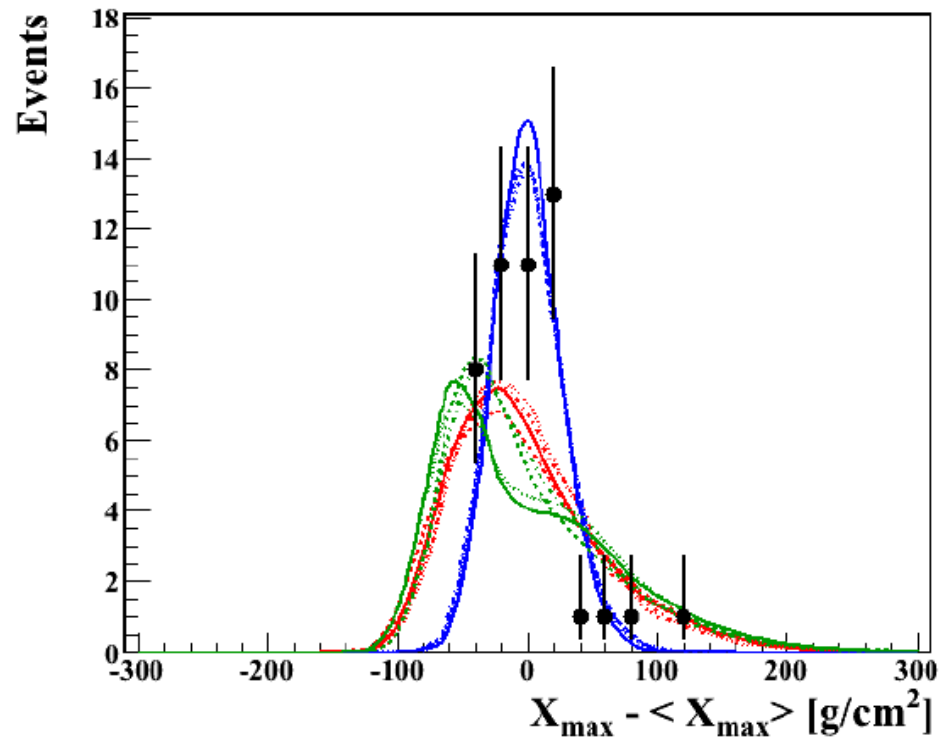
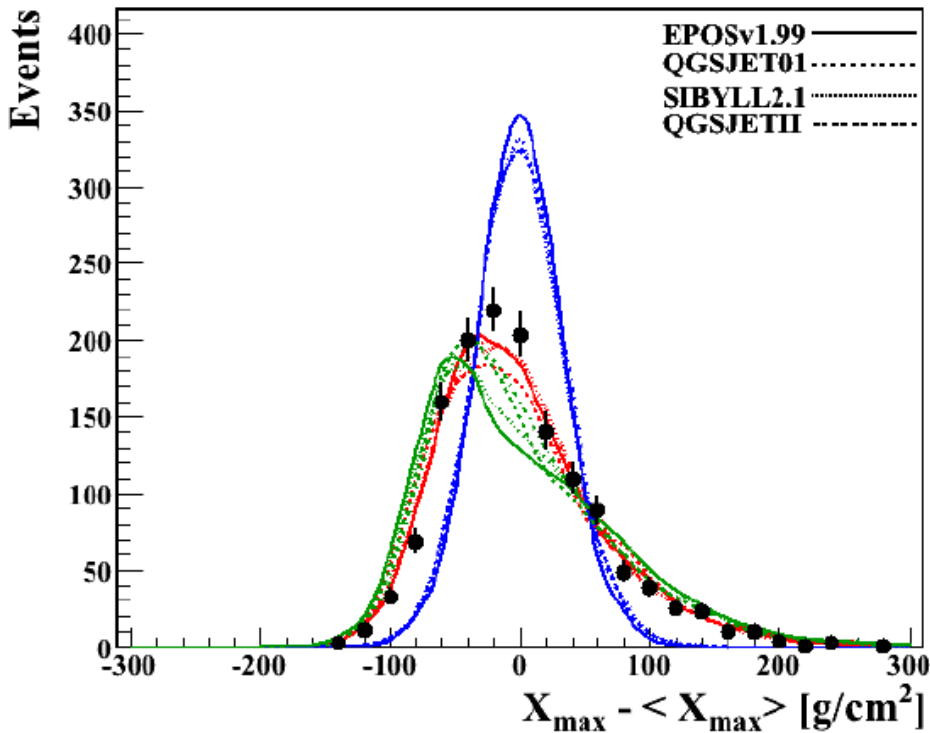
p Fe Mixed

Mixed: 50% p + 50% Fe

18.1 > log(E) > 18.0

P.Facal @ ICRC 2011

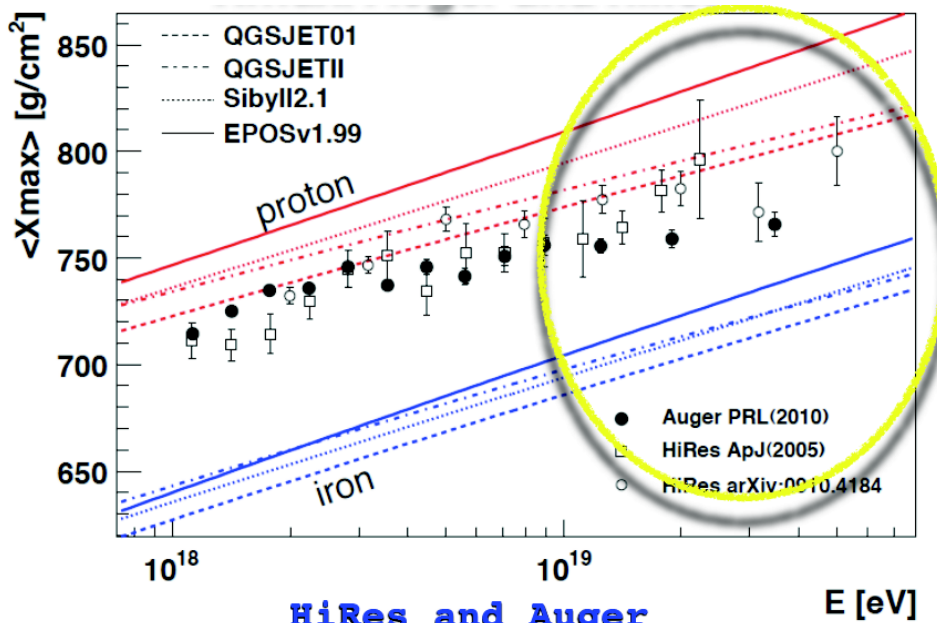
log(E) > 19.4



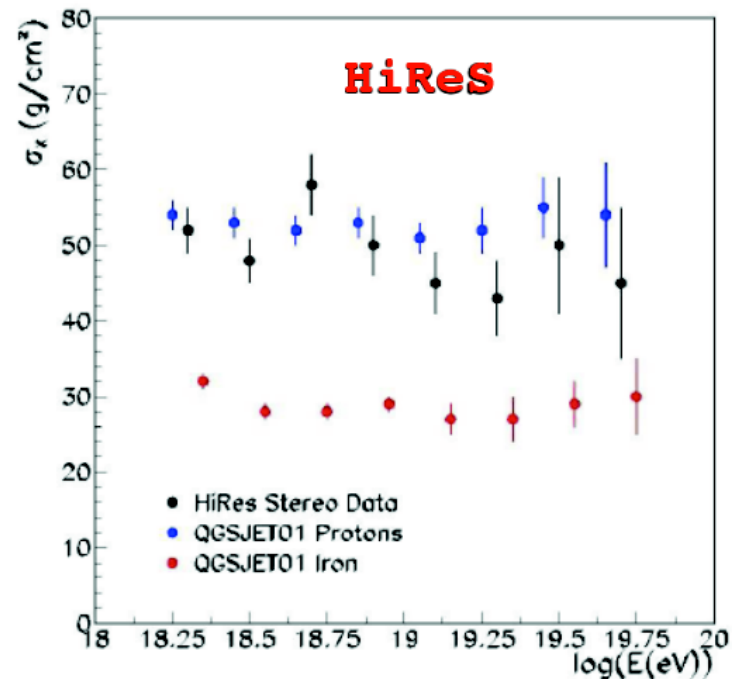
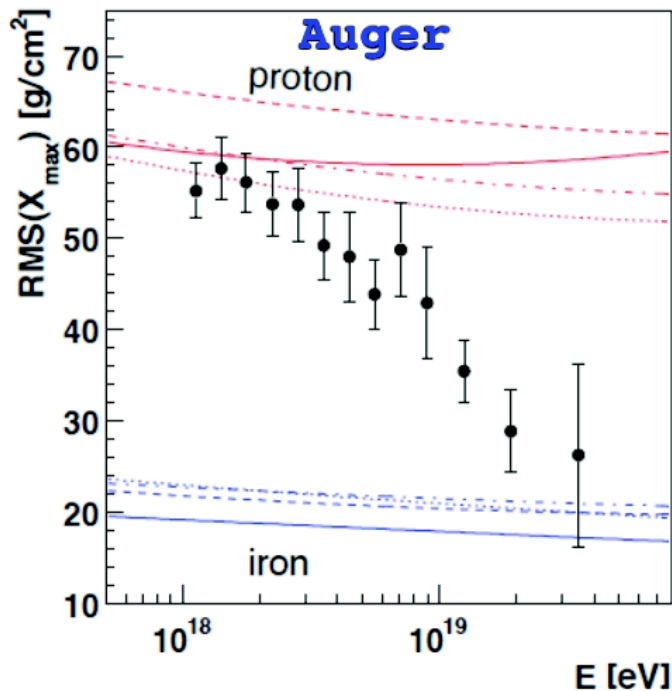
Fits light to heavier

HiRes vs Auger

Mass composition



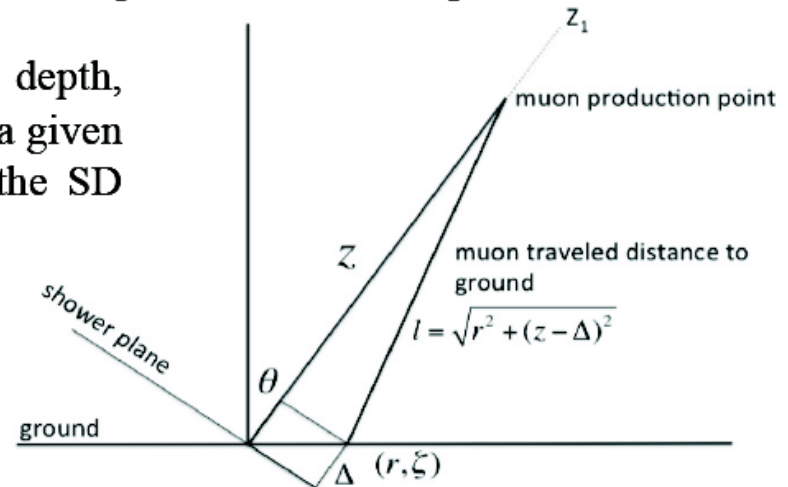
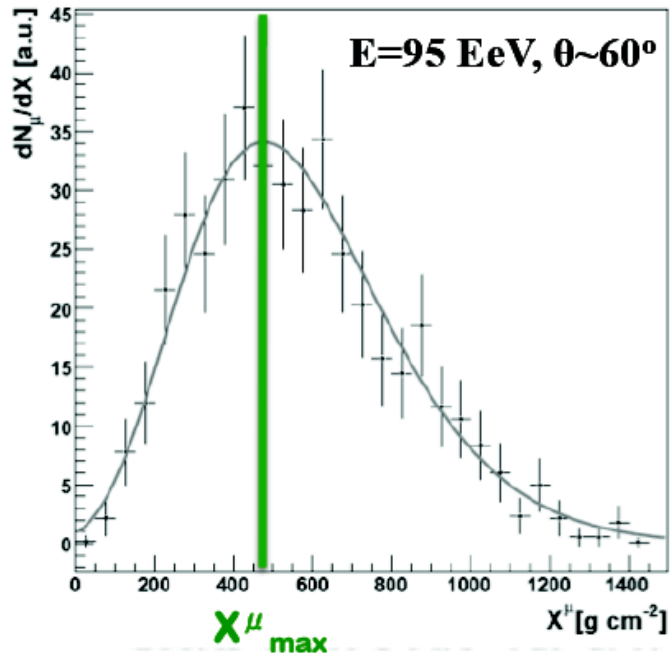
HiRes and Auger



Muon Production Depth

Muons are produced within a narrow cylinder centered at the shower axis. They travel along straight lines, practically unaffected by multiple scattering and bremsstrahlung.

Muon Production Depth (MPD): the depth, measured parallel to the shower axis, at which a given muon is produced. It can be obtained from the SD signals.



t_g , geometrical delay: the time difference between the arrival time of the muon and that of the time-reference shower plane.

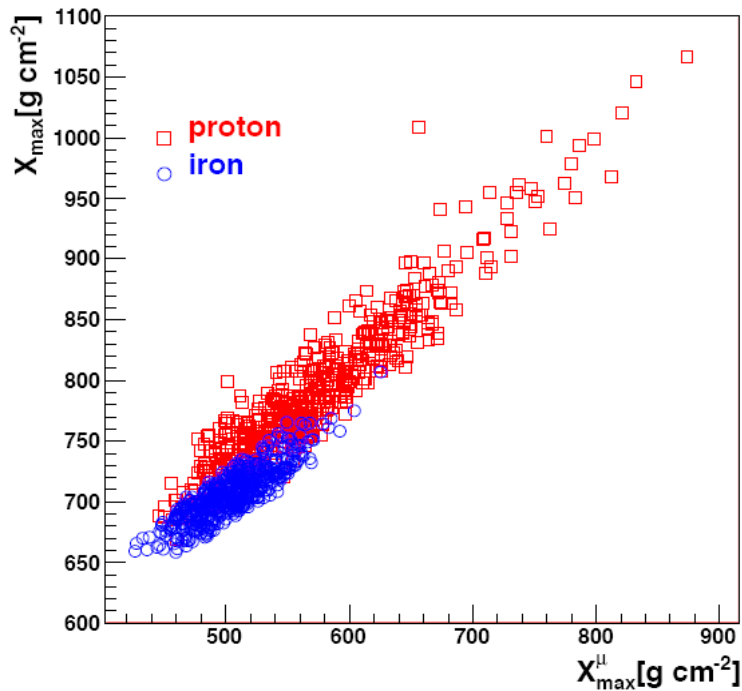
$$z = \frac{1}{2} \left(\frac{r^2}{ct_g} - ct_g \right) + \Delta$$

Event selection:

- $55^\circ < \theta < 65^\circ$
- $r > 1800$ m
- $E > 20$ EeV
- Gaisser-Hillas fit $\rightarrow X^\mu_{\max}$ (depth of maximum number of produced muons)
- Systematic uncertainty ≤ 11 g/cm²

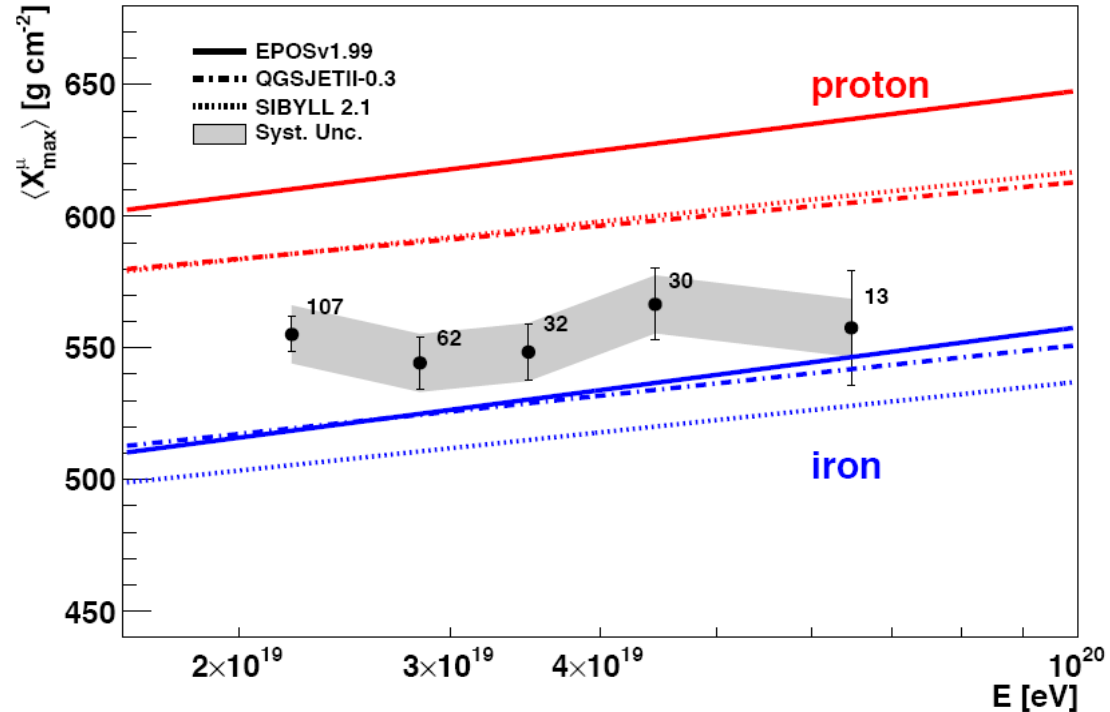
Mass Composition: X_{\max}^{μ}

X_{\max}^{μ} vs X_{\max}



- MC hybrid events
- Correlation with X_{\max}

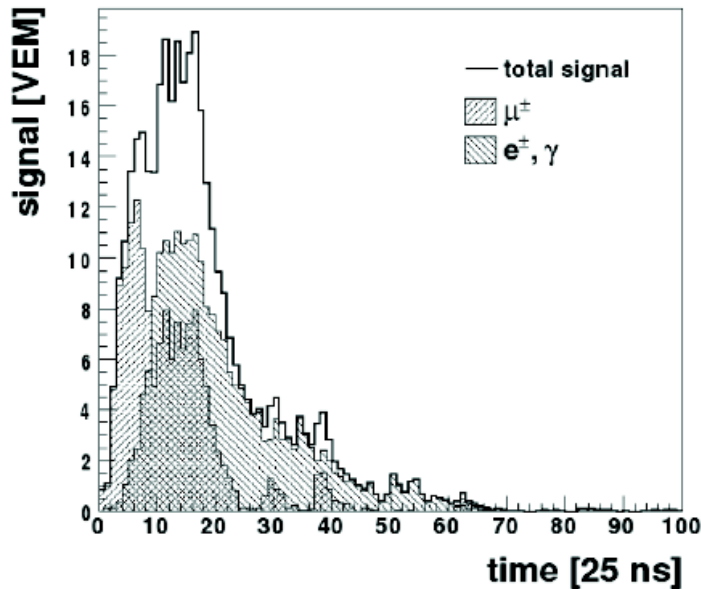
$\langle X_{\max}^{\mu} \rangle$ vs E



- 244 SD events (Jan 2004 – Dec 2010)
- $E > 20 \text{ EeV}$ $55^{\circ} < \theta < 65^{\circ}$

Composition using the azimuthal asymmetry in SD signals

The time structure of SD signals has information about shower development:

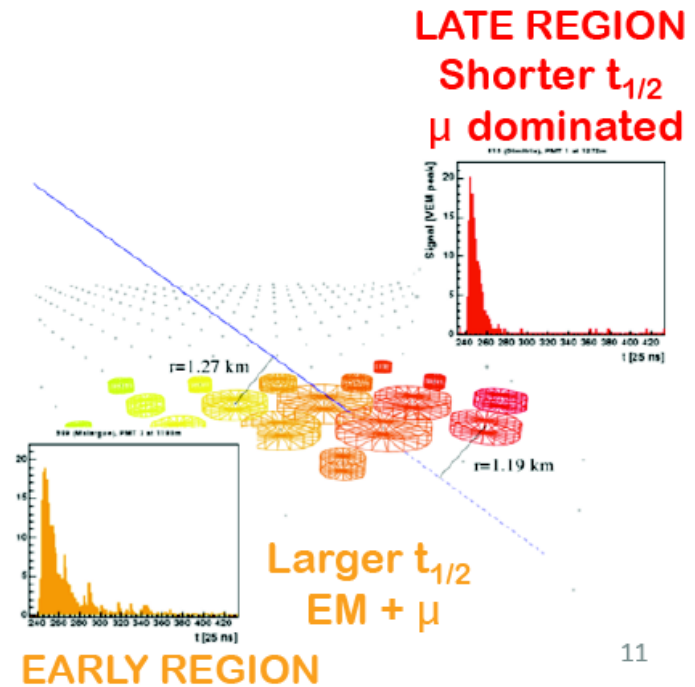


μ : less interacting. Dominate first portion of the signal.

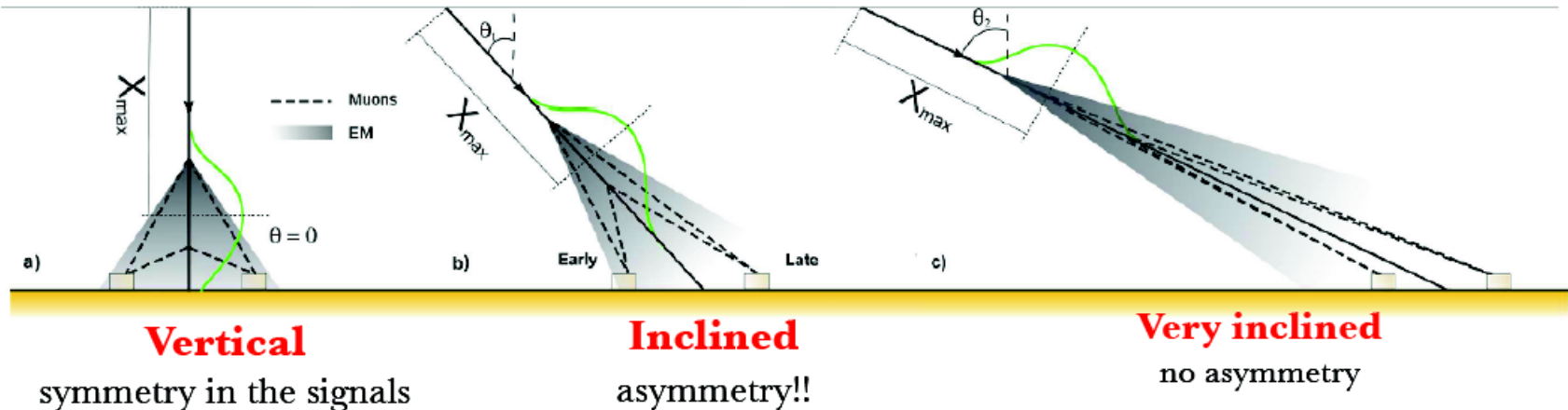
EM: multiple scattering. Spread out in time.

Risetime ($t_{1/2}$): time required to go from 10% to 50% of the total signal.

For non-vertical showers particles striking detectors in the different regions will have different stages of development because of the different path travelled.



Azimuthal asymmetry in SD signals



The early-late asymmetry as function of the zenith angle is expected to have a maximum which is correlated with X_{\max}

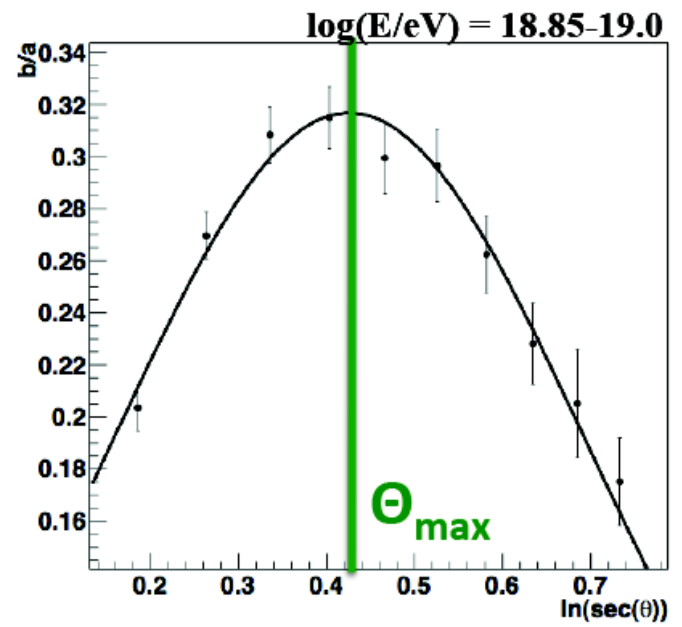
Observable: Θ_{\max} : $\sec\theta$ for which b/a is maximum

Different primaries will have different asymmetry profiles.

Event selection:

- $30^\circ < \theta < 60^\circ$
- $500 \text{ m} < r < 2000 \text{ m}$

$$\langle t_{1/2}/r \rangle = a + b \cos \zeta$$

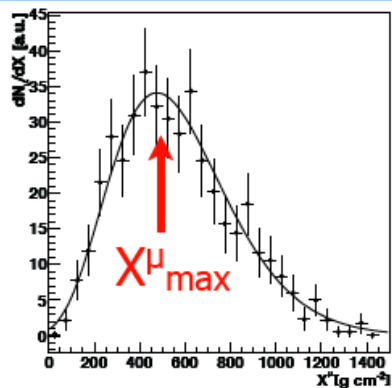


Systematic uncertainty $\approx 10\%$ of p-Fe separation

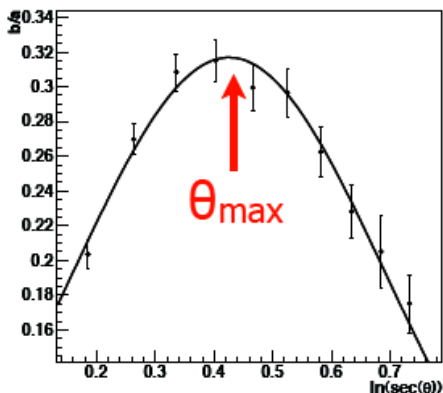
Comparison of Methods

#709: Garcia Pinto

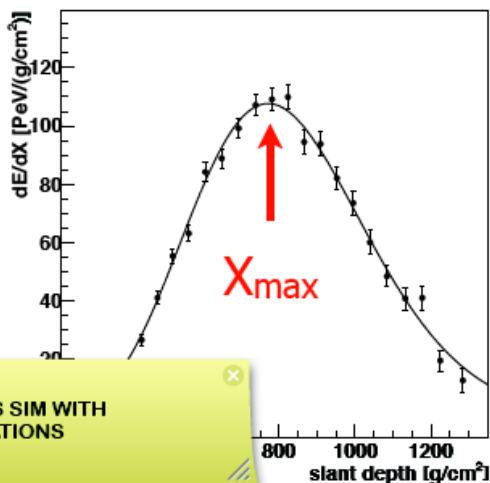
Muon Production Depth
from timing differences



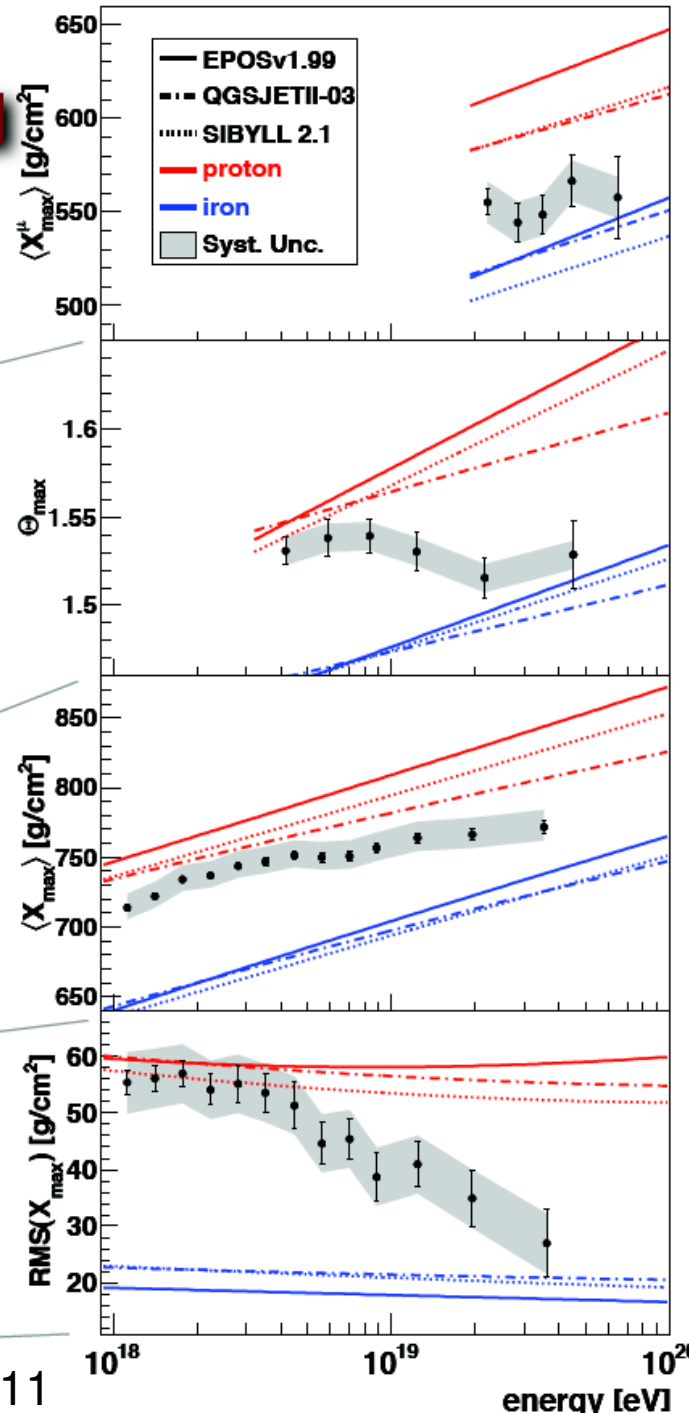
Shower Maximum from
asymmetry of rise times



X_{max} from FD



RMS(X_{max}) from FD



PERHAPS SIM WITH
FLUCTUATIONS

Results

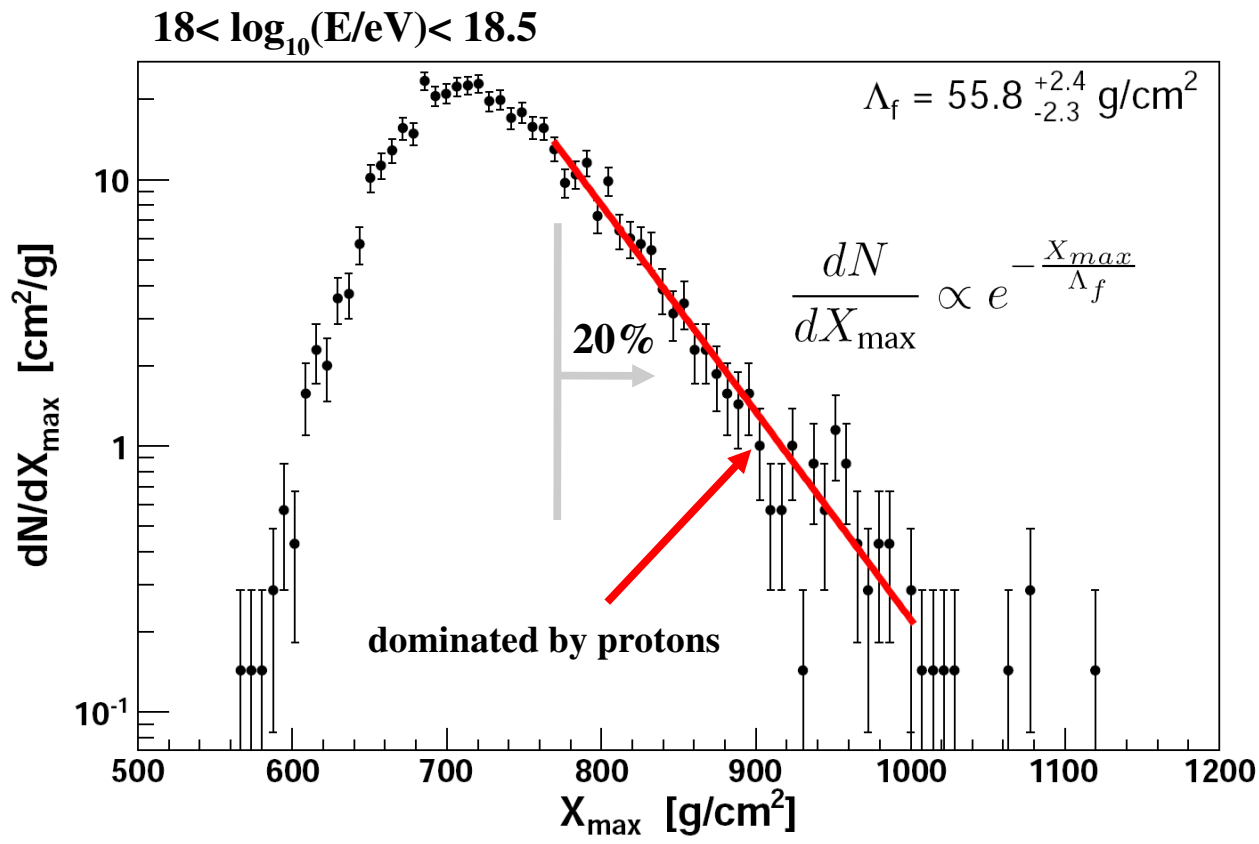
- Energy spectrum
- Mass composition
- **Hadronic Interactions**
- Search for photons and neutrinos
- Astrophysics

Measurement of the p-air cross-section

Tail of the distribution of $\langle X_{\max} \rangle$ sensitive to cross-section

Ellsworth et al. Phys. Rev. D26 (1982) 336
 Baltrusaitis et al. Phys. Rev. Lett. 52 (1984) 1380

Fly's Eye \rightarrow



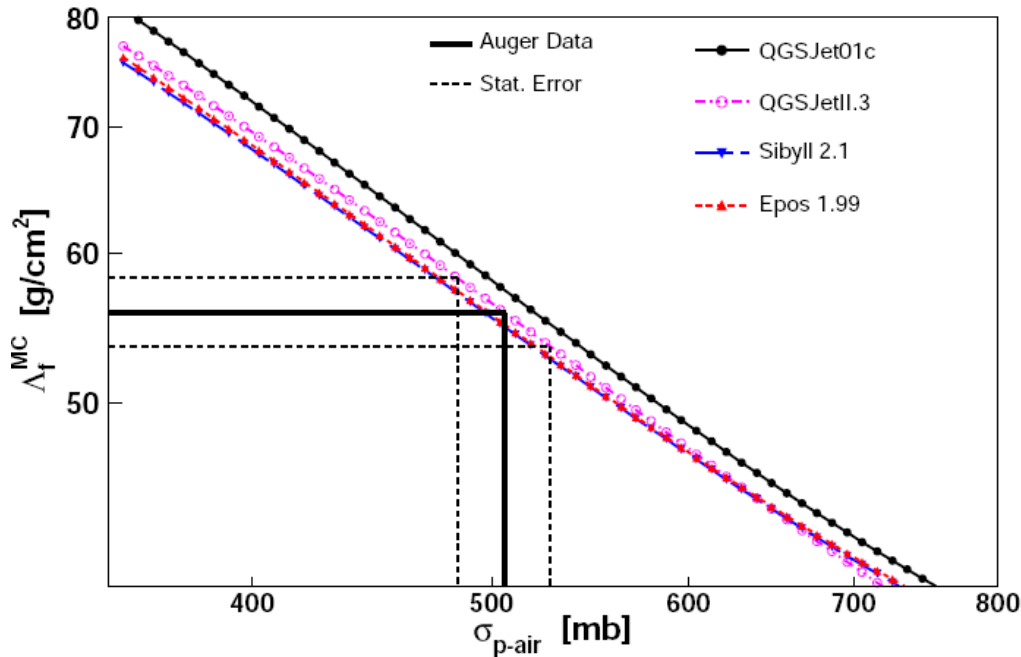
Dedicated analysis to select a proton-enriched data sample

Why 20%?
 15% helium contamination produces a bias at the level of the statistical uncertainties

Use simulations to correlate Λ_f^{MC} with cross-sections

Λ_f^{MC} adjusted to reproduce the measured Λ_f

Retrieving cross-sections



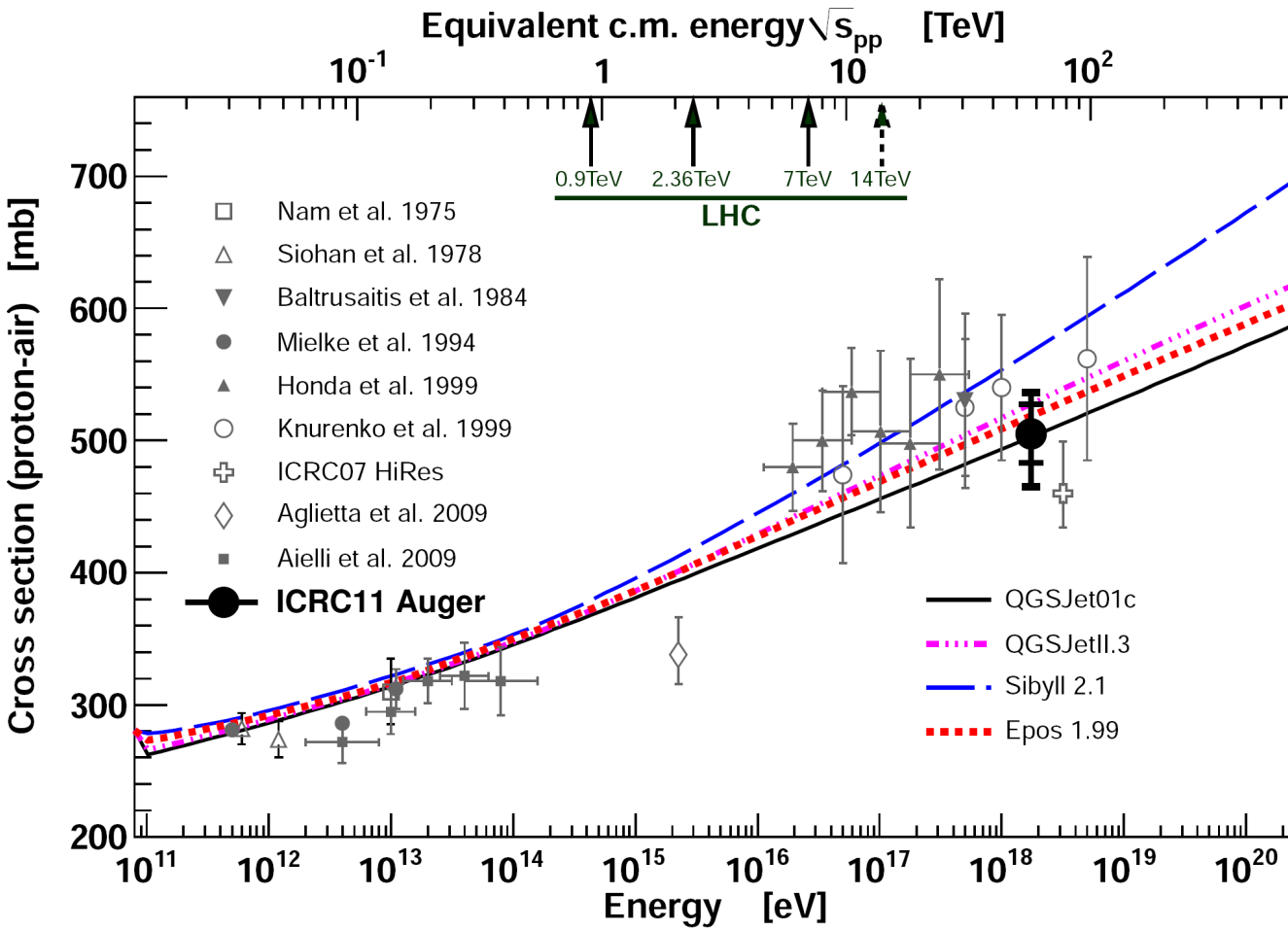
Correlation between Λ^{MC} and true cross-sections for different models

This method relies on simulations

Model	Rescaling factor at $10^{18.24}$ eV	$\sigma_{\text{p-air}}/\text{mb}$
QGSJet01	1.04 ± 0.04	524 ± 23
QGSJetII.3	0.95 ± 0.04	503 ± 22
SIBYLL 2.1	0.88 ± 0.04	497 ± 23
EPOS 1.99	0.96 ± 0.04	498 ± 22

Corrections to be applied to simulations (i.e. on true cross-sections) in order to match the measured Λ

$$m(E, f_{19}) = 1 + (f_{19} - 1) \frac{\lg(E/10^{15} \text{ eV})}{\lg(10^{19} \text{ eV}/10^{15} \text{ eV})},$$



Energy well above the LHC measurements

Systematic Uncertainties

- hadronic models
- energy scale
- simulations

Total: -15 mb, +20 mb

$$\langle E \rangle \sim 1.7 \text{ EeV} \quad \sqrt{s} = 57 \text{ TeV}$$

$$\sigma_{p\text{-air}} = (505 \pm 22_{\text{stat}} \left(\begin{smallmatrix} +26 \\ -34 \end{smallmatrix} \right)_{\text{syst}}) \text{ mb}$$

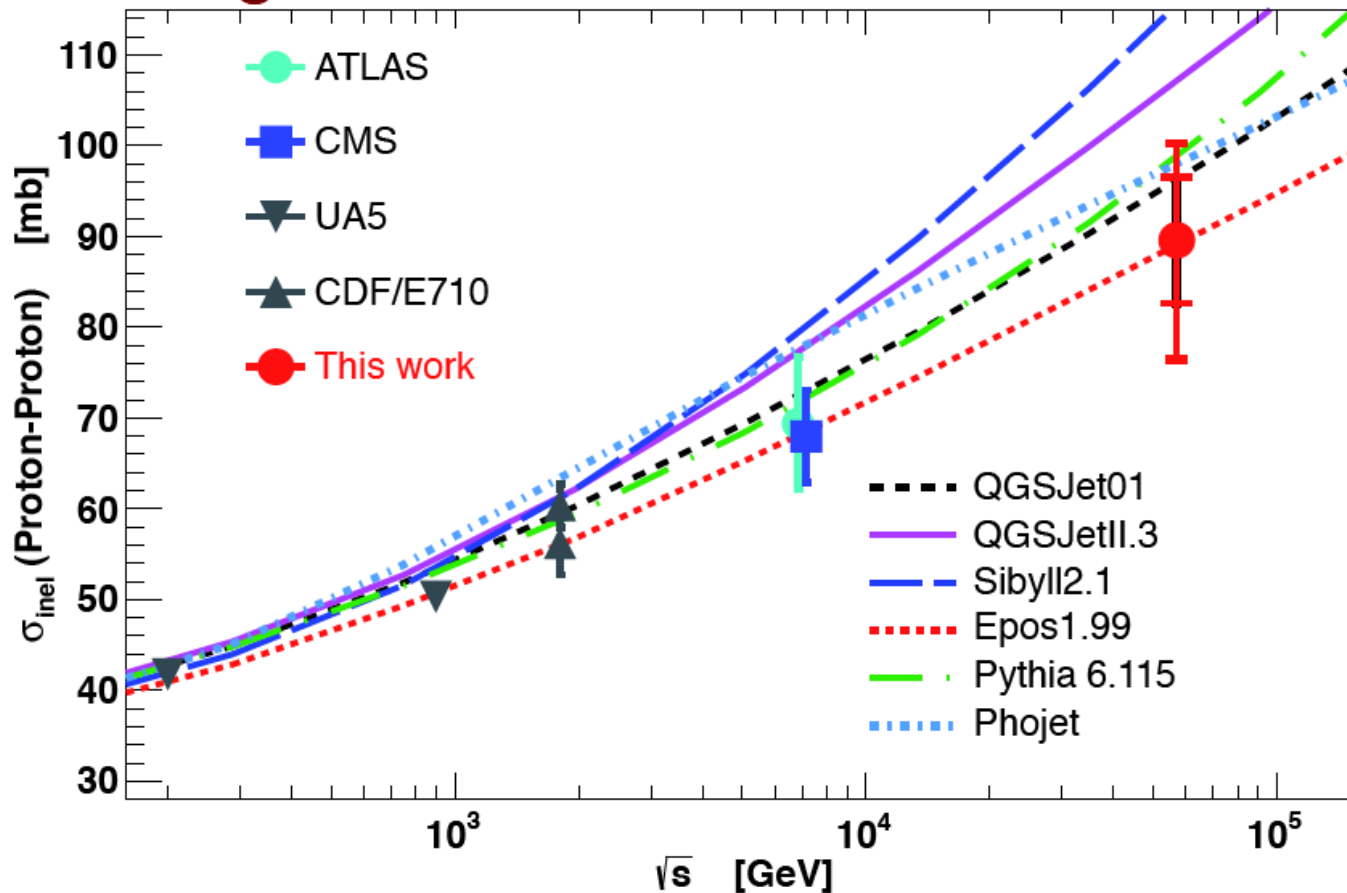
Additional Uncertainties due to diverse contaminations:

- photon fraction 0.5% +10 mb
- helium fraction 10% -12 mb
- helium fraction 25% -30 mb

p-p Cross Section at \sqrt{s} 57 TeV

#946:
Ulrich

using Glauber model

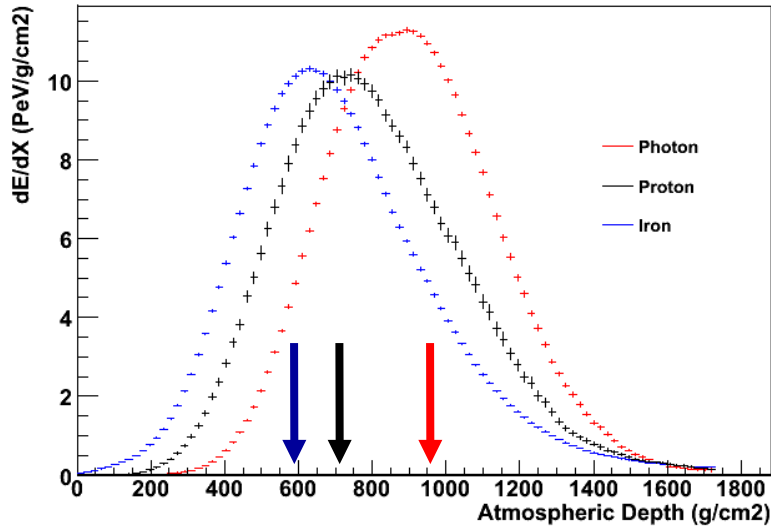


$$\sigma_{pp} = (90 \pm 7_{\text{stat}} \left(\begin{smallmatrix} +8 \\ -11 \end{smallmatrix} \right)_{\text{sys}} \pm 1.5_{\text{Glauber}}) \text{ mb}$$

Results

- Energy
- Mass composition
- Hadronic Interactions
- **Search for photons and neutrinos**
- Astrophysics

Search for photon primaries

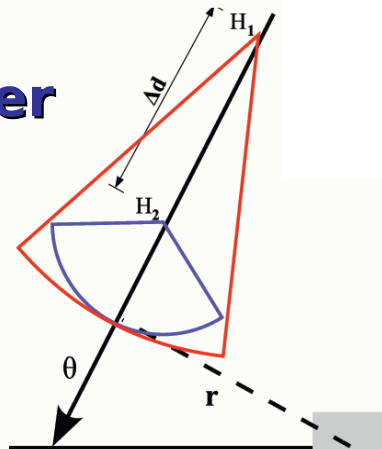


Photon showers develop deeper in the atmosphere

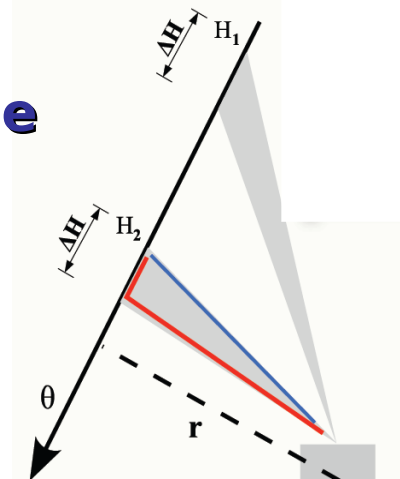
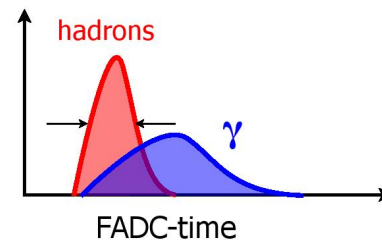
FD: search for events with deep X_{max}

SD: search based on signal time structure

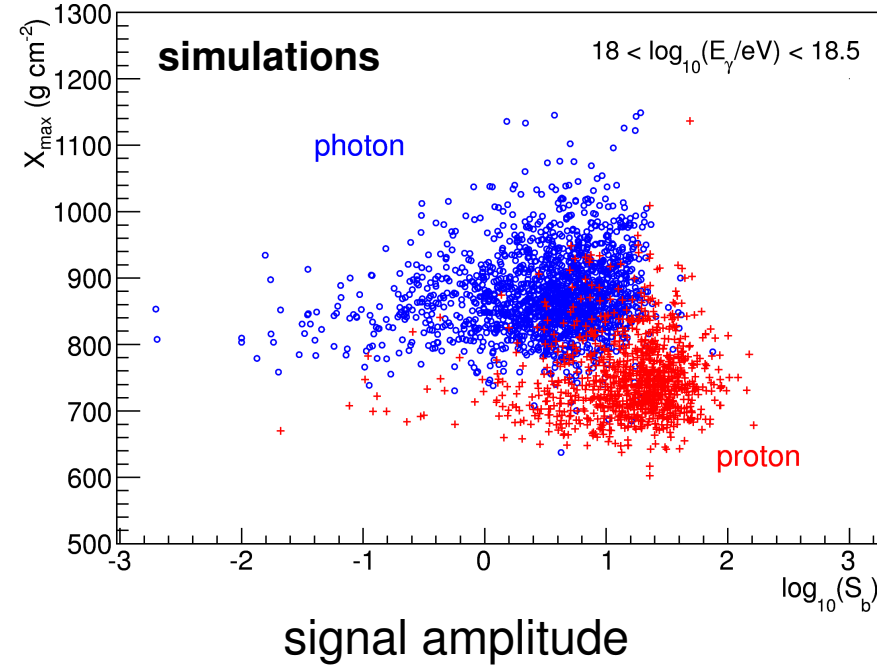
Deeper showers larger curvature



Slower signal, longer risetime



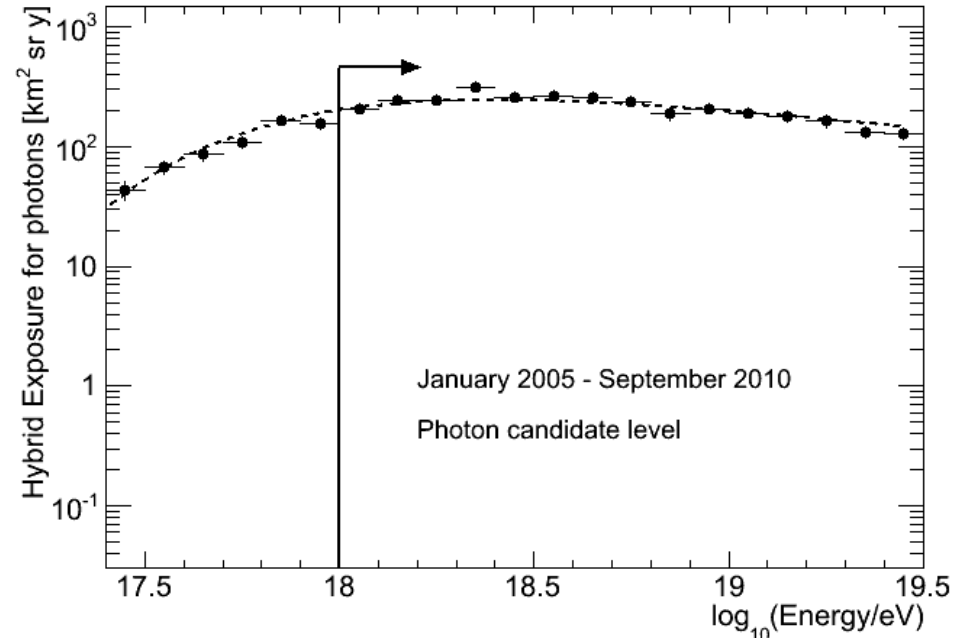
(hybrid) photon/hadron separation



- **deep shower**
large X_{max} (from **FD**)

- **structure of the LDF**
different time structure and smaller signal (from **SD**)

Hybrid Exposure for photons



Realistic and time dependent

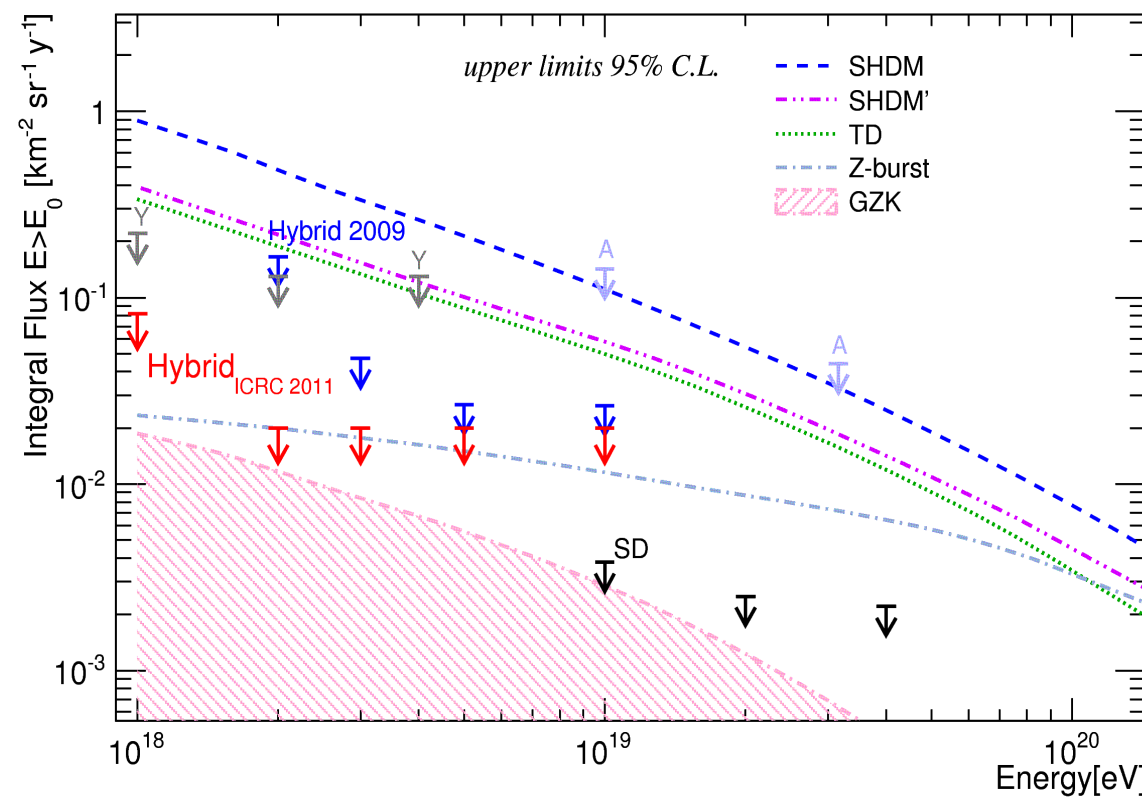
actual DAQ and atmospheric conditions taken into account (same approach used for the hybrid spectrum)



Proton background less than 1%

Upper limit to the integral photon flux

M. Settimo @ ICRC 2011



flux and fraction upper limits down to the EeV region

top-down models severely constrained

- favour astrophysical origin of UHECR
- reduce systematics in measurements of energy spectrum, p-air cross section, mass composition

Upper limits to the integral photon fraction assuming the Auger Spectrum

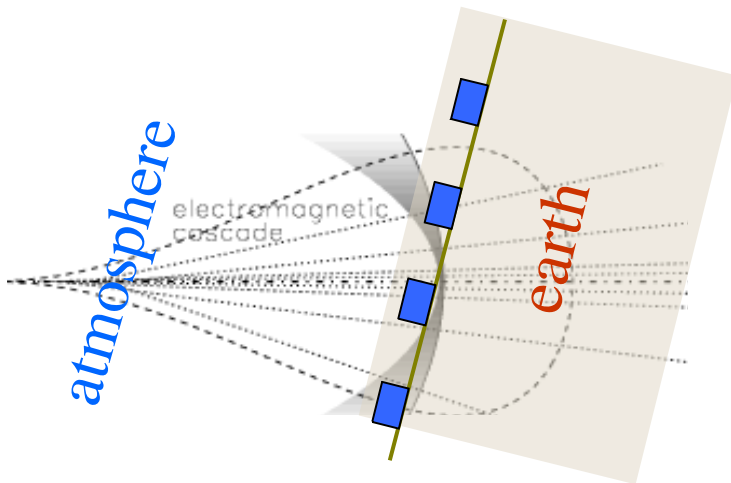
0.4%, 0.5%, 1.0%, 2.6% and 8.9% for $E > 1, 2, 3, 5$ and 10 EeV

Number of candidates

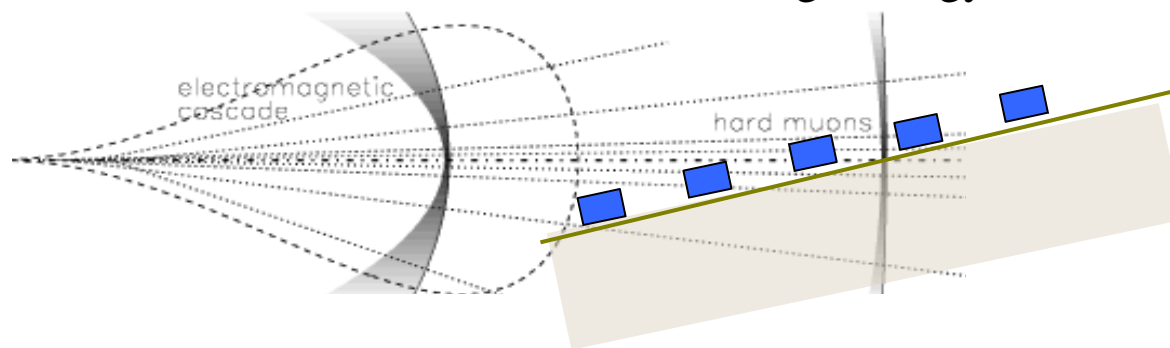
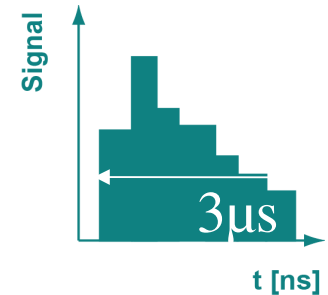
6, 0, 0, 0, and 0 for $E > 1, 2, 3, 5$ and 10 EeV

GZK region within reach in the next years

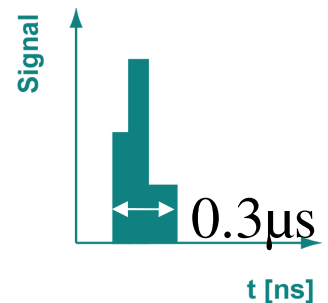
Search for neutrinos



Almost vertical
muons + electromagnetic



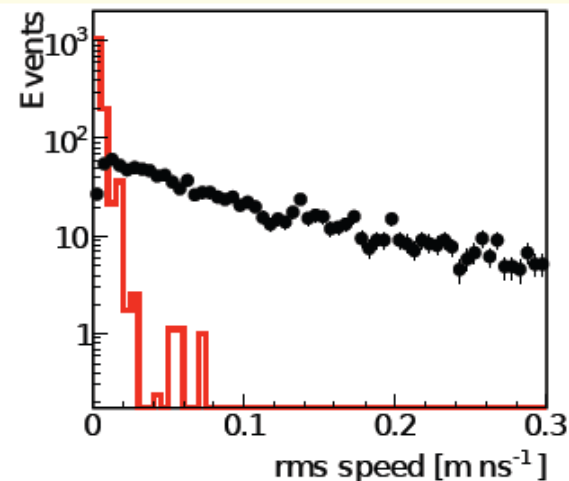
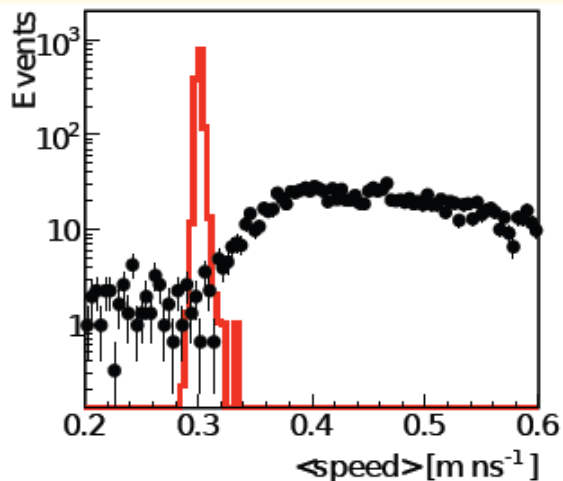
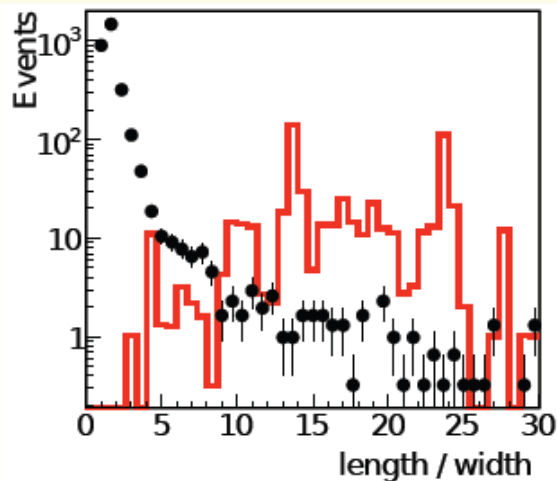
Very inclined, thin flat front
high energy muons



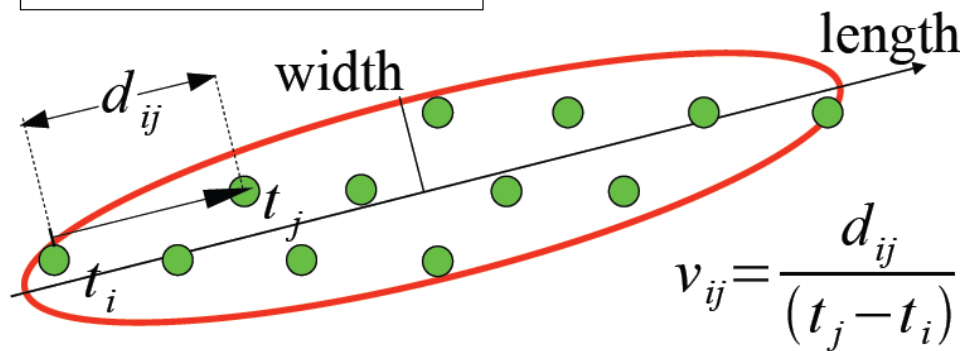
Important for neutrino detection: observable only if almost horizontal

Neutrino signature: an inclined shower with large electromagnetic component

Neutrino-like event selection



Inclined Showers



Similar selection rules for down-going

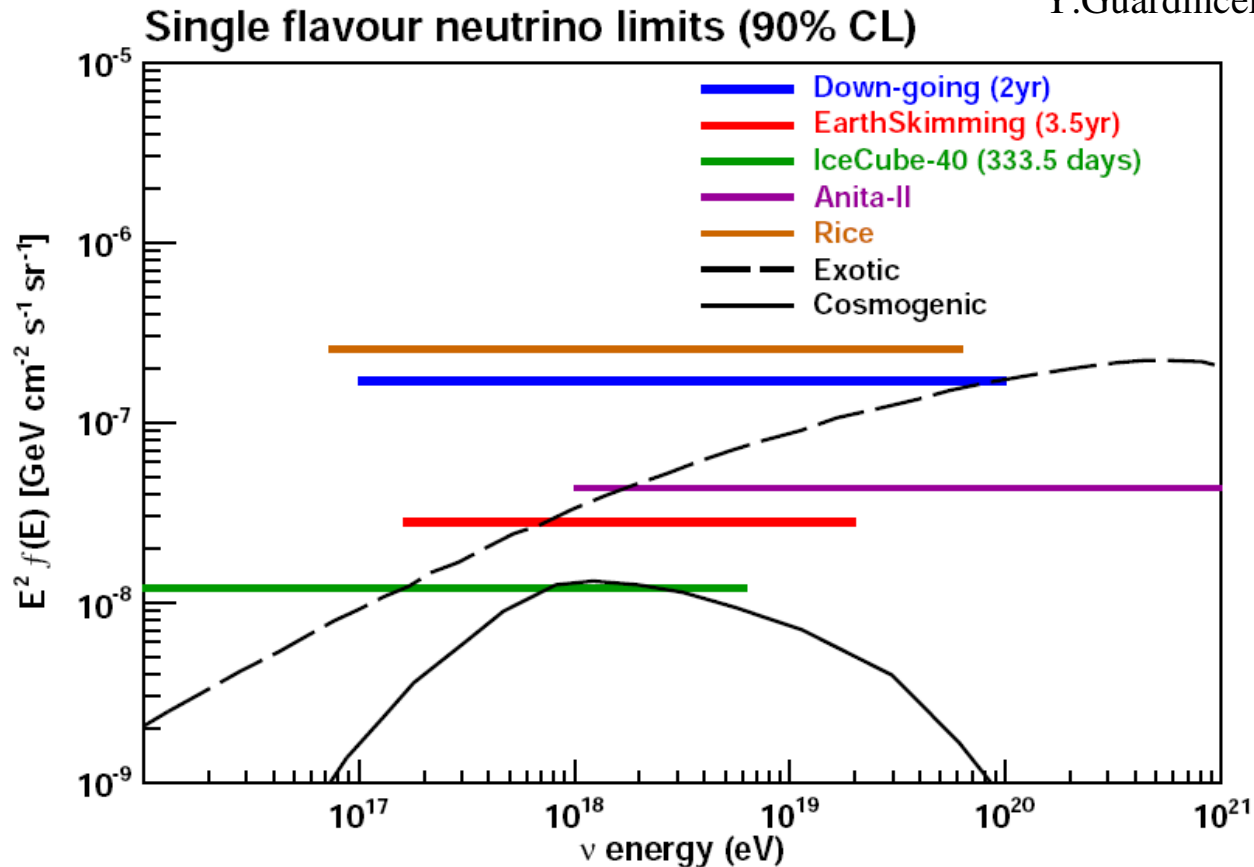
Data

**Simulated
neutrino signal**

Earth-skimming
Length/width > 5
0.29 < speed < 0.31 m/ns
rms < 0.08 m/ns

Upper limit on the diffuse neutrino flux

Y.Guardincerri @ ICRC 2011



$$k < 2.8 \times 10^{-8} \text{ GeV cm}^{-2} \text{ s}^{-1} \text{ sr}^{-1} \text{ in } 1.6 \times 10^{17} \text{ eV} < E < 2.0 \times 10^{19} \text{ eV}$$

$$k < 1.7 \times 10^{-7} \text{ GeV cm}^{-2} \text{ s}^{-1} \text{ sr}^{-1} \text{ in } 1 \times 10^{17} \text{ eV} < E < 1 \times 10^{20} \text{ eV}$$

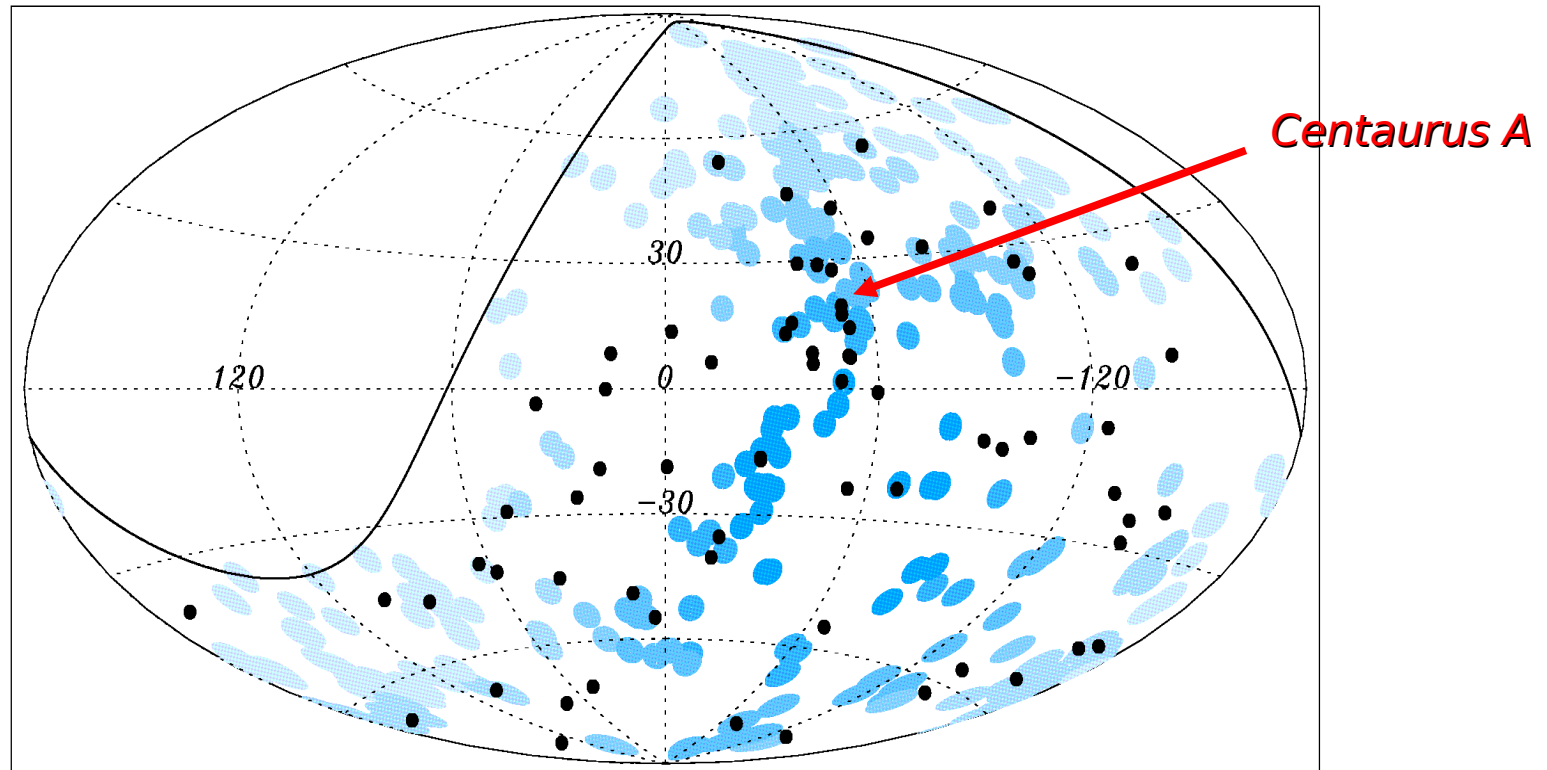
Results

- Energy spectrum
- Mass composition
- Hadronic Interactions
- Search for photons and neutrinos
- **Astrophysics**

Anisotropy at the highest energy

Astropart. Phys. 34 (2010) 314

Jan 2004
Dec 2009

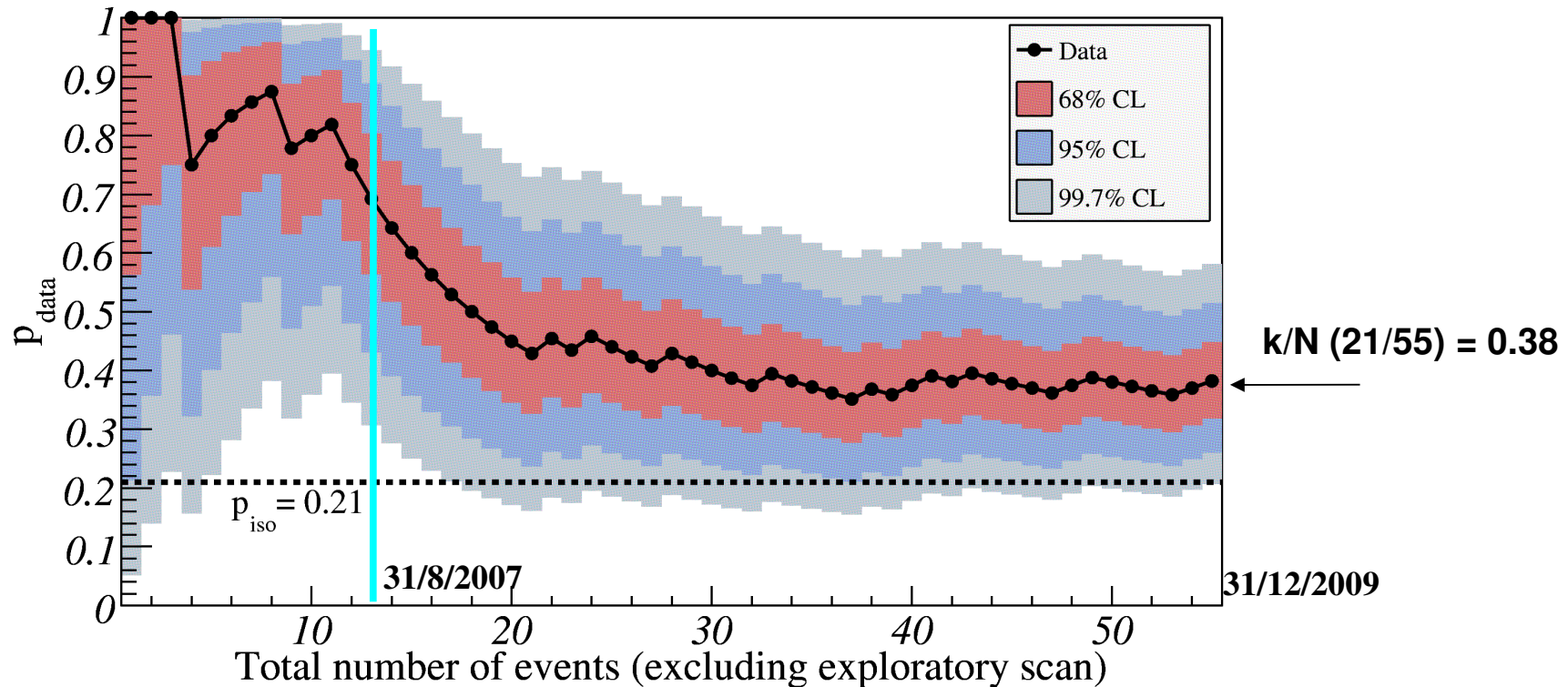


The 69 events with Energy > 55 EeV detected by the Pierre Auger Observatory
Blue circles of radius 3.1° centered at the positions of the 318 AGNs < 75 Mpc in the VCV catalog. The exposure-weighted fraction of the sky covered by the blue circles is 21% (fraction of correlating events under the hypothesis of isotropy)

Limitations of the catalogue: incomplete and inhomogeneous

Degree of correlation

Astropart. Phys. 34 (2010) 314



Degree of correlation $p_{\text{data}} = k/N$ vs total number of time-ordered events:

the 68%, 95% and 99.7% confidence level intervals around the most likely value are shaded.

The isotropic value is $p_{\text{iso}} = 0.21$. The current estimate of the signal is 0.38 (+0.07, -0.06).

Facts and open issues

- the degree of correlation has decreased (from 69% to 38%)
- probability from an isotropic distribution $\sim 3 \cdot 10^{-3}$
- with the current degree of correlation about four years of new data are required for a 5σ significance

Anisotropy consistent with a proton based composition

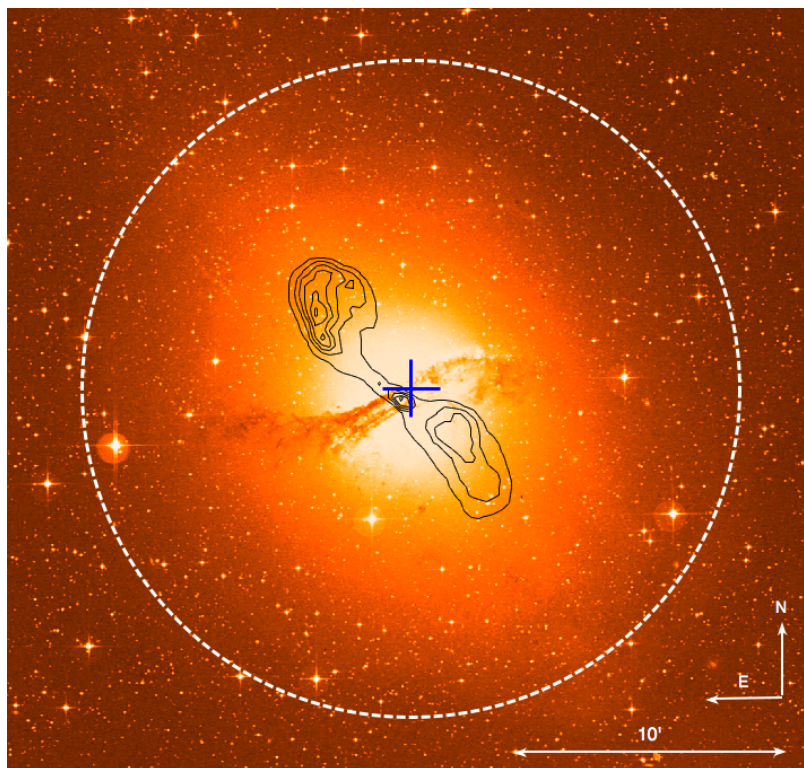
Xmax measurement suggest mixed composition (though not measured for $E > 55$ EeV)

Anisotropy not confirmed by HiRes (lower statistics, northern Hemisphere)

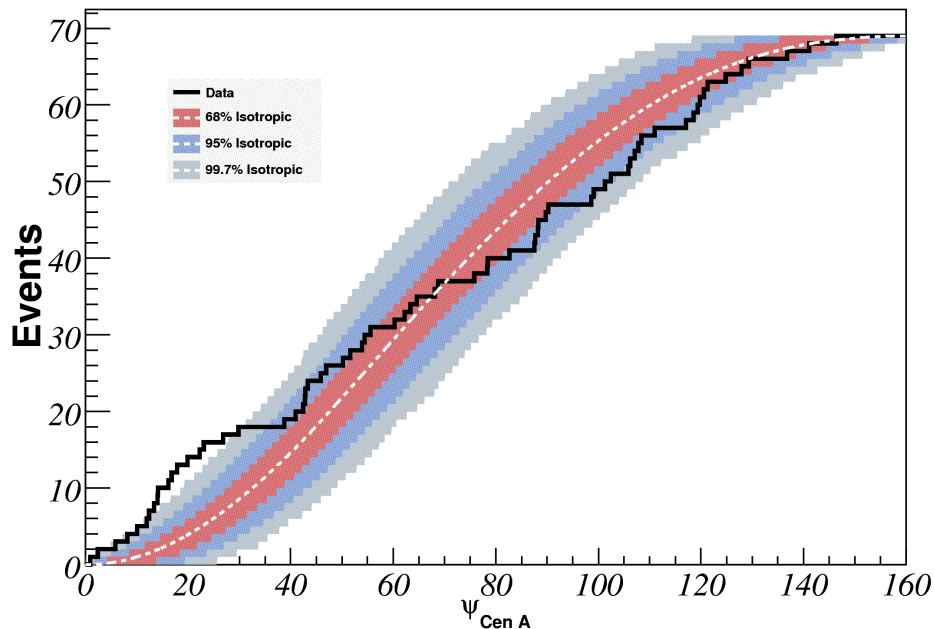
TA has a similar degree of correlation: 40% (8/20) con $p_{\text{iso}} = 25\%$

Centaurus A

Astropart. Phys. 34 (2010) 314



CEN A: optical image, radio contours (VLA), VHE best fit position and 95% C.L. (HESS).
From <http://arxiv.org/pdf/0903.1582v1>



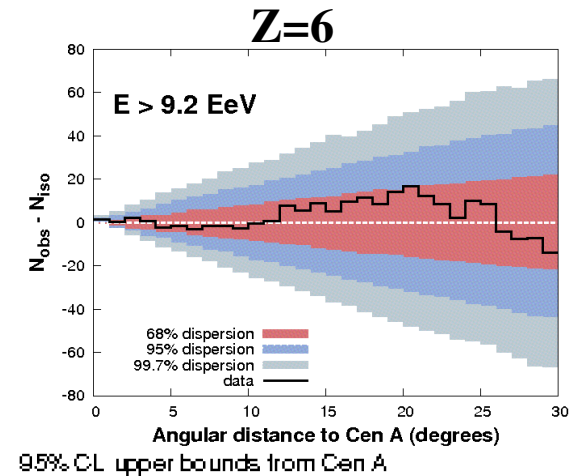
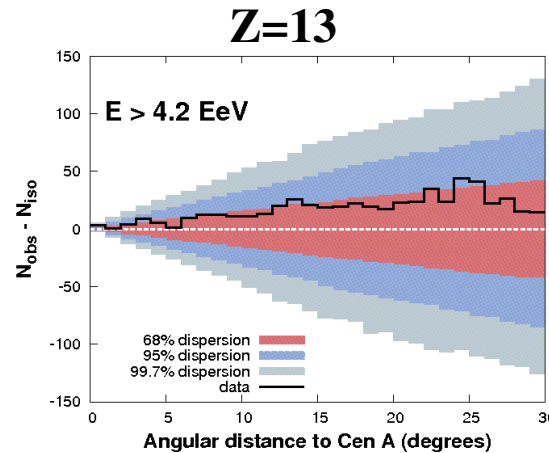
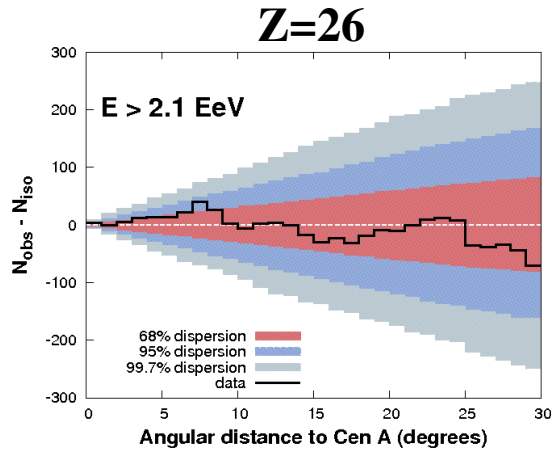
Cumulative number of events with energy $E \geq 55$ EeV as a function of angular distance from the direction of Cen A.

The bands correspond to the 68%, 95%, and 99.7% dispersion expected for an isotropic flux. 13 events fall in this area (18°) vs. 3.2 expected from isotropic flux.

Anisotropy and chemical composition

If the excess at $E_{\text{thres}} > 55 \text{ EeV}$ is due to nuclei (Z), the proton counterpart should be observed at energy above E_{thres}/Z

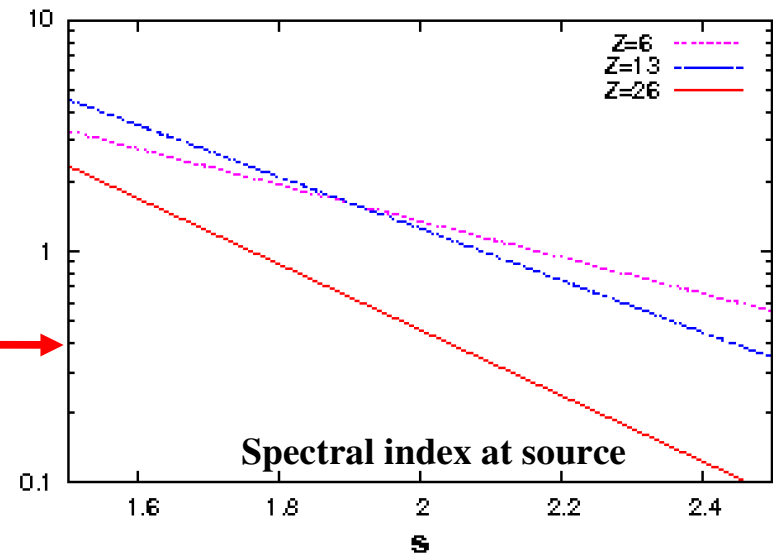
Lemoine & Waxman JCAP 11 (2009) 009



No excess observed from CEN A at lower energies

Upper limit to the proton fraction at the source (within the model assumption)

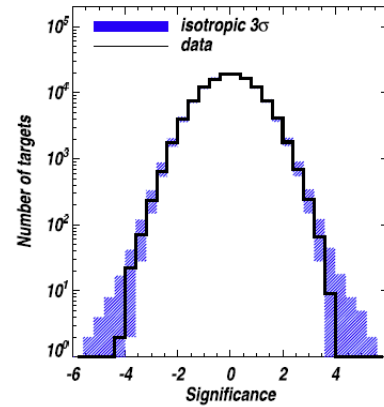
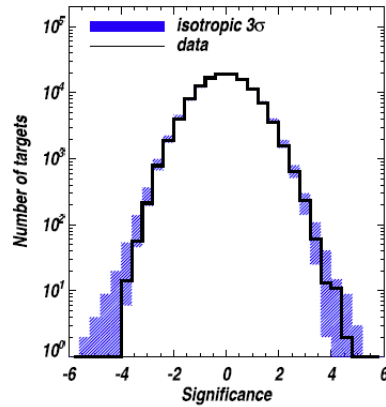
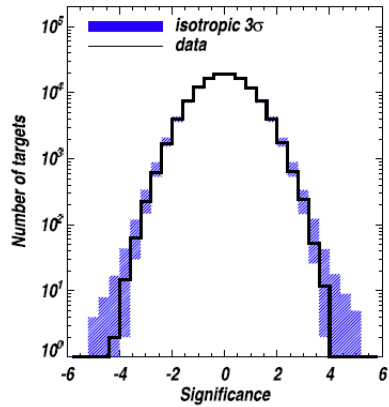
f_p / f_Z



Search for neutron point-sources

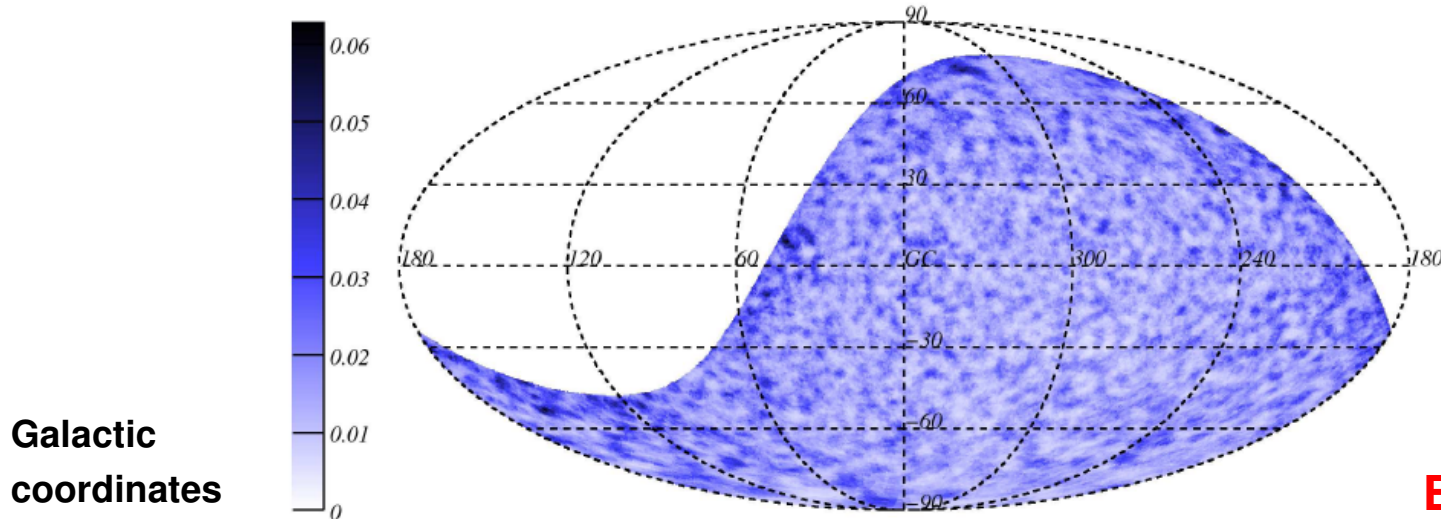
Neutron mean decay length: $\lambda_n = (9.2 \times E)$ kpc \longrightarrow

They could arrive from GC



No significant excess observed

Upper limits 95% CL (km⁻²yr⁻¹)



Enhancements and future plans

Extension towards the lower energies

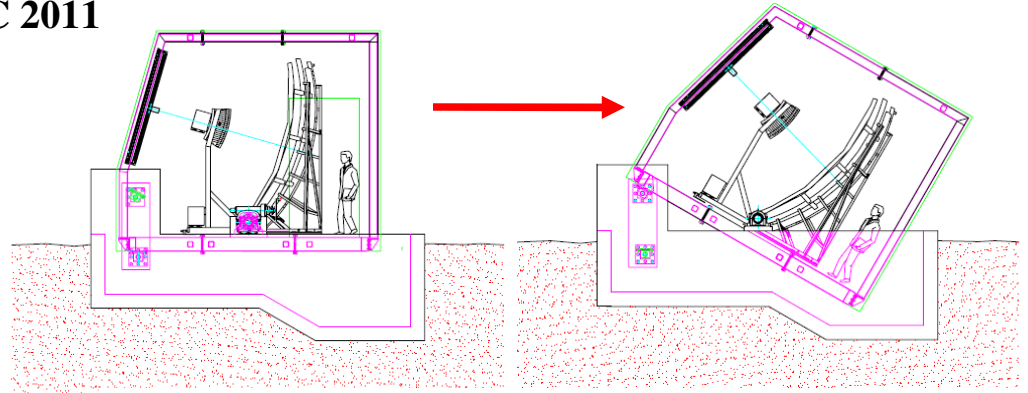
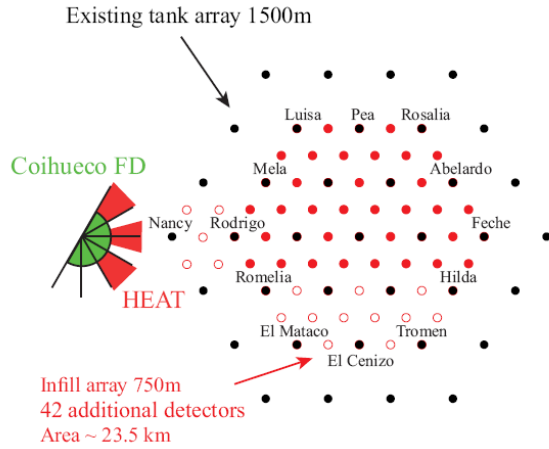
- improve detector performance at the transition to extragalactic component between $\sim 10^{17}$ and 10^{18} eV (HEAT and AMIGA)
- cross calibration with other experiments

The Pierre Auger Observatory as an ideal site to test and develop new detection techniques

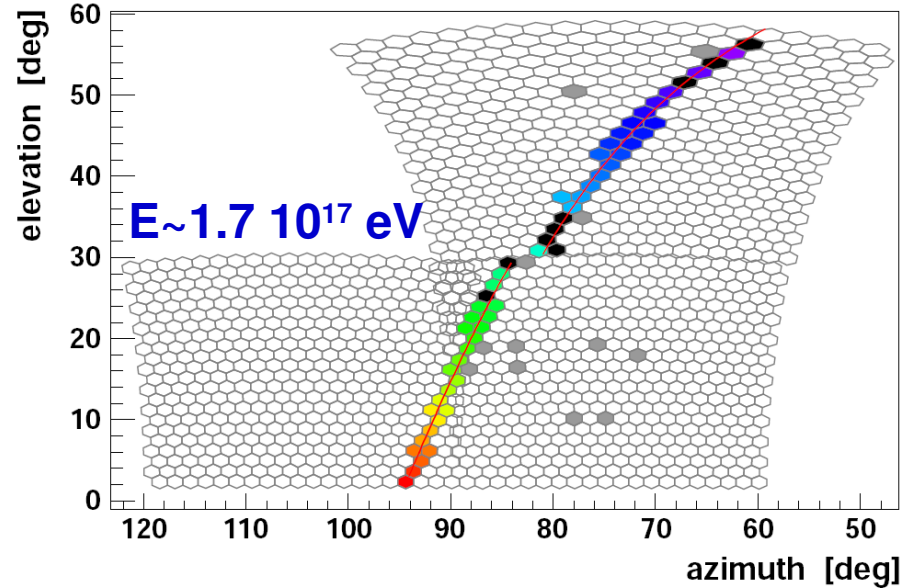
- Radio detection (AERA)
- Microwave detection (several projects)

FD Auger enhancement: HEAT

H-J Mathes @ ICRC 2011



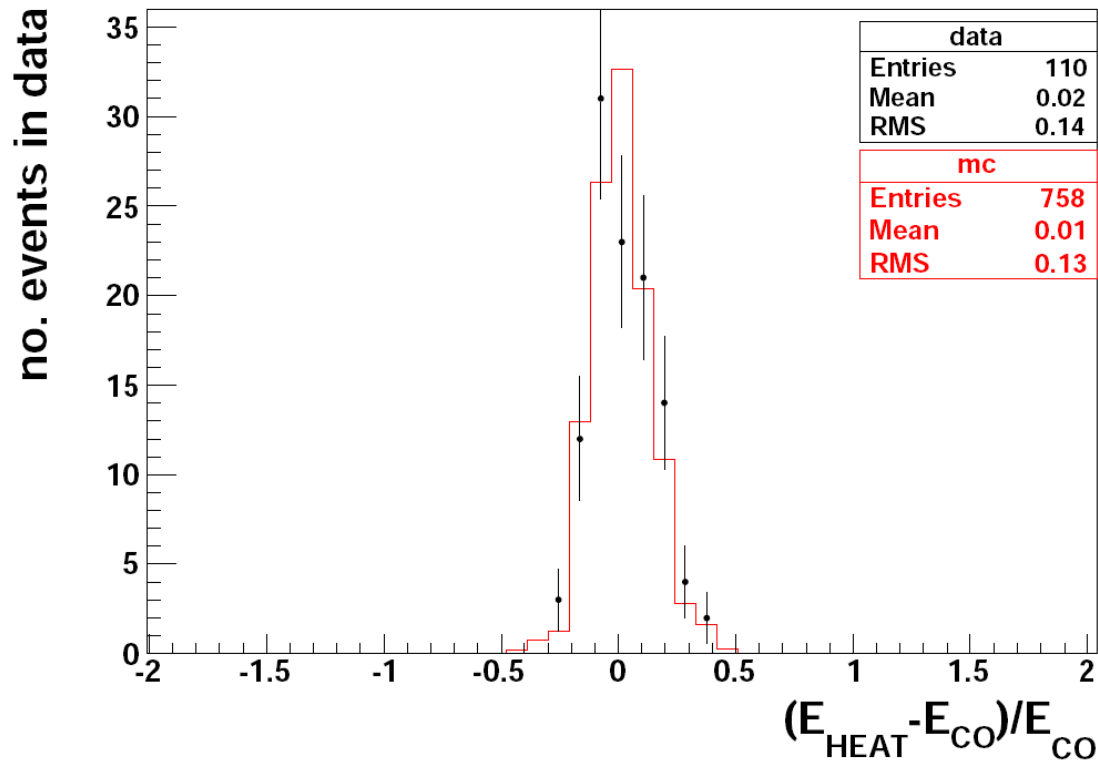
3 telescopes nearby Coihueco
30° up to 60° elevation



Higher elevation
lower energies ($\sim 10^{17}$ eV) unbiased
observation of longitudinal profile

Taking data since Sept. 2009

First data used for alignment and calibration



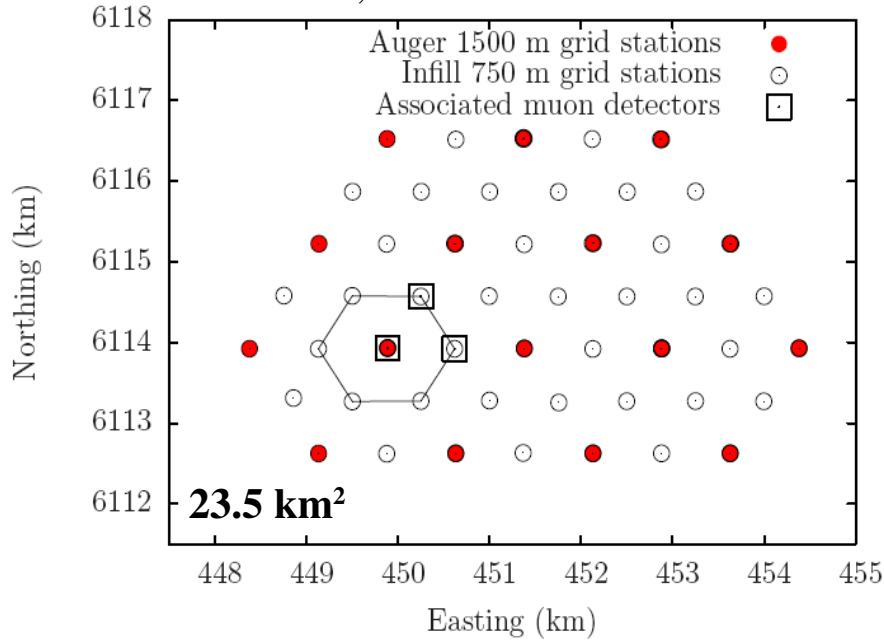
Energy reconstruction

- cross-calibration of HEAT (working in downward mode) and Caihueco
- agreement with simulations

Plenty of new high-quality data are being collected

SD Auger enhancement: AMIGA

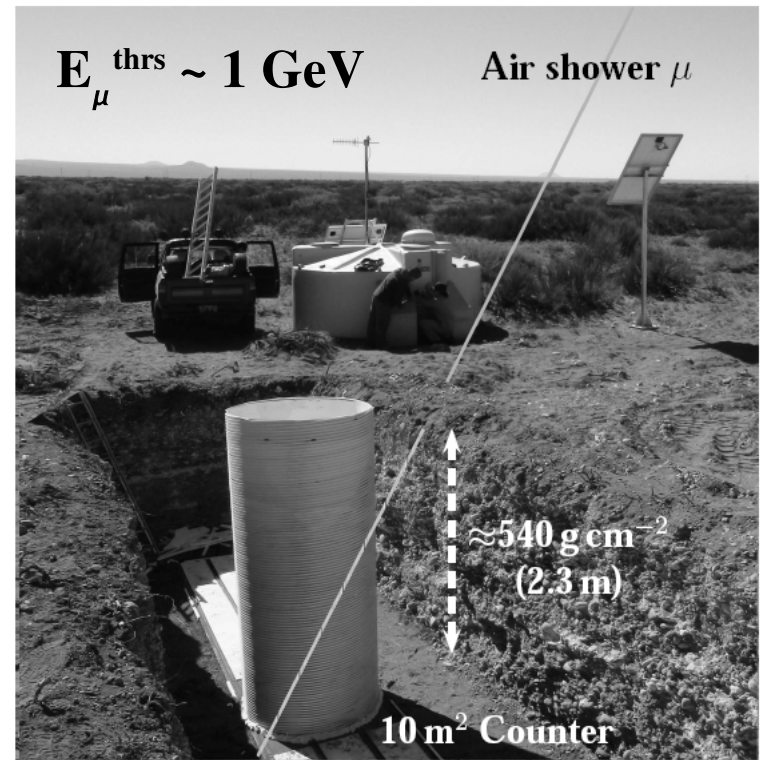
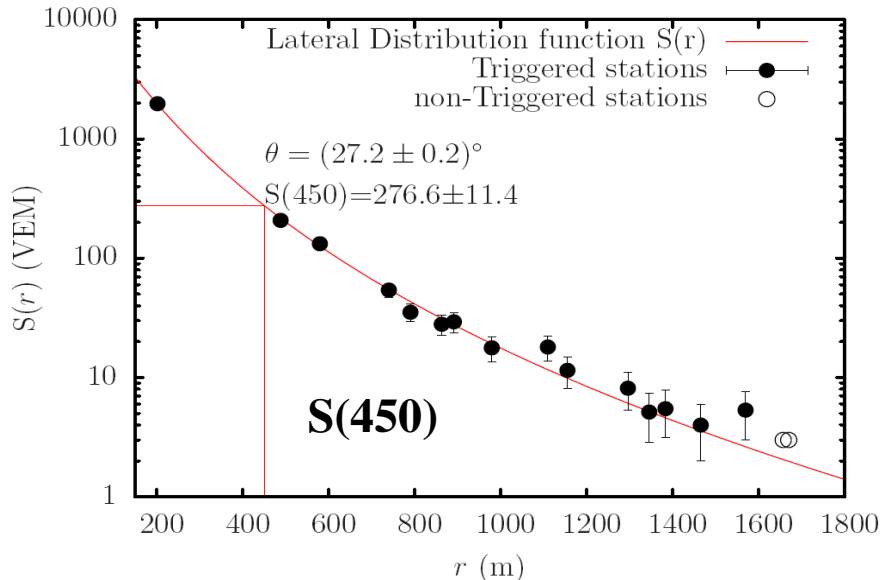
I. Maris, F. Sanchez @ ICRC 2011



INFILL array (Cherenkov stations) and Muon detectors (scintillators)

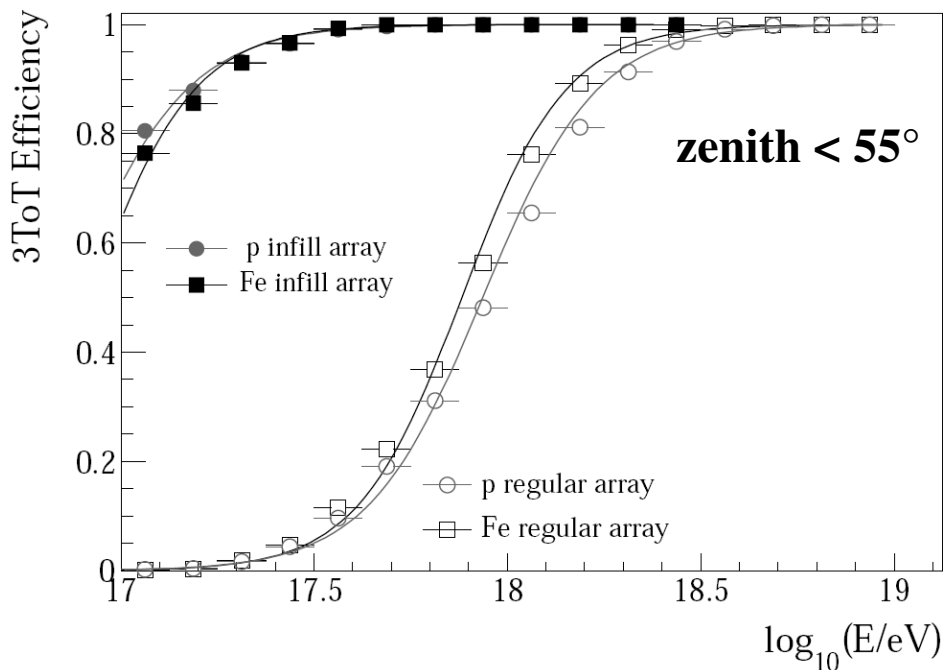
- 61 station with spacing 750 m deployed
- 4 buried scintillator modules installed

Exposure: (35.7 ± 1.3) km² sr yr



700 (20, 4) events/ month $E > 10^{17.5}$ (18, 18.5) eV

Infill array performance



S(450) -> particle density at 450 m
- S35 corrected for the zenith angle dependence
- 22% (13%) uncertainty at 3 (10) VEM

Imminent result:
the energy spectrum down to $3 \cdot 10^{17}$ eV

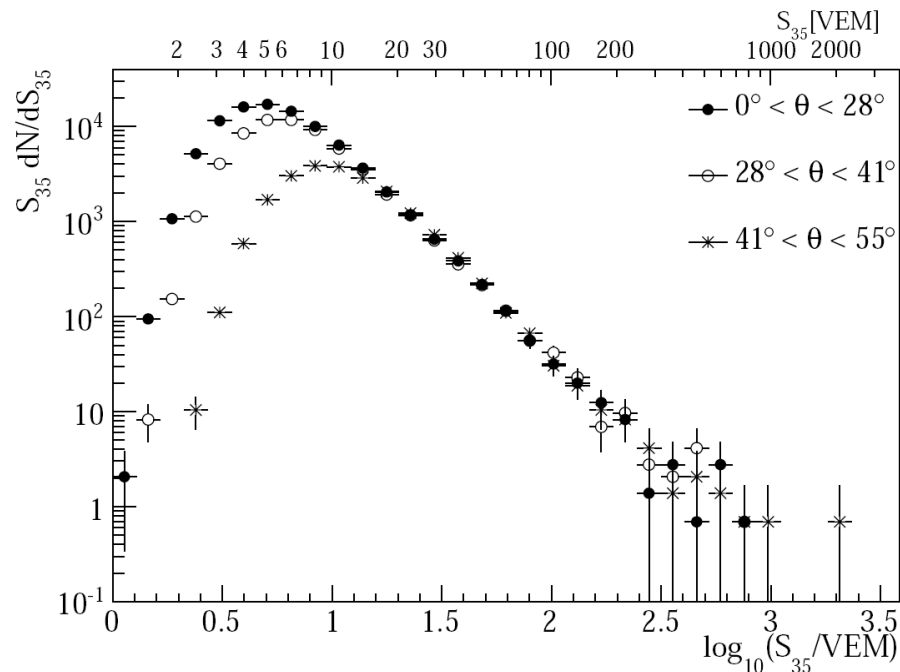
Full Efficiency above $3 \cdot 10^{17}$ eV

Angular resolution

1.3° for at least four stations

1° for at least six stations

About 200.000 fiducial events collected



AERA: Radio detection

B. Revenu, J.L Kelley @ ICRC 2011

Observation of radio emission from electromagnetic cascade

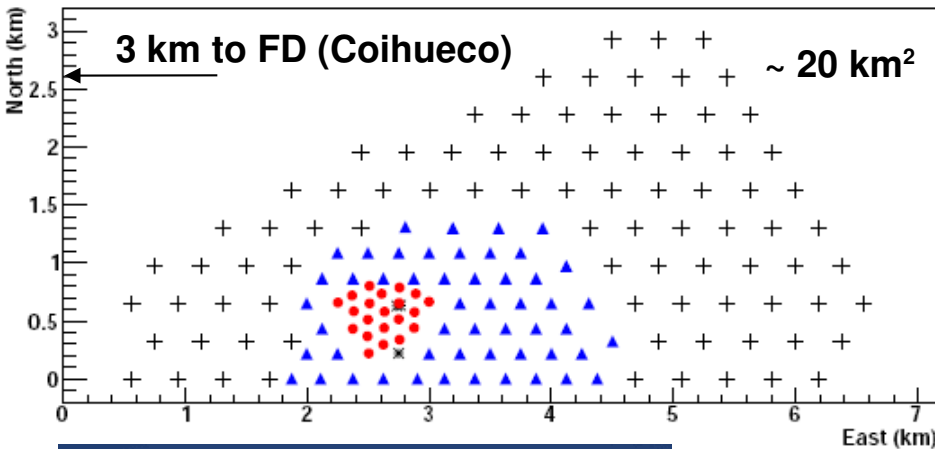
- geomagnetic field
- charge separation

VHF band 10-100 MHz

Deployed in 2010 (21 Radio stations, 150m)
stage 2 (250 m)
stage 3 (350 m)

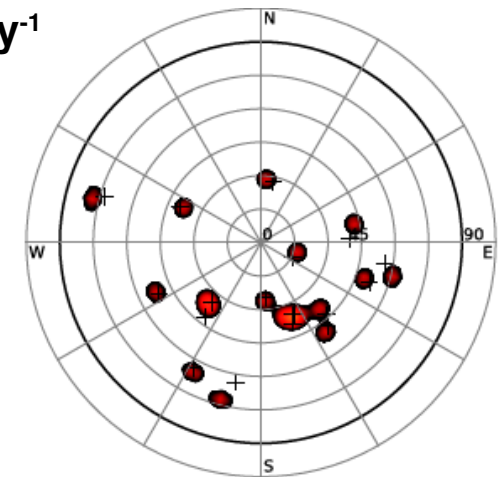
First physical radio-hybrid events

Radio/SD 0.5 day^{-1}



$E_{\text{thres}} \sim 10^{17} \text{ eV}$

**Logarithmic
periodic dipole
antenna (two
polarizations)**



Polar plot, SD and radio reconstruction

First Radio/FD/SD super hybrid event observed

Microwave detection

Observation of microwave emission from electromagnetic cascade

Molecular Bremsstrahlung isotropic emission

P. Gorham et al., Phys. Rev. D, 2008, 78: 032007

Signal $\propto N_e^2$ quadratic scaling

Signal $\propto N_e$ linear scaling

~100% duty cycle – negligible atmospheric absorption

P. S Allison @ ICRC 2011

Radiometers in coincidence with SD



AMBER

2.4 m off-axis parabola
C Band: 3.4 - 4.2 GHz
ku band: 10.95 14.5 GHz
Total FoV $7^\circ \times 7^\circ$
First test at Hawaii, then
shipped to Argentina
Collecting first data



EASIER

GhZ Antenna
C Band: 3.4 - 4.2 GHz
Total FoV 60° to zenith
First test at Paris, then
shipped to Argentina
Collecting first data

Self-trigger same logic as FD

Observation of the
longitudinal profile

4.5 parabolic reflector
with a 53 pixel camera
Total FoV $20^\circ \times 10^\circ$
C Band: 3.4 - 4.2 GHz
**Data collected at
Chicago**, then shipped to
Argentina



MIDAS

$E_{\text{thrs}} \sim 2 \cdot 10^{18}$ eV (quadratic scaling)

$E_{\text{thrs}} \sim 1 \cdot 10^{19}$ eV (linear scaling)

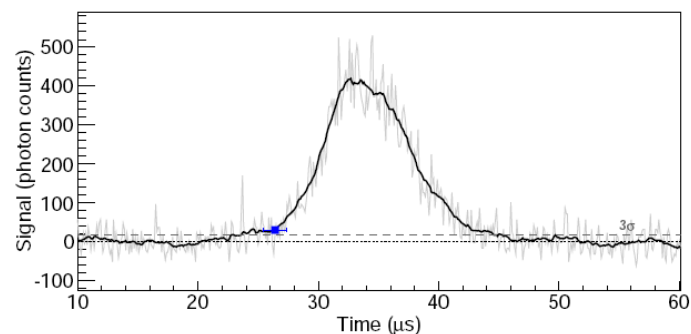
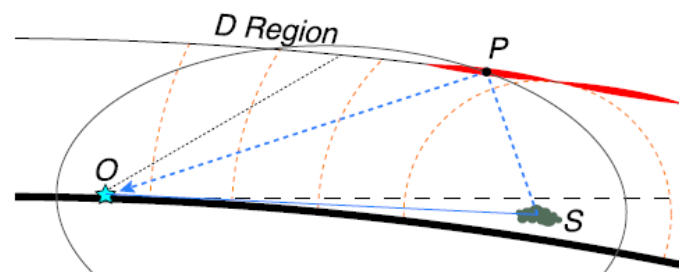
All operating (or very close to) at the Auger Site

Observation of elves with FD

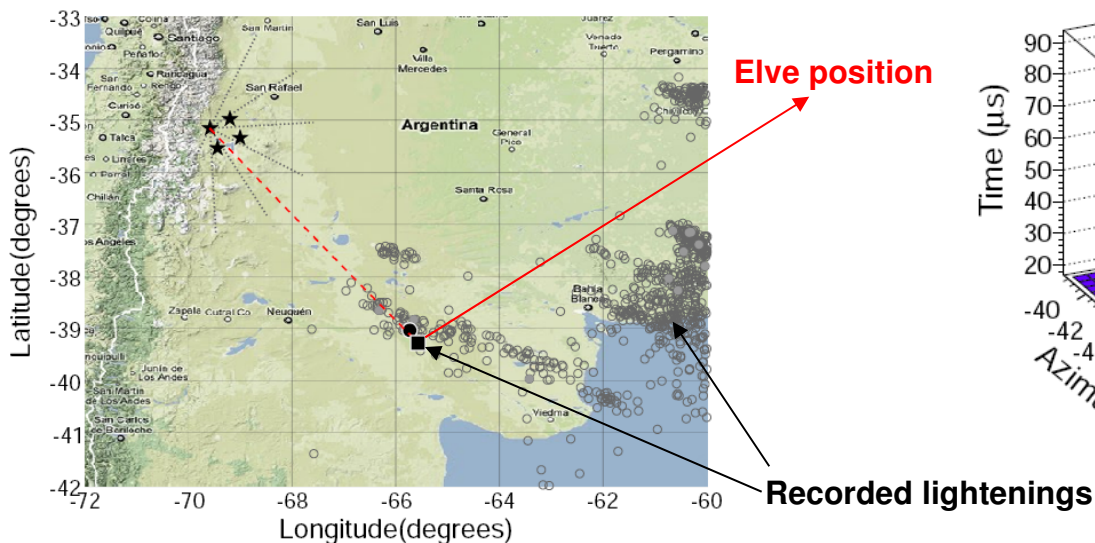
Transient phenomena in D-layer of the ionosphere at about 90 km (few ms long)

3 candidates observed in FD

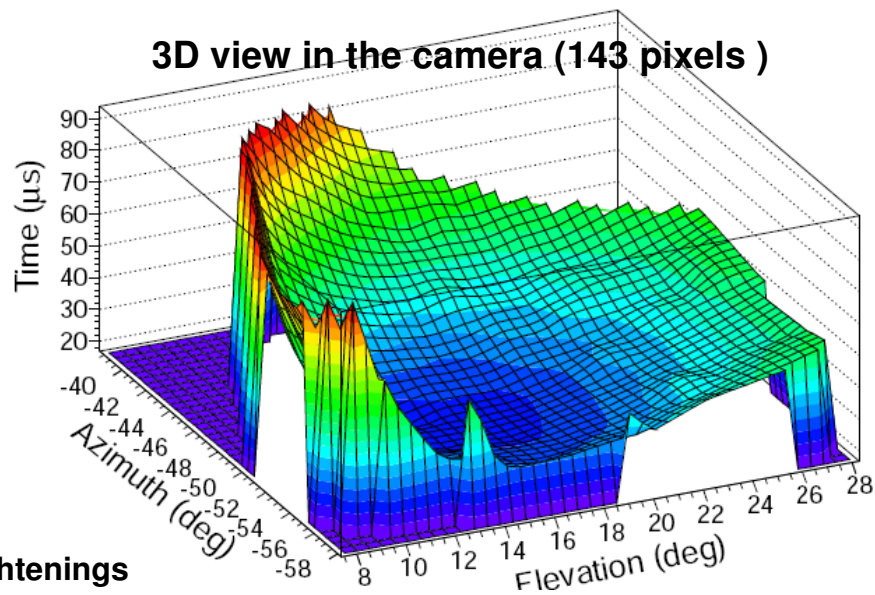
Site-Bay	GPS time	GMT time
LM - 6	800414142	18 May 2005 01:15:29
CO - 3	860806213	17 April 2007 00:49:59
LL - 1	861081389	20 April 2007 05:16:15



Reconstruction performed with FD



3D view in the camera (143 pixels)



Summary of results

Spectrum

- flux suppression established ($E > 4 \cdot 10^{19}$ eV)
- ankle observed at about $4 \cdot 10^{18}$ eV

Composition

- mixed scenario: light dominated at low energies, heavier with increasing energy (interpretation is model dependent)

Hadronic interactions

- first measurement at $\sqrt{s} = 57$ TeV

Arrival directions

- the degree of correlation with VCV catalog has decreased
- definitive conclusions must await additional data

Photons and neutrinos

- flux photon limits above 1 EeV (top-down model disfavored)
- updated limits on the diffuse flux

Outlook and future

The Pierre Auger Observatory takes data smoothly since 2004

- construction completed in 2008

Extensions towards the lower energies (HEAT and AMIGA) r

- study the transition from galactic to extragalactic CR component
- allow cross-calibration with other experiments

The Pierre Auger Observatory for new detection techniques

Radio detection (AERA), radio hybrid events collected

Microwave detection, several detectors being installed

“In order to make further progress, particularly in the field of cosmic rays, it will be necessary to apply all our resources and apparatus simultaneously and side-by-side.”

V.H.Hess, Nobel Lecture, December 1936

Back-up slides

Anisotropy at the highest energy

Data Set

01/01/2004 –
31/08/2007

27 high energy events

$E > 57$ EeV

Angular radius of 3.1°

$D_{\max} = 75$ Mpc

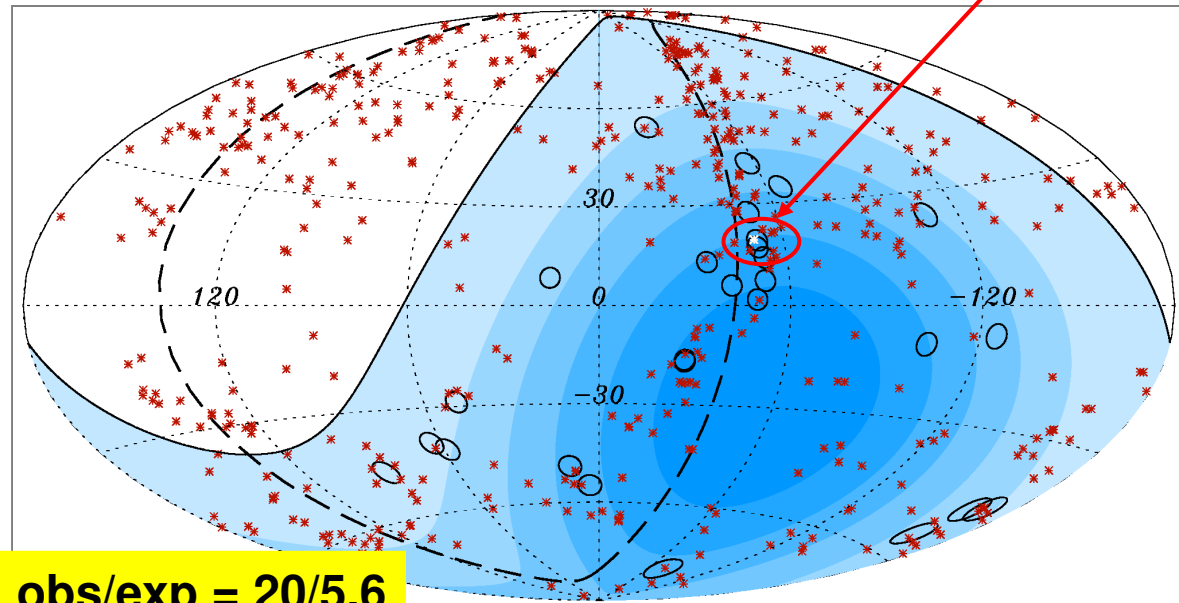
Taking as reference the catalog by Véron-Cetty and Véron (2006)

20/27 events correlate with nearby AGN

Limitations of the catalogue: incomplete and inhomogeneous

Science, vol 318, issue 5852, 09/11/07

Centaurus A



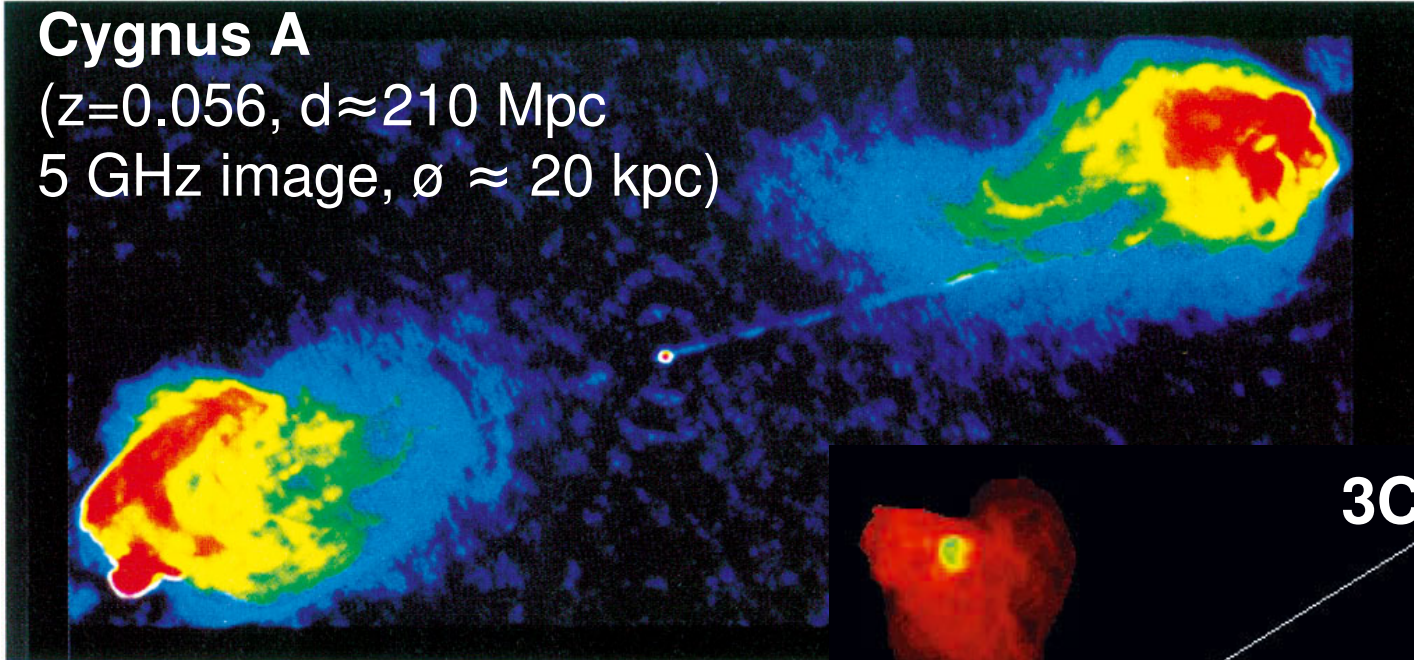
- events with $E > 57$ EeV, angular radius $\psi = 3.1^\circ$,
- ✱ 472 AGN within $D_{\max} = 75$ Mpc (318 in the Auger FOV)

Isotropic chance probability < 1%

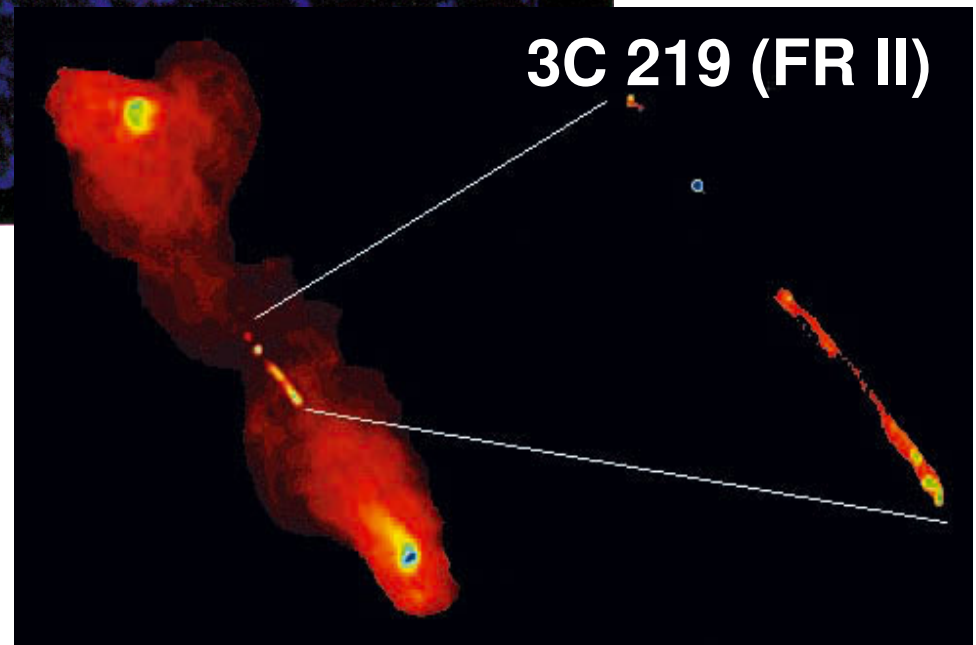
Cosmic Rays: astrophysical sources

Cygnus A

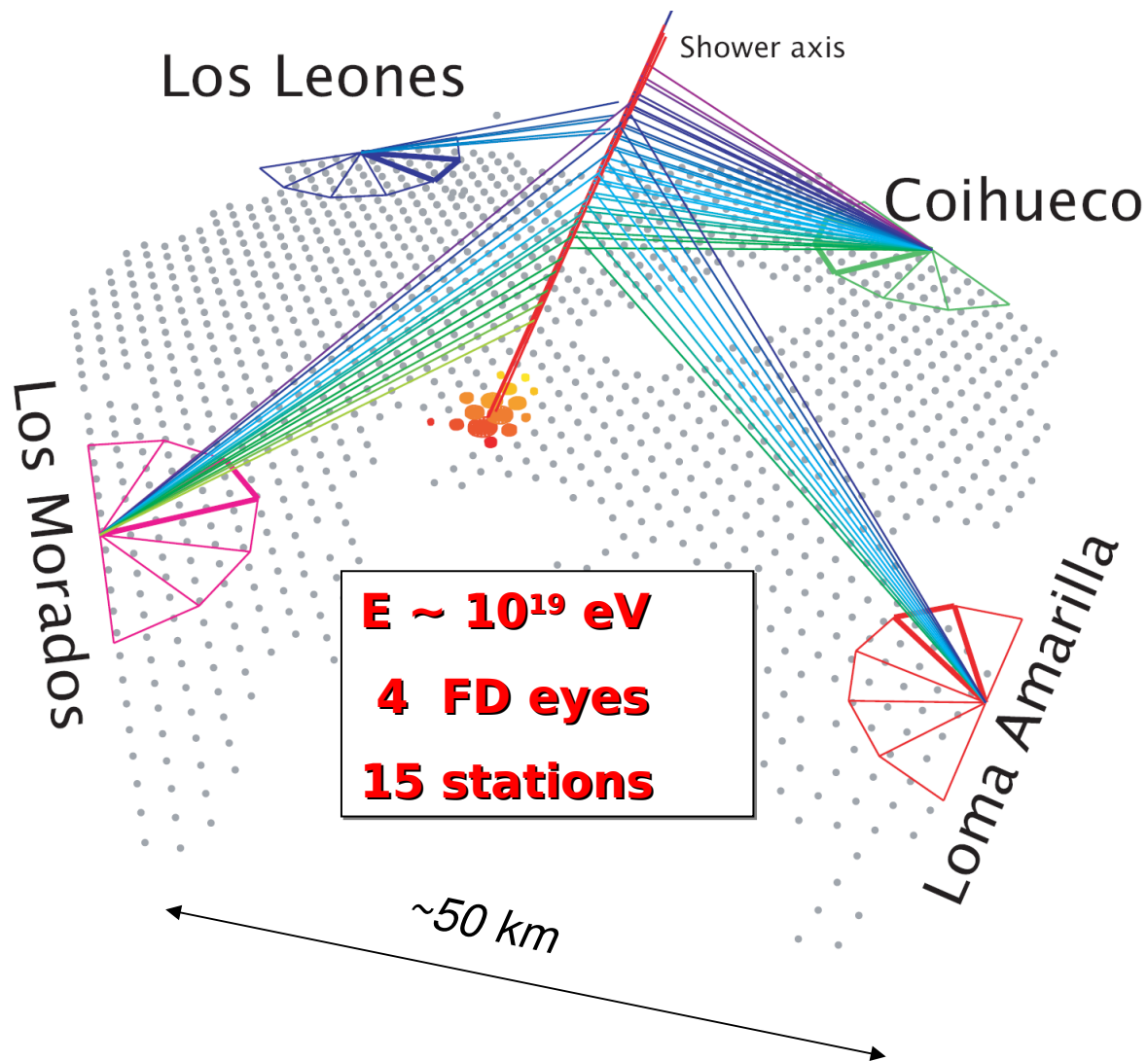
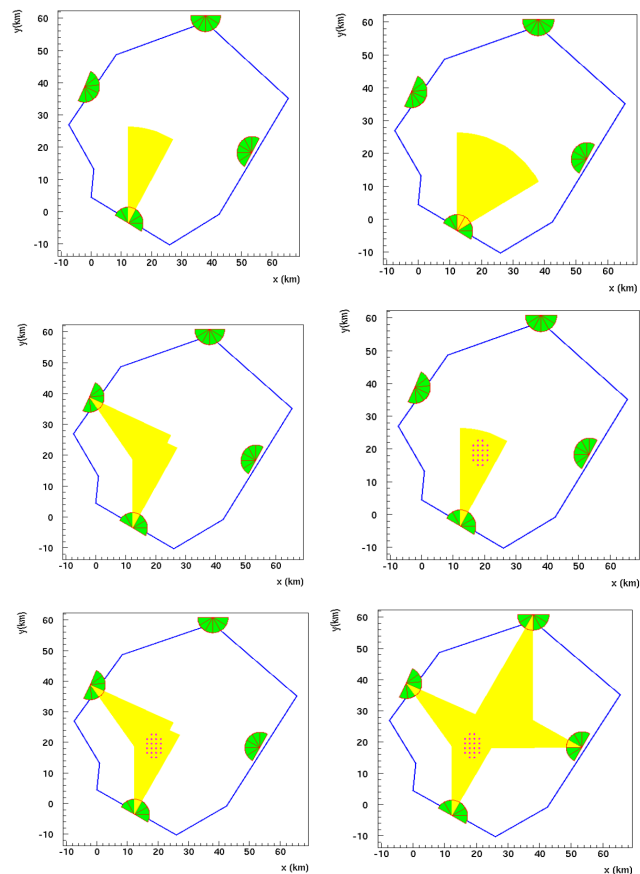
($z=0.056$, $d \approx 210$ Mpc
5 GHz image, $\varnothing \approx 20$ kpc)



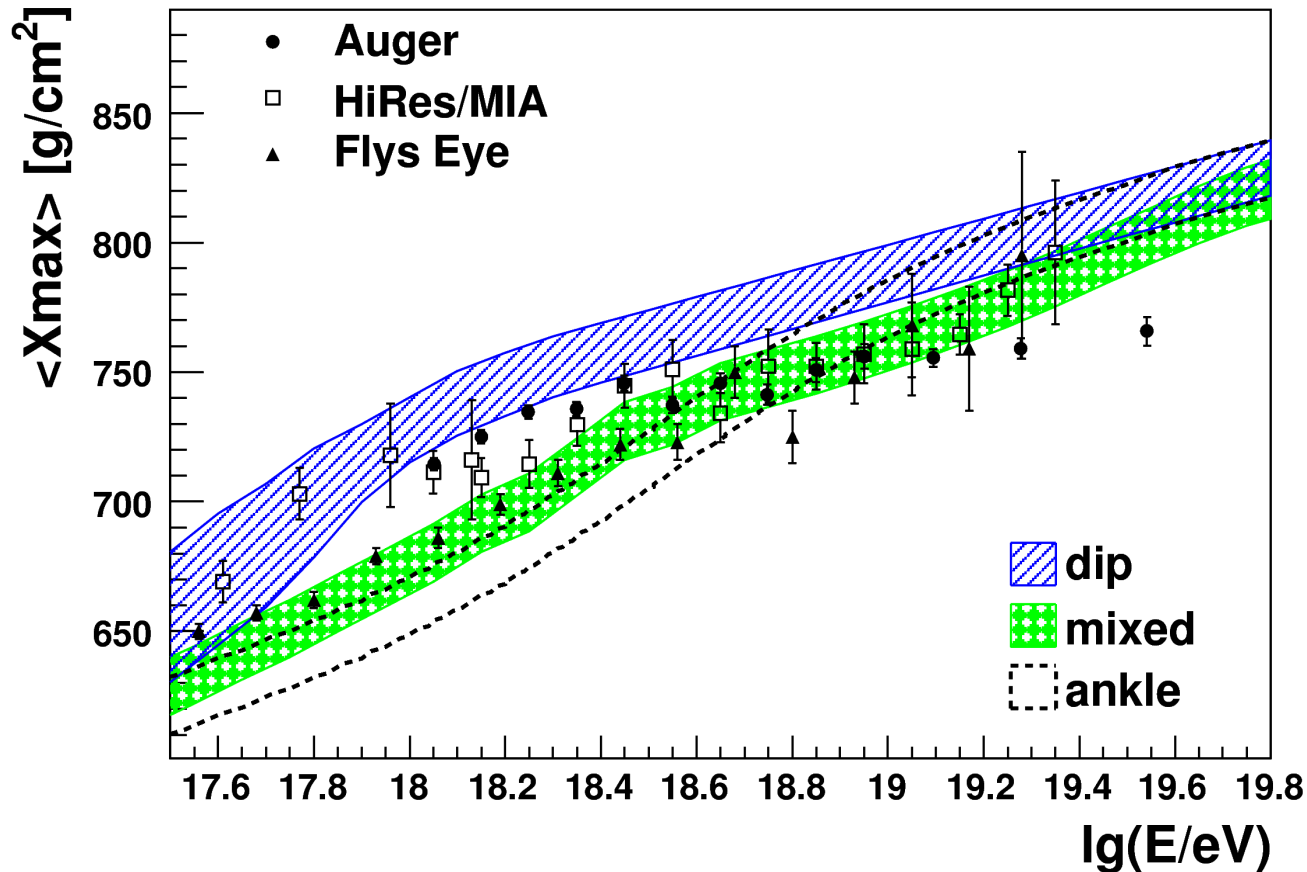
AGN radio-lobes:
(Rachen&Biermann,1993)
AGN Jets:
(Norman et al.,1995)



Event topologies



Data compared to models

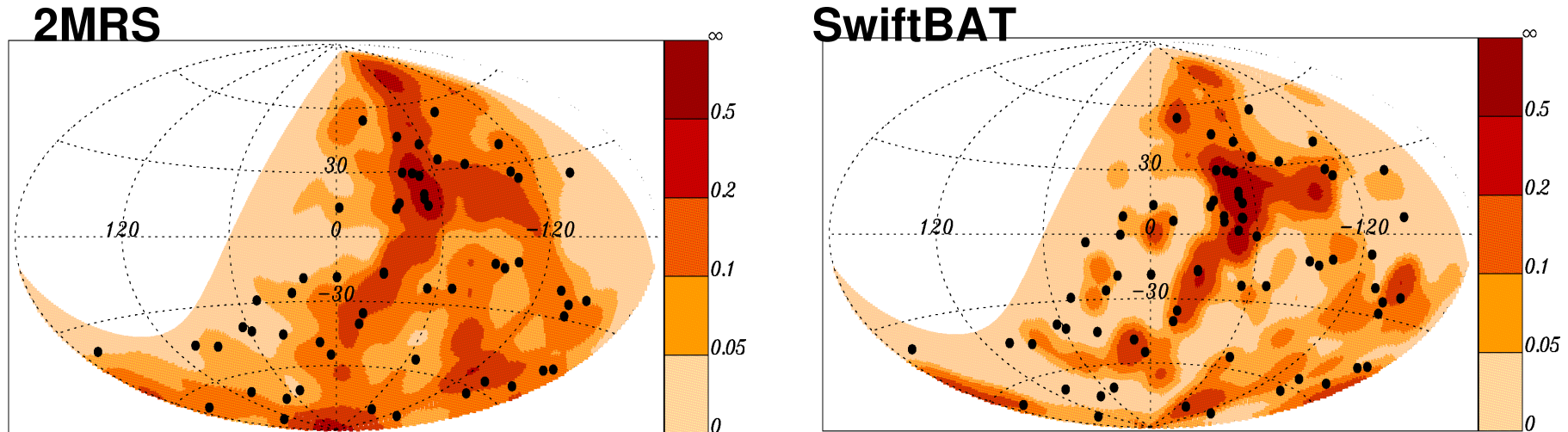


Courtesy of Michal Unger

none of the model satisfactory explains data yet (shape, absolute value)
→ constraints by studying X_{\max} distribution (known syst. unc.)

A posteriori searches

Astropart. Phys. 34 (2010) 314



5 σ detection requires more data (165 for $P=6 \cdot 10^{-7}$)

→ tests on other catalogues: 2MRS (IR) & SwiftBAT (X-rays)

Not only muons hit the tank!!!!



**Bird droppings
together with dry
weather degrade
solar panels.**

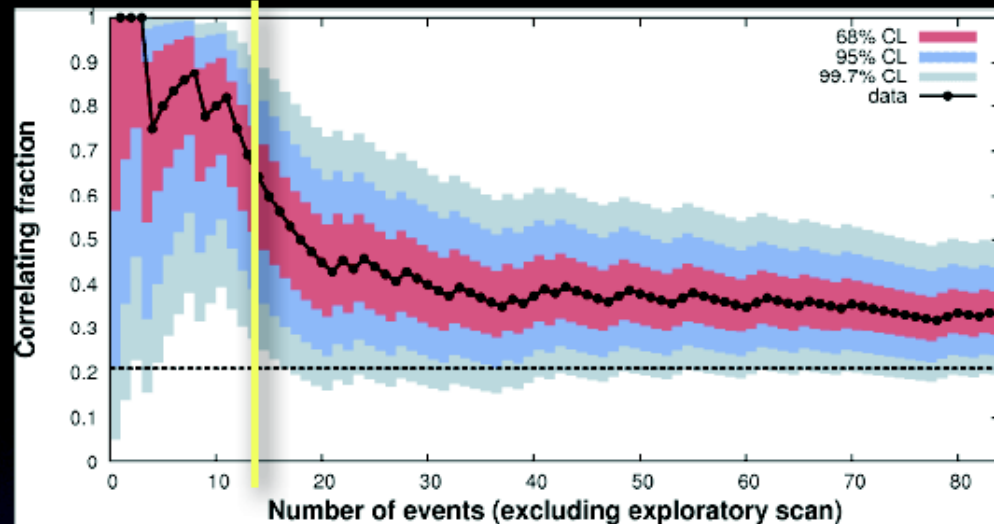


**Bird nests behind
solar panels
sometimes catch
fire.**

Frazione di eventi di $E > 55$ EeV che correlano con le posizioni degli AGN “vicini” del catalogo VCV

Pierre Auger Collaboration (2011) presentato ICRC 2011 (Beijing)

Science 318: 9/13 ~69% di eventi correlati



frazione = k/N
 k : eventi che correlano
 N numero di eventi totali

$f = (33 \pm 5)\%$
 $f_{iso} = 21\%$, Totali 28/84
 $P = 0.006$

frazione aumenta escludendo piano galattico
 $f = 46 \pm 6\%$ ($f_{iso} = 24\%$)

Telescope Array (2011)

frazione di correlati è 40% (8/20) mentre l'aspettazione da un flusso isotropo è il 25%

frazione degli eventi correlati del 69% (9/13) convertita nell'emisfero nord è il 73%

